UNIVERSIDADE ESTADUAL DE CAMPINAS
Faculdade de Engenharia Química

JEAN FELIPE LEAL SILVA

# Process development for sugarcane conversion to ethyl levulinate: a route for a viable biodiesel additive

*Desenvolvimento de um processo de conversão de cana-de-açúcar a levulinato de etila: uma rota para um aditivo de biodiesel viável*

Campinas
2018

JEAN FELIPE LEAL SILVA

# Process development for sugarcane conversion to ethyl levulinate: a route for a viable biodiesel additive

# *Desenvolvimento de um processo de conversão de cana-de-açúcar a levulinato de etila: uma rota para um aditivo de biodiesel viável*

Dissertation presented to the School of Chemical Engineering of the University of Campinas in partial fulfillment of the requirements for the degree of Master in Chemical Engineering.

*Dissertação apresentada à Faculdade de Engenharia Química da Universidade Estadual de Campinas como parte dos requisitos exigidos para a obtenção do título de Mestre em Engenharia Química.*

Supervisor/*orientador*: Prof. Dr. Rubens Maciel Filho

*ESTE EXEMPLAR CORRESPONDE À VERSÃO FINAL DA DISSERTAÇÃO DEFENDIDA PELO ALUNO JEAN FELIPE LEAL SILVA, E ORIENTADA PELO PROF. DR. RUBENS MACIEL FILHO*

Campinas
2018

**Agência(s) de fomento e nº(s) de processo(s):** FAPESP, 2016/10450-1
**ORCID:** https://orcid.org/0000-0002-9915-5859

Ficha catalográfica
Universidade Estadual de Campinas
Biblioteca da Área de Engenharia e Arquitetura
Luciana Pietrosanto Milla - CRB 8/8129

L473d

Leal Silva, Jean Felipe, 1991-
Process development for sugarcane conversion to ethyl levulinate: a route for a viable biodiesel additive / Jean Felipe Leal Silva. – Campinas, SP : [s.n.], 2018.

Orientador: Rubens Maciel Filho.
Dissertação (mestrado) – Universidade Estadual de Campinas, Faculdade de Engenharia Química.

1. Biocombustível. 2. Processos químicos. 3. Energia renovável. 4. Simulação de processos. 5. Biomassa. I. Maciel Filho, Rubens, 1958-. II. Universidade Estadual de Campinas. Faculdade de Engenharia Química. III. Título.

Informações para Biblioteca Digital

**Título em outro idioma:** Desenvolvimento de um processo de conversão de cana-de-açúcar a levulinato de etila: uma rota para um aditivo de biodiesel viável
**Palavras-chave em inglês:**
Biofuel
Chemical processes
Renewable energy
Process simulation
Biomass
**Área de concentração:** Engenharia Química
**Titulação:** Mestre em Engenharia Química
**Banca examinadora:**
Rubens Maciel Filho [Orientador]
Marija Tasic
Luís Fernando Mercier Franco
**Data de defesa:** 30-07-2018
**Programa de Pós-Graduação:** Engenharia Química

UNIVERSITY OF CAMPINAS
*UNIVERSIDADE ESTADUAL DE CAMPINAS*
School of Chemical Engineering
*Faculdade de Engenharia Química*

**Process development for sugarcane conversion to ethyl levulinate: a route for a viable biodiesel additive**

***Desenvolvimento de um processo de conversão de cana-de-açúcar a levulinato de etila: uma rota para um aditivo de biodiesel viável***

Author/*autor*: Jean Felipe Leal Silva

Supervisor/*orientador*: Prof. Dr. Rubens Maciel Filho

The dissertation was approved by the following members of the examining committee:

*A banca examinadora composta pelos membros abaixo aprovou esta dissertação:*

Prof. Dr. Rubens Maciel Filho – Chair/*Presidente*
School of Chemical Engineering – University of Campinas

Prof. Dr. Marija Tasic
Faculty of Technology, University of Nis

Prof. Dr. Luís Fernando Mercier Franco
School of Chemical Engineering – University of Campinas

The minute with the signatures of members of the examining committee can be found in the students' academic life file.

*A ata de defesa com as respectivas assinaturas dos membros encontra-se no processo de vida acadêmica do aluno.*

Campinas, July 30th 2018

To my parents, who have always supported me in pursuing this project; to my friends, who know how much I value them for the great times we have spent together; and to my will of self-improvement, which keeps helping me to become a better man and citizen of the world.

## Acknowledgments

Graduate School (*Vol. I – The Master's degree*) was a challenge, but thankfully I was not alone in this journey. First, I would like to thank my parents, who supported my decisions in life and have always been by my side. Next, I thank those who helped to direct me into the path of graduate school in one way or another: Livia Lima, Simone Silva, Prof. Marcos Benevuto Jardim, Prof. Milton Campos, Prof. Peter Van Puyvelde, Nadya Zyakina, Tassia Junqueira, and Bruno Klein. My classmates from the bachelor's degree also kept saying (countless times) that I have the talent for research, so I suppose they also motivated me a lot.

In my time in the Laboratory of Process Optimization, Control and Design (LOPCA), I have met some wonderful people, who will always have a special place in heart: Andressa, Bárbara, Carla, Daniel, Emília, Ercília, Gabriela, Ingrid, Júnia, Laís, Larissa, Nahieh, and Rebecca. Thank you all for sharing knowledge and laughs – this is priceless, and keeping good company is fundamental to maintain a good rhythm in our work. As we all have seen in *The Shining*: *"all work and no play makes Jack a dull boy."* Also, I would like to thank our colleagues who stay in the background to keep the laboratory running: Maria Ingrid, Silvana Campos, and Cristiano Roberto.

I would like to give a special thanks to those who helped me to reach my research goals: Rebecca Grekin, Emília Lopes, Ingrid Motta, Andressa Marchesan, Nahieh Toscano, Daniel Assumpção, Prof. Adriano Mariano, Prof. Maria Regina Wolf Maciel, and of course, Prof. Rubens Maciel Filho – my supervisor whose guidance was fundamental to lead me in the right path. Research is a combination of efforts, and I am grateful for your contributions. I would like to thank the professors who gave me the opportunity to be their teaching assistant: Prof. Maria Teresa Moreira Rodrigues and Prof. Reginaldo Guirardelo. I also would like to thank the examining committee in my qualifying and defense exams, Prof. Luís Fernando Mercier Franco, Prof. Marija Tasic, Prof. Adriano Mariano, and Prof. Simone Monteiro e Silva. Your contributions were fundamental to improve this work.

Finally, I acknowledge the São Paulo Research Foundation (FAPESP) for the financial support (MS grant #2016/10450-1 and thematic project #2015/20630-4), and the School of Chemical Engineering of the University of Campinas for the structure, fundamental in the development of the project presented in this dissertation.

*"I have stolen ideas from every book I have ever read. My principle in researching a novel is 'Read like a butterfly, write like a bee', and if this story contains any honey, it is entirely because of the quality of the nectar I found in the work of better writers."*

Philip Pullman, in *The Amber Spyglass* (*His Dark Materials*, book 3)

## Resumo

Levulinato de etila é um derivado do ácido levulínico com potencial para ser utilizado num futuro próximo como um aditivo de diesel e biodiesel devido às suas características únicas, como alto teor de oxigênio e origem renovável. Ele é obtido da esterificação do etanol com ácido levulínico, sendo o segundo um produto da hidrólise de hexoses. Porém, a produção em larga escala do levulinato de etila não é possível atualmente devido a barreiras tecnológicas. O objetivo deste projeto de mestrado foi propor e investigar um processo de hidrólise de biomassa com foco na produção de ácido levulínico e a sua posterior conversão a levulinato de etila, levando em conta os fatores econômicos que são mais importantes na redução dos custos de produção. Uma revisão de possíveis rotas já exploradas na literatura demonstrou o grande potencial em produzir levulinato de etila a partir de bagaço de cana-de-açúcar no Brasil. Ao longo do projeto, várias etapas foram estudadas individualmente de modo a complementar lacunas existentes para simular o processo de produção do levulinato de etila. Finalmente, de posse destes resultados, este trabalho apresenta a simulação de uma biorrefinaria e a otimização de parâmetros operacionais para minimizar o custo de produção do levulinato de etila. Foi demonstrado que a carga de sólidos na hidrólise é o principal fator impactante no custo de produção de levulinato de etila, uma vez que ela eleva a concentração final de ácido levulínico no hidrolisado. Também foi demonstrado que é possível obter levulinato de etila a um custo equivalente a aproximadamente metade do valor atual de diesel com baixo teor de enxofre. Condições que levam à redução no custo de produção do levulinato de etila incluem a hidrólise em condições menos severas (menor carga de catalisador e menor temperatura), mesmo que este cenário não represente a melhor seletividade possível. Outro fator fundamental para o sucesso econômico do processo consiste em remover grande parte das hemiceluloses em etapa anterior à hidrólise da celulose. A análise de risco da biorefinaria otimizada em comparação com um projeto de produção de eletricidade a partir do bagaço de cana demonstrou que a produção de químicos derivados de biomassa como furfural, levulinato de etila e ácido fórmico representa um investimento menos arriscado e mais rentável do que a produção de eletricidade, considerando que a questão de operabilidade do reator não represente um empecilho para o desenvolvimento do projeto. Finalmente, os resultados demonstram a viabilidade da produção de levulinato de etila a partir do bagaço de cana e apresentam um melhor entendimento dos fatores que impactam a rentabilidade de processo. Portanto, estas observações servirão como ferramenta para outros pesquisadores da área direcionarem melhor as suas pesquisas em escala de bancada.

Palavras-chave: biocombustível, processos químicos, energia renovável, simulação de processos, biomassa

## Abstract

Ethyl levulinate is a derivative of levulinic acid with the potential to be used in the near future as a diesel and biodiesel additive because of its unique characteristics, such as high oxygen content and renewable origin. Ethyl levulinate is the product of the esterification of ethanol with levulinic acid, being the later obtained from hydrolysis of hexoses. However, the large-scale production of ethyl levulinate is unfeasible these days due to the lack of proper conversion technology. The objective of this master's project was to propose and investigate a process of hydrolysis of biomass focusing on the production of levulinic acid and its further conversion to ethyl levulinate, considering the economic factors that are the most important in reducing the production costs. A review of the possible routes demonstrated the enormous potential of producing ethyl levulinate in Brazil using sugarcane bagasse as feedstock. During the project, several steps of the production of ethyl levulinate were studied individually to cover gaps in the literature that were fundamental in the development of more accurate process simulation to produce ethyl levulinate. Finally, using these results, this work presents the simulation of a biorefinery and the optimization of operating parameters to minimize the production cost of ethyl levulinate. Solids loading in the hydrolysis reactor was demonstrated to be the main factor impacting the production cost of ethyl levulinate because of its high impact in the final concentration of levulinic acid in the hydrolysate. Results indicated that production of ethyl levulinate at about half of the price of ultra-low-sulfur diesel in Brazil (energy basis) is economically viable. Conditions that led to lower production costs included hydrolysis in less severe conditions (lower catalyst dosage and lower temperature), even though this scenario does not represent the best possible selectivity. Another fundamental factor for the economic success of the processes consists of removing part of the hemicelluloses before hydrolysis of cellulose in a different step. Risk analysis of the optimized biorefinery compared to an optimized ethanol distillery producing electricity from bagasse showed that production of biomass-derived chemicals such as furfural, ethyl levulinate, and formic acid represents a safer and more profitable investment than producing only electricity from the surplus bagasse. Overall, the results demonstrated the viability of ethyl levulinate production using sugarcane bagasse as feedstock and presented a better understanding of the factors that impact the profitability of the process. Therefore, these observations will serve as a tool for other researchers to developed better processes for conversion of biomass to levulinic acid and derivatives in the future by having a better grasp of the economics behind it.

Keywords: biofuel, chemical processes, renewable energy, process simulation, biomass

## List of Figures

## List of Tables

## Nomenclature

| | |
|---|---|
| AA | acetic acid |
| CAPEX | capital expenditure |
| CC | cellulose conversion |
| CCD | central composite design |
| CEPCI | chemical engineering plant cost index |
| CHP | cogeneration of heat and power |
| CL | catalyst loading |
| DOE | design of experiments |
| EL | ethyl levulinate |
| EL-f | scenario with ethyl levulinate production from bagasse, future price |
| EL-p | scenario with ethyl levulinate production from bagasse, premium price |
| EL-t | scenario with ethyl levulinate production from bagasse, today's price |
| ET-t | scenario without ethyl levulinate production from bagasse, only electricity |
| FF | furfural |
| FA | Formic acid |
| GVL | γ-valerolactone |
| HMF | 5-hydroxymethylfurfural |
| IAPWS | The International Association for the Properties of Water and Steam |
| IGP-M | general index for market prices |
| IRR | internal rate of return |
| L/D | length to diameter ratio |
| LA | levulinic acid |
| LHV | lower heating value |
| LLE | liquid-liquid equilibria |
| MTHF | 2-methyltetrahydrofuran |
| MSP | minimum selling price |
| NRTL | nonrandom, two-liquid model |
| OPEX | operational expenditure |
| PURE32 | Aspen Plus databank (version 8.6) |

| | |
|---|---|
| RT | reactor temperature |
| SL | solids loading |
| ULSD | ultra-low-sulfur diesel |
| UNIFAC | UNIQUAC functional group activity coefficient model |
| UNIQUAC | universal quasichemical activity coefficient model |

## Symbols

*Latin letters*

| | |
|---|---|
| $A_i$ | coefficient of a general equation |
| $A_0$ | pre-exponential factor |
| $a_{ij}$ | coefficient in NRTL model for interaction between species $i$ and $j$ |
| $B$ | second coefficient of a virial expansion of molar density of a gas |
| $B_i$ | coefficient of a general equation |
| $B_{ij}$ | second virial coefficient characterizing pair interactions between species $i$ and $j$ |
| $b_{ij}$ | coefficient in NRTL model for interaction between species $i$ and $j$ |
| $C_i$ | coefficient of a general equation |
| $\boldsymbol{C}_i$ | concentration term of species $i$ for driving force expression |
| $c_i$ | parameter in Boston-Mathias alpha function |
| $c_{ij}$ | coefficient in NRTL model for interaction between species $i$ and $j$ |
| $D_i$ | coefficient of a general equation |
| $d_i$ | parameter in Boston-Mathias alpha function |
| $d_{ij}$ | coefficient in NRTL model for interaction between species $i$ and $j$ |
| $e_{ij}$ | coefficient in NRTL model for interaction between species $i$ and $j$ |
| $\hat{f}_i^I$ | fugacity of component $i$ in a mixture in phase I |
| $f_{ij}$ | coefficient in NRTL model for interaction between species $i$ and $j$ |
| $G_{ij}$ | coefficient of NRTL equation |
| $i$ | component or step |
| $j$ | term in a mathematical expression |
| $K_i$ | constant in adsorption expression for component $i$ |
| $k_i$ | kinetic factor of step $i$ or preexponential factor of forward and reverse reactions |
| $M$ | number of terms in adsorption expression |
| $m$ | number of variables in the surrogate model |
| $m'$ | exponent of adsorption expression |
| $m_i$ | exponent for sulfuric acid concentration |
| $n$ | number of cases used in data regression of the surrogate model |

| | |
|---|---|
| $N$ | number of components in the mixture |
| $P$ | pressure |
| $P_c$ | critical pressure |
| $P_i^{sat}$ | vapor pressure of component $i$ |
| $R$ | gas constant (8.3144598(48) J/(mol.K)) |
| $R_i$ | reaction rate for step $i$ |
| $r_{gyr}$ | radius of gyration |
| $\boldsymbol{S}$ | matrix of independent variables |
| $T$ | temperature |
| $T_c$ | critical temperature |
| $T_r$ | reduced temperature |
| $V_i$ | molar volume |
| $\boldsymbol{x}$ | vector of independent variables |
| $x_i$ | mole fraction of component $i$ in liquid phase |
| $\hat{\boldsymbol{y}}$ | vector of predicted responses |
| $y_i$ | mole fraction of component $i$ in vapor phase |
| $\boldsymbol{y_s}$ | vector of sampled responses |
| $Z$ | compressibility factor |

*Greek letters*

| | |
|---|---|
| $\alpha_i$ | alpha function, cohesion function, or reaction order (component $i$, forward reaction) |
| $\alpha_{ij}$ | non-randomness parameter (NRTL) |
| $\beta_i$ | reaction order (component $i$, reverse reaction) |
| $\gamma_i$ | activity coefficient of component $i$ |
| $\varepsilon$ | energy parameter |
| $\xi$ | angle averaged polar effect |
| $\sigma$ | molecular size parameter |
| $\eta$ | association or solvation parameter for pure or unlike interactions |
| $\lambda$ | concentration exponent of individual terms in adsorption exponent |
| $\kappa$ | characteristic constant of the alpha function |

| | |
|---|---|
| $\mu$ | molecular dipole moment |
| $\tau_{ij}$ | dimensionless interaction parameters of molecules $i$ and $j$ (NRTL) |
| $\hat{\phi}_i$ | fugacity coefficient of component $i$ in a mixture |
| $\phi_i^{sat}$ | fugacity coefficient of pure component $i$ at $T$, $P_{sat}$ |
| $\omega$ | acentric factor |

# Table of Contents

## Preface

This Master's dissertation corresponds to the results of the FAPESP master's project 2016/10450-1 (Process development for sugarcane conversion to ethyl levulinate: a route for a viable biodiesel additive - *Desenvolvimento do processo de conversão de cana-de-açúcar a levulinato de etila: uma rota para um aditivo de biodiesel viável*). The results of this project were divided into six parts. Parts 1 to 5 represent individual steps either required to develop a better understanding of the process to convert biomass into ethyl levulinate or required to cover knowledge gaps fundamental for the process simulation of EL production. Part 6 represents the simulation of the biorefinery and depends on the results of the other five parts.

The content of each part was defined to represent a single, independent work. Up to the publication of the dissertation, the following papers/manuscripts were published and included in the list of references of the dissertation with the following numbers:

- [15] J. F. Leal Silva, R. Grekin, A. P. Mariano, R. Maciel Filho, *Energy Technol.* **2018**, 6, 613–639.
- [29] J. F. Leal Silva, A. P. Mariano, R. Maciel Filho, *Biomass and Bioenergy* **2018**, 119, 492–502.
- [92] J. F. Leal Silva, R. Maciel Filho, M. R. Wolf Maciel, *Chem. Eng. Trans*. **2018**, 69, 373–378.
- [95] J. F. Leal Silva, M. R. Wolf Maciel, R. Maciel Filho, *Chem. Eng. Trans*. **2018**, 69, 379–384.

Article 5 will include the results presented in Appendix I of this master's dissertation. Article 6 corresponds to the results presented in the main text of this master's dissertation.

# 1. Introduction

Several studies in the past years have demonstrated the potential of using biomass as a precursor of chemicals, both for environmental and economic reasons. However, fermentative processes still face many challenges to use lignocellulosic sugars as feedstock. Conversion of cellulose to levulinic acid (LA) followed by conversion to ethyl levulinate (EL) represents an alternative to fermentative processes. The economic and technical feasibility of this route is the center point of discussion in this work.

## 1.1. Biomass conversion technologies and the levulinate family

The use of non-renewable sources for chemicals and energy by society, such as petroleum and natural gas, has driven the concentration of carbon dioxide in the atmosphere to unprecedented levels.[1] Examples of renewable alternatives to petroleum include solar and wind power for electricity supply and biomass for energy and chemical supplies. Biomass has the benefit of using the carbon dioxide present in the atmosphere as a carbon source. On the other hand, the use of petroleum means necessarily that carbon is being removed from the soil and put in the atmosphere in the form of carbon dioxide. Even though the use of biomass represents a considerable advance regarding the carbon cycle, its use as a source for chemicals and energy still hampered due to challenges related to processing and profitability.

One of the main suggestions for biomass processing is the reduction of the holocellulose (total polysaccharide fraction of biomass) into fermentable sugars. This process comes with a series-selectivity challenge because the monosaccharides decompose into furanic compounds which are toxic to fermentative organisms. Alternatively, instead of sugars, the furanic compounds and their derivatives can be sought as the final goal of holocellulose decomposition, leading to furfural (FF) and LA (4-oxopentanoic acid, $CH_3C(O)(CH_2)_2COOH$, CAS number 123-76-2, 116.11 g/mol) as the main products. Both FF and LA are very reactive chemicals and lead to a plethora of other chemicals, thus representing great building block candidates.

Researchers have been struggling to design a reliable process for biomass conversion into LA and derivatives. Many of the problems are related to either cumbersome reactor operation or reaction conditions that lead to poor selectivity. In this work, reaction conditions to convert sugarcane bagasse into LA and later into EL were investigated using process simulation, technoeconomic analysis, and risk analysis.

## 1.2. Objectives of this work

Bearing the above comments in mind, the primary goal of this study was to find conditions for economical operation of a biorefinery producing EL to help other researchers in the future to develop processes having in mind the big picture of the biorefinery. Reaction conditions such as the proportion of biomass to liquid, catalyst dosage, conversion, and temperature in a two-step reactor process, each of which focused on conversion of different biomass polysaccharides, were studied via statistical analysis. All these conditions were analyzed always having in mind the final cost of EL at the gate of the biorefinery to meet the specific objectives of this work, which include:

- Defining a set of operating conditions that decrease the production cost of EL
- Impact of variations of operating conditions in production cost of EL
- Effect of reactor configuration on the yield of hydrolysis products
- Impact of selectivity and humins formation in process economics
- Risk assessment of a biorefinery producing EL
- Impact of FF on economic results

## 1.3. Organization of the dissertation

Development of a robust biorefinery model depends on reliable process data. Consequently, methodology and theoretical background play a critical role in process simulation. Simulation of EL production depends on data that was already available in the literature or data that was obtained during this master's project. Contributions of these other works are described throughout the dissertation.

Details regarding process design and simulation are available in chapter 4, and details on the methodology used in the technoeconomic analysis are available in section 3.3. Results of the minimum selling price (MSP) of EL are presented in section 5.1, followed by a statistical analysis of variables impacting this economic parameter. Economic analysis is provided in detail in section 5.3 only for the optimized biorefinery compared to a benchmark scenario. Risk analysis included the impact of market uncertainties and different pricing conditions for FF and EL.

## 1.4. Main contributions of this work

Simulation plays an important role in the development of new chemical processes: adequate modeling can discard unpromising routes and avoid laborious experimental work. Moreover, it provides the opportunity to easily connect the effect of inputs and outputs via sensitivity analysis, making the results of experimental models more valuable and easier to assess. This work also presents a sensitivity analysis of the production cost of EL considering both technical and economic aspects. This way, other researchers may discuss their findings based on their real impact on the final cost of EL, instead of only based on yield and selectivity. Moreover, since both EL and LA are commodities, the observations obtained from technoeconomic analysis of EL production can easily be extended to LA and other LA derivatives.

# 2. Literature survey

Several steps are involved in the development of biorefineries, which today are praised as a solution to make viable the commercialization of a variety of green chemicals. This section explains the choice of the chemical on which this work focuses (ethyl levulinate - EL) and shows the knowledge gaps that were proposed to be solved by this project.

## 2.1. From biomass to building blocks

Limited resources and pollution have driven society to develop alternatives to petroleum-based products. These alternatives, based on renewable resources, need to be engineered to cover the demand that today belongs to well-established chemicals. There is much concern involved in making this paradigm shift as stealthy as possible. A great example is the automobile industry: cars with internal combustion engine have been in existence for more than a century.[2] Although the shift from internal combustion engine cars to electric cars is recognized as a trend in the near future in developed countries, developing countries such as China, India, and Brazil may still need to rely on internal combustion engines for decades. Moreover, resources for battery manufacturing are limited, and recycling of rare earth elements seems challenging.[3–5] Therefore, renewable alternative to fuels, the so-called biofuels, have been developed to be used in the same engines like those of fossil fuels.

While searching for biofuels, several molecules have been identified as promising candidates to replace other commodities. Interesting options include succinic acid and 2,5-

furandicarboxylic acid. Succinic acid can be used to replace maleic anhydride in the production of butanediol and tetrahydrofuran, with applications in the polymer industry.[6] 2,5-furandicarboxylic acid is another example because it has a structure very similar to terephthalic acid, which is used in manufacturing of polyethylene terephthalate (referred to as PET, PETE, Terylene, or Dacron), the most common polyester resin in the world.[7] These options of base molecules, called bio-based building blocks, have the potential to replace their fossil counterparts given that they can be produced at a similar or lower cost. However, the cost issue represents a significant challenge.[8]

Biomass is recognized, in general, as a low-cost feedstock alternative. Nevertheless, conversion technologies for biomass fail into realizing the potential of this low cost due to poor yields or expensive process technology (catalyst, equipment, energy demand, etc.), as observed in the industrial endeavors on the cellulosic ethanol field.[9] A significant part of this challenge resides in the fractionation step of biomass, in which the focus is to decompose the biomass into molecules which can be transformed into valuable chemicals. Biomass is composed of cellulose, hemicelluloses, and lignin. Cellulose is a polymer consisting solely of repeating units of glucose. Hemicelluloses correspond to a series of polymers whose proportions depend on plant species: xylans, arabinans (pentose polymers), mannans, glucans, galactans (hexose polymers), etc.[10] Lignin, as hemicelluloses, is not as well organized as cellulose: it is an amorphous tridimensional polymer of syringyl, *p*-hydroxyphenyl, and guaiacyl, along with several other differently substituted aromatic units, and its decomposition into chemicals is very challenging.[11] Today, most of the efforts in biomass fractionation into valuable chemicals focus on cellulose and hemicelluloses owing to the range of possibilities related to the conversion of carbohydrates into building blocks.

### 2.1.1. The concept of biorefineries

One option to circumvent the cost issue in biomass processing is the development of robust biorefineries. Oil refineries produce an extensive array of products, and it is possible to transform part of heavy fractions into products that can be obtained from light fractions and vice-versa. The same idea of exploring the possibilities of each fraction of biomass and integrating several processes to obtain different products can be explored in the conversion of biomass, which is the basis behind the concept of the biorefinery.

### 2.1.2. Economies of scale

Biorefinery projects should focus on large-scale processing of biomass to be economically feasible.[12,13] The integration of several processes requires, for example, the production of more utility, and sharing the production of utilities among several production trains decreases the specific cost per unit of energy because of economies of scale. Yet, a practical limitation of a biorefinery size is the logistics of biomass: biomass difficult to be transported unlike oil that is transported via pipelines, and biomass has low density, presents moisture, and occupies large volumes. Thus, transportation for long distances considerably increases the feedstock cost. Mathematical models have demonstrated the potential of paying for long-distance transportation to allow the construction of larger projects, and the development of larger biorefinery models may become possible in the future.[14]

### 2.1.3. Process integration

One of the main hurdles alleviated by the concept of the biorefinery is that some parts of the processes can be integrated. For instance, the production of utilities can be centralized on a single unit. In another example, considering conventional and cellulosic ethanol processes, parts of the fermentation and distillation processes can be combined, leading to larger equipment and reduced costs.[12] Another important aspect of the biorefinery is that different precursors of a chemical can be produced in the same site, which also results in reduced production costs.[13,15] The flexibility of using the same feed stream to similar processes is also proven to have a positive impact in the economics of a biorefinery project, as in the case of the flexibility in the production of ethanol and butanol.[16]

### 2.1.4. Levulinic acid and ethyl levulinate

Valuable acid dehydration products from monosaccharides include 5-hydroxymethylfurfural (HMF), LA, and FF. Among these, the only chemical with a sizeable market today is FF, which is used as a solvent and as a precursor of furans used in the fabrication of furanic resins.[17] LA has an extensive potential as a building block for molecules to be used in pharmaceuticals, food additives, agricultural products, solvents, polymers, and also as a precursor of

biofuels.[15] However, realizing the full potential of LA depends on the development of a biomass fractionation process with high selectivity and reliable operability.[18]

#### *2.1.4.1. Synthesis of levulinic acid*

The production of HMF and LA, which derive from cellulose (Figure 1), depends on severe hydrolysis conditions because of the well-structured nature of cellulose. Such severe conditions end up compromising the selectivity of the process as furans (HMF and FF) react with sugars to produce an valueless residue, called humins.[19] In contrast, hydrolysis of hemicelluloses is easily attained in mild conditions. For instance, production of FF is carried out in temperatures in the range of 150 °C (using sulfuric acid as catalyst – Quaker Oats process) to 180 °C (no use of catalyst – Rosenlew process).[20] On the other hand, patents on LA production report temperatures in a first reactor in the range of 210-230 °C.[21] Hence, conditions to improve the yield of LA need to be developed carefully taking into account several reaction variables because of the steps involved.

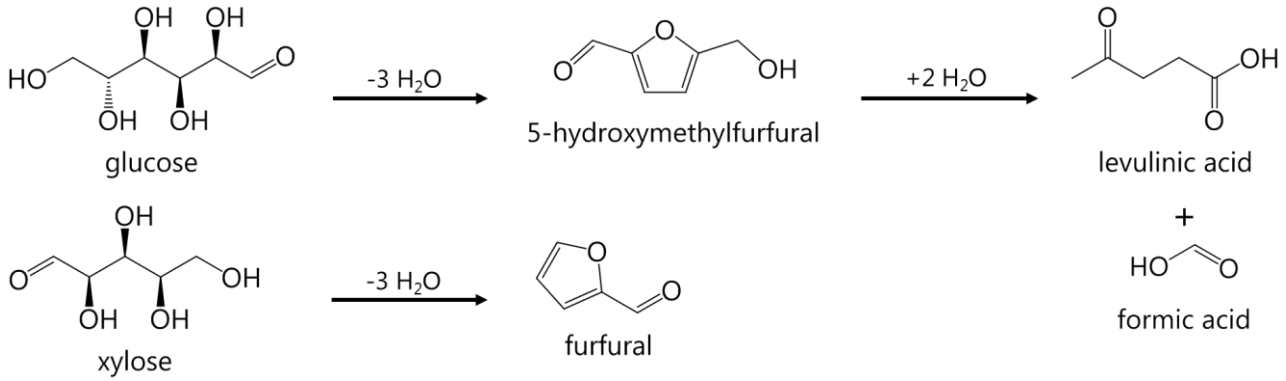


*Figure 1. Dehydration products from hexoses (*e.g.*, glucose) and xylose (*e.g.*, xylose).*

### 2.1.5. Levulinic acid as a building block

LA is a 5-carbon molecule with two organic functions: ketone and carboxylic acid. The presence of these two functions and the length of the carbon chain open a wide range of reaction possibilities for LA, which rendered its fame as one of the top 12 building blocks derived from biomass.[22] Possible derivatives of LA are exemplified in Figure 2.

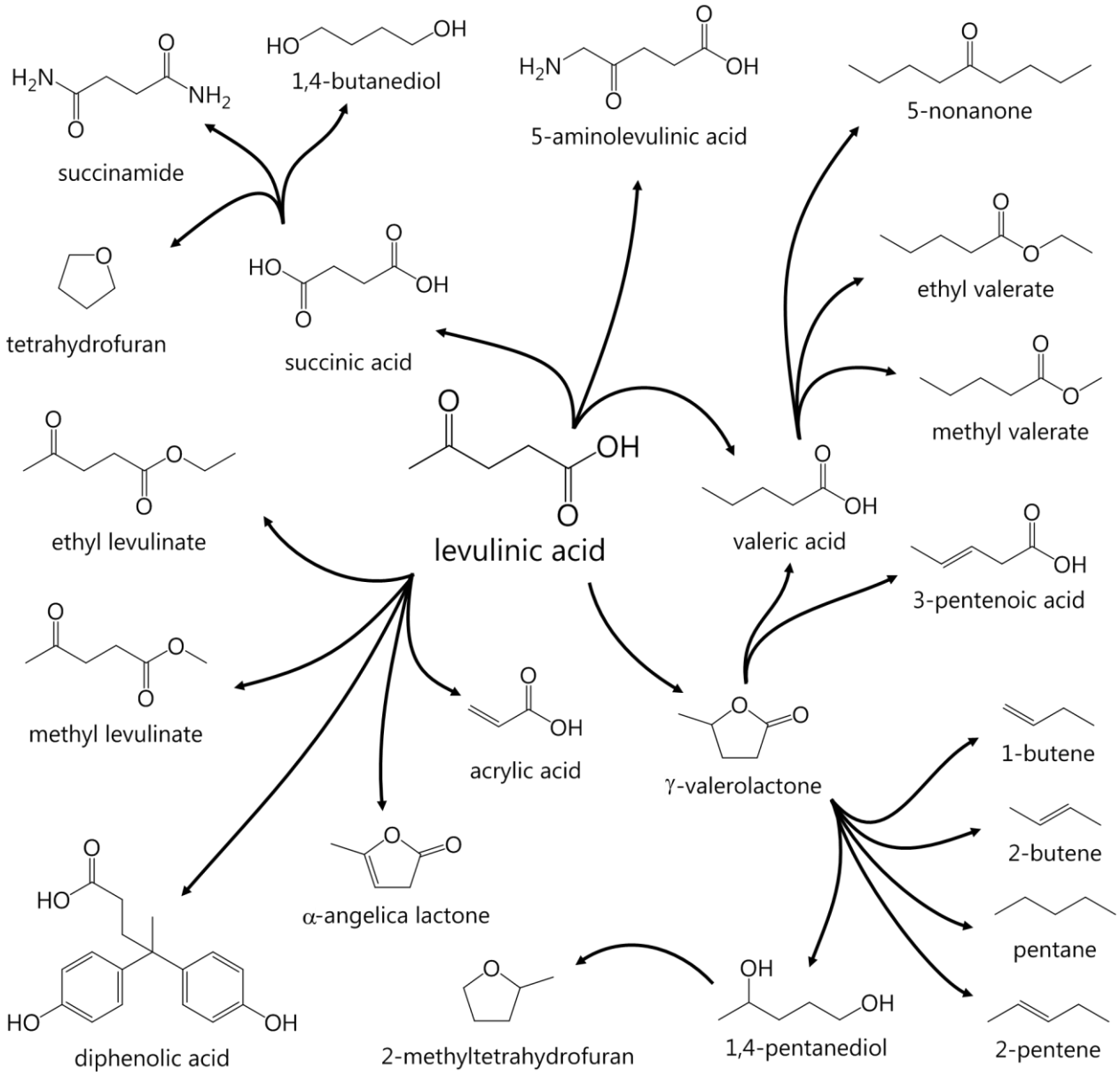


*Figure 2. Derivatives of LA.*[15,23–26]

Conversion of LA to these derivatives can be carried out via simple reactions that do not require expensive catalysts. For instance, single-step hydrogenation in the presence of a suitable catalyst, such as Cu,[27] can reduce the ketone group to an alcohol, which will react with the carboxylic acid in the other side of the carbon chain to yield γ-valerolactone (GVL).[28] Reduction followed by deoxygenation of the ketone group yields valeric acid, precursor of valerate biofuels.[25,26] Another simple reaction that can yield a whole family of LA derivatives is esterification with alcohols such as

methanol, ethanol, and butanol. Levulinate esters have applications as biofuel additives, and renewable routes to these alcohols are available either from renewable syngas or sugar fermentation.[15]

#### *2.1.5.1. The levulinate family derived from hemicelluloses*

Dehydration of sugars derived from xylan and arabinan yields FF. Though FF has a large market, the production capacity of a single plant of average capacity (50 kt/y) can cover more than 10% of the existing market.[17] Consequently, alternative applications for FF need to be developed, since its production cannot be dissociated from the production of LA. FF itself cannot be used as fuel as it is very unstable. Chemical upgrade of FF via hydrogenation can lead to 2-methyltetrahydrofuran (MTHF), which can be blended into gasoline, or LA and EL, as shown in Figure 3.

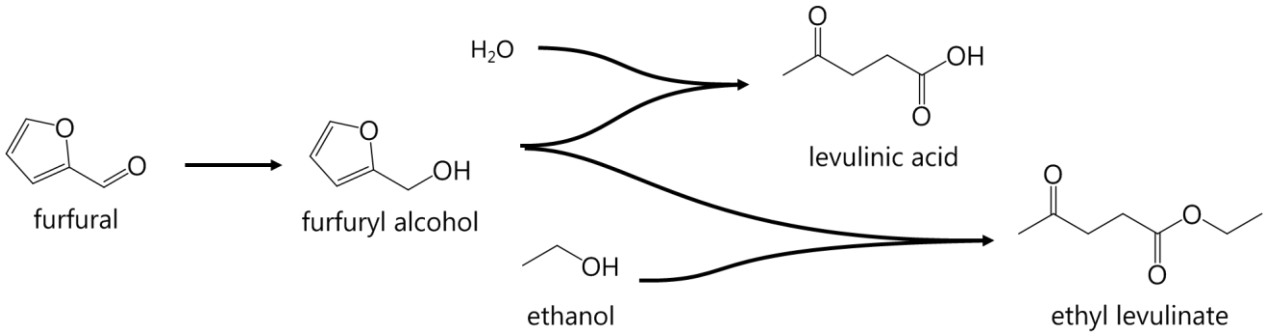


*Figure 3. LA and EL derived from FF.*[29]

### 2.1.6. Importance of ethyl levulinate

Levulinate esters such as methyl levulinate, EL, or butyl levulinate have been tested in diesel engines as additives.[30,31] Methanol, the precursor of methyl levulinate, is mainly produced from syngas, which in turn is typically obtained via steam reforming of natural gas and naphtha.[32] Also, methyl levulinate is highly polar, fully miscible in water, and separates from hydrocarbon fuels at low temperatures. Hence, levulinates of higher alcohols are desirable because they are less polar than methyl levulinate, providing a better blending option.[33] EL has the advantage that its production uses ethanol, which is traditionally produced from renewable resources. Butanol can also

be obtained from renewable resources.[16] Still, it has a higher cost than ethanol and methanol. Therefore, EL is the levulinate ester with the highest potential.

Use of biodiesel in cold environment has limitations because of the self-ignition requirement for fuel in diesel engines.[15] Historically, the self-ignition requirement has led refiners to produce diesel with different qualities according to region and season in which the fuel is commercialized.[34] These qualities, the so-called cold flow properties, represent fuel standards required for commercialization: cloud point, pour point, and cold filter plugging point.[35]

Biodiesel has worse cold flow properties than regular diesel.[35] Historically, this problem has been overcome by subjecting diesel (in which biodiesel will be blended) to a more onerous hydrotreating process. Blends of EL have been tested as an alternative solution to the problem. According to Joshi *et al.* (2011), the addition of 20 vol% EL in biodiesel from cottonseed oil and poultry fat reduced cloud point in 4-5 °C, pour point in 3-4 °C, and cold filter plugging point in 3 °C.[31] Tests for cold flow properties were run with regular diesel as well. Nevertheless, improvements were not as noticeable as with biodiesel.[36] Performance tests have shown that fuel blends using up to 5% EL and biodiesel have similar power and torque to an engine running with pure diesel. Brake specific fuel consumption and energy consumption were decreased with the fuel blends, suggesting improved combustion. Also, hydrocarbon and carbon monoxide emissions decreased significantly.[37]

Soot emission is strongly associated with aromatics content, and diesel hydrotreating is also the chemical process required to reduce aromatics content in diesel to meet regulations in determined jurisdictions.[34] Soot is related to incomplete combustion of fuel, which is a consequence of the diesel engine design: liquid fuel injection occurs when the piston reaches the end of the compression stroke, and combustion takes place immediately (Figure 4). Notice that, at this moment, oxygen and fuel are not well mixed, which leads to incomplete combustion (*i.e.,* soot formation). The presence of oxygen in biodiesel (10-12 wt%) and EL (33 wt%) provides better distribution of oxygen atoms throughout the fuel, thus reducing soot emissions.[15,38] Therefore, dilution of diesel using EL has the potential to decrease the requirement of a very intensive diesel hydrotreating process. A similar conclusion is valid for sulfur content because biodiesel and EL are free of sulfur and hydrotreating is also the key process for diesel desulfurization.

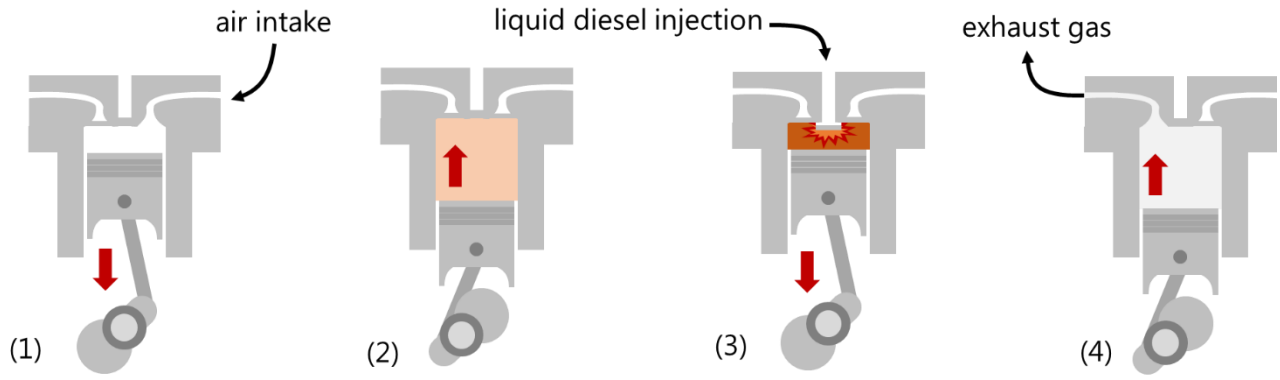


*Figure 4. Four stroke diesel engine cycle: (1) induction, (2) compression, (3) power, and (4) exhaust.*

While LE (24.34 MJ/kg) has about half of the lower heating value (LHV) of diesel (ultra-low-sulfur diesel, ULSD, 42.83 MJ/kg),[30] its density of 1016 kg/m$^3$ is higher, which helps to avoid a significant decrease in mileage[1].[15] For example, comparing ULSD and a blend of ULSD with 10% of EL by volume, the LHV in volumetric basis drops 3.0%, against a decrease of 4.3% when LHV is compared in mass basis.[30] The use of the energy density to determine a price for EL may render impractical commercialization because the price of the product may be too low for companies to turn a profit.[29] However, bearing in mind all of its benefits, pricing EL above the current energy price of ULSD may be acceptable, and may even occur naturally as a consequence of blending mandates.

## 2.2. Process simulation of ethyl levulinate production

In the process simulation of a biorefinery producing ethyl levulinate, a series of equations are solved to determine the concentrations of any species in equilibrium conditions by equating the fugacity $\hat{f}_i$ of each species in any phase of the mixture (I, II, III, and so on):

$$\hat{f}_i^I = \hat{f}_i^{II} = \hat{f}_i^{III} = \cdots \quad (1)$$

For the vapor phase, the fugacity is a function of the fugacity coefficient $\hat{\phi}_i$, temperature, and pressure:

$$\hat{f}_i^{vapor}(T,P) = y_i \hat{\phi}_i(T,P)P \quad (2)$$

[1] Mileage is defined as miles (or distance in other unit) travelled on a specific volume of fuel.

And in the liquid phase, fugacity is a function of the activity coefficient $\gamma_i$:

$$\hat{f}_i^{liquid}(T,P) = \gamma_i x_i \phi_i^{sat}\left(T, P_i^{sat}\right) P_i^{sat} \exp\left(\frac{V_i\left(P - P_i^{sat}\right)}{RT}\right) \quad (3)$$

#### *2.2.1.1. Modeling of vapor and gas phase*

Substances such as carboxylic acids strongly associate in the vapor phase, in a phenomenon described by Nothnagel *et al*. (1973) as Chemical Theory of Vapor Imperfection.[39] According to this theory, an association of molecules in the vapor phase leads to a molar volume which is less than the corresponding volume of an ideal gas under the same conditions (negative deviation):

$$i + j \leftrightarrow ij \quad (4)$$

Such behavior is proven to occur in systems with molecules such as acetic acid (AA), which present strong intermolecular hydrogen bonding, and occurs even instantly in systems with molecules less prone to interaction, such as argon. In these systems, modeling must account for this deviation considering the actual number of species to correctly correlate pressure, volume, and temperature. Examples of equations of state that model this behavior include Nothnagel, Abrams, and Prausnitz (1973),[39] and Hayden and O'Connell (1975)[40]. Among these examples, the Hayden-O'Connel equation of state, a variation of the virial equation of state, was chosen because it is recommended for low up to medium pressures (up to 15 bar).[41] In the simulated process, only one equipment operates at a pressure higher than 15 bar, though at subcooled liquid conditions.

For a given set of pressure $P$ and temperature $T$, the compressibility factor $Z$ is given by the Hayden-O'Connell equation as follows:[40,41]

$$Z = 1 + \frac{BP}{RT} \quad (5)$$

$B$, the second virial coefficient which characterizes pair interactions between molecules $i$ and $j$, can be described as a function of molar fractions $y_i$ and $y_j$ and the sum of several temperature-dependent contributions from molecular configurations: free pair, metastably bound, and bound.[42] The Hayden-O'Connell equation of state considers that the bound contribution in chemically bonding species can be broken into two different contributions: bound and chemical.[41]

$$B = \sum_i \sum_j y_i y_j B_{ij}(T) \tag{6}$$

$$B_{ij} = \left(B_{free-nonpolar}\right)_{ij} + \left(B_{free-polar}\right)_{ij} + (B_{metastable})_{ij} + (B_{bound})_{ij} + (B_{chem})_{ij} \tag{7}$$

For nonpolar, non-associating species:

$$B_{free-nonpolar} = f_1(\sigma_{np}, \varepsilon_{np}, \omega_{np}, T) \tag{8}$$

$$\sigma_{np} = g_1\left(\omega_{np}, T_c, P_c\right) \tag{9}$$

$$\varepsilon_{np} = g_2\left(\omega_{np}, T_c\right) \tag{10}$$

$$\omega_{np} = f_2\left(r_{gyr}\right) \tag{11}$$

For polar (dipole moment $\mu$ > 1.45 D), associating species:

$$B_{free-polar} = f_3(\sigma_{fp}, \varepsilon_{fp}, \omega_{np}, T) \tag{12}$$

$$\sigma_{fp} = g_3\left(\sigma_{np}, \omega_{np}, \xi\right) \tag{13}$$

$$\varepsilon_{fp} = g_4\left(\varepsilon_{np}, \omega_{np}, \xi\right) \tag{14}$$

$$\xi = g_5\left(\sigma_{np}, \varepsilon_{np}, \omega_{np}, p, T\right) \tag{15}$$

For chemically bonding species:

$$B_{metastable} + B_{bound} + B_{chem} = f_4(\sigma_c, \varepsilon_c, P, T) \tag{16}$$

$$B_{chem} = f_5(\sigma_c, \varepsilon_c, \eta, T) \tag{17}$$

$$\sigma_c = g_3\left(\sigma_{np}, \omega_{np}, \xi\ \right) \tag{18}$$

$$\varepsilon_c = g_6\left(\varepsilon_{np}, \omega_{np}, \xi, \eta\right) \tag{19}$$

The following mixing rules are applied:

$$\varepsilon = 0.7\left(\varepsilon_i \varepsilon_j\right)^{1/2} + 0.6\left(\frac{1}{\varepsilon_i} + \frac{1}{\varepsilon_j}\right) \tag{20}$$

$$\sigma = \left(\sigma_i \sigma_j\right)^{1/2} \tag{21}$$

$$\omega_{np} = (\omega_{n,pi} + \omega_{n,pj})/2 \tag{22}$$

$$P = \left(P_i P_j\right)^{1/2} \tag{23}$$

And the fugacity coefficient of a component $i$ in a mixture of $N$ components is given by:

$$\ln(\hat{\phi}_i) = \left(2\sum_{j=1}^{N} y_i B_{ij} - B\right)\frac{P}{RT} \quad (24)$$

Sections of the biorefinery that do not handle carboxylic acids and require a different modeling approach include: sugarcane separation in juice and bagasse, sugarcane juice treatment and conditioning, fermentation of sugarcane juice to ethanol, ethanol recovery, biomass furnace, steam generation system, and cooling water system. Separation of sugarcane and fermentation of sugarcane juice to ethanol was not simulated step-by-step, as explained in chapter 4. As for the utility systems, the steam tables from the IAPWS (The International Association for the Properties of Water and Steam) 1995 formation were used, because this implementation of steam table is the most accurate available in Aspen Plus 8.6.[43] Lastly, gases in the biomass furnace were modeled using the Peng-Robinson equation of state with the Boston-Mathias modification for the alpha function and standard mixing rules.[41,44] The Boston-Mathias modification for the alpha function improves predictability for $T \geq T_{c,i}$:

$$\alpha_i(T) = \left(\exp\left(c_i\left(1 - T_{r,i}^{d_i}\right)\right)\right)^2, for\ T > T_{c,i} \quad (25)$$

$$d_i = 1 + \kappa_i/2 \quad (26)$$

$$c_i = 1 - 1/d_i \quad (27)$$

$$\kappa_i = 0.37464 + 154226\omega_i - 0.26992\omega_i^2 \quad (28)$$

For $T < T_{c,i}$, the standard alpha function is used:[45]

$$\alpha_i = \left(1 + \kappa_i\left(1 - T_{r,i}^{1/2}\right)\right)^2 \quad (29)$$

The required parameters for these calculations, ($T_c$ , $P_c$, $\omega$, etc.), are available in databanks, such from PURE32 databank from Aspen Plus.[46]

#### *2.2.1.2. Modeling of liquid phase*

Activity coefficients of components in the liquid phase were estimated using the NRTL (nonrandom, two-liquid) model. The NRTL model was used because it demonstrates better agreement with data for the class of components included in the simulation of this biorefinery.[47] In this model, the activity coefficient of a component *i* in a mixture is calculated as follows: [48]

$$\ln(\gamma_i) = \frac{\sum_j x_j \tau_j G_{ji}}{\sum_k x_k G_{ki}} + \sum_j \left( \frac{x_j G_{ij}}{\sum_k x_k G_{kj}} \right) \left( \tau_{ij} - \frac{\sum_m x_m \tau_{mj} G_{mj}}{\sum_j x_k G_{kj}} \right) \quad (30)$$

where:

$$G_{ij} = \exp(-a_{ij}\tau_{ij}) \quad (31)$$

$$\tau_{ij} = a_{ij} + \frac{b_{ij}}{T} + e_{ij}\ln(T) + f_{ij}T \quad (32)$$

$$\alpha = c_{ij} + d_{ij}(T - 273.15\ K) \quad (33)$$

and $\tau_{ii} = 0$, $G_{ii} = 1$, and $a_{ij}, b_{ij}, e_{ij}$, and $f_{ij}$ are unsymmetrical. For most of the components considered in the simulation, only binary interaction parameters $a_{ij}$, $a_{ji}$, $b_{ij}$, and $b_{ji}$ combined with $c_{ij}$ were enough to describe the non-ideal behavior of mixtures. Values for each of these parameters can be obtained via regression of experimental data, and the NRTL model has the capability to model multicomponent systems using only binary data.[47]

## 2.3. Process optimization

A generalized study of several routes to EL demonstrated that for any specific biomass feedstock, operating parameters such as biomass to solvent ratio, number of reaction stages, and conversion of cellulose and hemicelluloses play a vital role in the economics of the process.[15]

Optimizing the production cost of EL includes other variables, such as feedstock (biomass and ethanol) cost, electricity price, and capital, just to mention a few. Consequently, coupling the optimization of EL production cost to the simulation of a complete biorefinery may develop into a very onerous computational task. In this work, this whole process was simplified by fixing a few conditions and using an appropriate sampling method to establish a simplified mathematical model of the biorefinery. This simplified model will provide the basis for process optimization.

### 2.3.1. Surrogate model and design of experiments

Surrogate models are employed when an outcome of an experiment cannot be easily directly measured. Such model mimics the behavior of the complex simulation model while being computationally cheaper to evaluate. Surrogate models are proven to be very useful for optimization, design space exploration, prototyping, and sensitivity analysis.[49]

Consider a problem with $m$ variables whose response is obtained by an unknown or very complicated function y: $\mathbb{R}^m \rightarrow \mathbb{R}$. Running this function over a space of $n$ sites corresponds to a matrix $\boldsymbol{S}$ of $m \times n$ dimensions and results in a vector $\boldsymbol{y_s}$ of $n$ responses:

$$\boldsymbol{S} = \left[\boldsymbol{x^{(1)}}, \boldsymbol{x^{(2)}}, \dots, \boldsymbol{x^{(n)}}\right]^T \in \mathbb{R}^{m \times n} \tag{34}$$

$$\boldsymbol{x} = \{x_1, x_2, \dots, x_m\} \in \mathbb{R}^m \tag{35}$$

$$\boldsymbol{y_S} = \left[y^{(1)}, y^{(2)}, \dots, y^{(n)}\right]^T = \left[y(\boldsymbol{x^{(1)}}), y(\boldsymbol{x^{(2)}}), \dots, y(\boldsymbol{x^{(n)}})\right]^T \in \mathbb{R}^n \tag{36}$$

The sampled data ($\boldsymbol{S}$, $\boldsymbol{y_S}$) can be fitted to any desirable equation. In the Response Surface Methodology, this data set can be fitted to a quadratic model which yields the predicted variable $\hat{y}$ and provides a great compromise between accuracy and computational expense:[50]

$$\hat{y}\,(\boldsymbol{x}) = A_0 + \sum_{i=1}^{m} B_i x_i + \sum_{i=1}^{m} C_{ii} x_i^2 + \sum_{i=1}^{m} \sum_{j \geq i}^{m} D_{ij} x_i x_j \tag{37}$$

where $A_0$ is a constant, $\boldsymbol{B}$ is the vector of linear coefficients, $\boldsymbol{C}$ is the vector of quadratic coefficients, and $\boldsymbol{D}$ is the vector of quadratic interaction coefficients, all to be determined. This equation has:

$$1 + m + m + \binom{m}{2} = 1 + 2m + \frac{m!}{2!\,(m-2)!} = 1 + 2m + \frac{m \times (m-1) \times \cancel{(m-2)!}}{2\cancel{(m-2)!}} \tag{38}$$
$$= \frac{m^2 + 3m + 2}{2}$$

parameters to be determined via regression. Therefore, the least number of $n$ cases required is:

$$n \geq \frac{m^2 + 3m + 2}{2} \tag{39}$$

Appropriate sampling inside the design space is critical to obtain a surrogate model that safely predicts the values of the response. Sampling is usually done via Design of Experiments (DOE) methods, such as the Central Composite Design (CCD).

# 3. Methodology

The study of optimized operating conditions via process simulation requires a careful definition of the applied methodology, along with details that are fundamental to ensure that the process simulation mimics the real process. This section provides the theoretical background and the methods used in the execution of this work.

## 3.1. Optimization variables and design of experiments

In the production of EL, four variables were chosen: solids loading[2] (SL, $x_1$), cellulose conversion[3] (CC, $x_2$), catalyst loading[4] (CL, $x_3$), and the second reactor temperature[5] (RT, $x_4$). Conditions of the first reactor were based on the Rosenlew process (see section 4.2).[20] In a fully orthogonal and rotational CCD, star points are defined to allow for estimation of curvature. In the case of a CCD with 4 variables, such star points are in a distance of $(2^4)^{1/4} = 2$ from the center point of the design.[51] Upper and lower limits on the design space were chosen based on previous literature

[2] Solids loading (SL) is defined in this work as the mass of dry biomass added with respect to the total feed (biomass, water, moisture, catalyst, and impurities) in mass basis.
[3] Cellulose conversion (CC) in the second reactor in molar basis.
[4] Catalyst loading (CL) is defined as mass of catalyst (sulfuric acid) with respect to the total feed in mass basis.
[5] Temperature of reactor (RT) feed. No additional heat is provided inside the reactor.

on the subject to correctly cover an adequate range of values for the process in question.[15,52,53] Table 1 presents a summary of the final design space used in the development of this work.

*Table 1. The final design space, with the lower and upper limits of the four variables.*

| Code | $-2$ | $-1$ | $0$ | $+1$ | $+2$ |
|---|---|---|---|---|---|
| SL | 4% | 8% | 12% | 16% | 20% |
| CC | 55% | 66% | 77% | 88% | 99% |
| CL | 1% | 2% | 3% | 4% | 5% |
| RT (°C) | 150.0 | 162.5 | 175.0 | 187.5 | 200.0 |

Most of the works on LA production focuses on SL values around 10%.[15] However, other works focused on the production of other lignocellulosic biofuels consider higher values (>18%), even though conversion is noticed to decrease.[54,55] This factor motivated the use of a wide range of values for SL. The same is true for CC: cellulose requires severe conditions to be hydrolyzed, but this may compromise LA yield, as the reaction of cellulose to LA, final product, requires an increase in the concentration of a furan intermediate which is very prone to polymerization and humins formation.[15] CL is limited to about 5% because results from the literature show that increasing the CL from 4% to 6% does not lead to great improvements in conversion.[56] Moreover, the kinetic model used to simulate the process covers a range of 0.11-0.55 mol/L of sulfuric acid, which roughly equates 1-5 wt%.[57] The second reactor, which focuses on cellulose conversion, has the inlet temperature (RT) range set according to patents of the Biofine process and the limitations of a kinetic model for cellulose conversion (150-200 °C).[52,53,57] The total number of cases necessary to run a CCD with four variables is 25 ($2^4$ fractional factorial points, $2 \times 4$ star points, and 1 central point – there is no sense in random experimental error in simulation experiments). Sample points were chosen using the software Statistica 13.3 (TIBCO Software Inc., 2017).

## 3.2. Biorefinery simulation

The biorefinery was simulated using the software Aspen Plus 8.6 (AspenTech, Inc., 2014)

with all biorefinery sections operating continuously – no batch processes were included in the process simulation. The following subsections of section 3.2 present parameters pertaining to the methodology to simulate the biorefinery process, whose design is presented in chapter 4.

### 3.2.1. Components

The following components were added to the simulation with data from Aspen Plus databank PURE32: water, sulfuric acid, glucose, xylose, ethanol, formic acid (FA), AA, LA, FF, MTHF, HMF, EL, potassium oxide, carbon dioxide, oxygen, and nitrogen. Additional properties of MTHF and HMF were retrieved from the National Institute of Standards and Technology database.[58] Other components were added to represent biomass: hemicelluloses, cellulose, lignin, and acetyl groups[6]. Acetyl groups were added as "acetic acid" and modified to solid according to the methodology applied by other authors in the field of simulation of biorefineries using sugarcane bagasse as feedstock.[59] Others components of biomass were added manually, with data available in Table 2.

*Table 2. User-defined entries for manually added components.*[59,60]

| Property | Entry in Aspen | Cellulose | Hemicelluloses | Lignin |
|---|---|---|---|---|
| Molecular weight (g/mol) | USERDEF/MW | 162.144 | 132.117 | 194.197 |
| Formula | - | $C_6H_{10}O_5$ | $C_5H_8O_4$ | $C_{10}H_{11.6}O_{3.9}$ |
| $\Delta H_{form,s}\ (kJ/mol)$ | USERDEF/DHSFM | -976.362 | -762.416 | -349.70 |
| Molar volume ($m^3$/mol) | VSPOLY-1/1 | 0.106 | 0.0864 | 0.0817 |
| $C_{p,s}$ (J/kmol.K)[a] | $C_1$, CPSPO1-1/1[a] | -11704 | -9536.3 | 31431.7 |
| | $C_2$, CPSPO1-1/2[a] | 672.07 | 547.62 | 394.427 |
| | $C_7$, CPSPO1-1/7[a] | 298.15 | 298.15 | 298.15 |
| | $C_8$, CPSPO1-1/8[a] | 1000.0 | 1000.0 | 1000.0 |

a) Coefficients of solid heat capacity equation: $C_{p,s} = C_1 + C_2 \times T$, for $C_7 \leq T \leq C_8$

[6] Bagasse's hemicelluloses are a series of polymers (xylan, arabinan, etc.) with acetyl groups.

### 3.2.2. Thermodynamic data

In the simulations, all possible interactions between molecules included in the sections handling carboxylic acids must be taken into account to properly model the vapor phase of the system using the Hayden-O'Connell equation of state. Considering only the species occurring in the presence of carboxylic acids (FA, AA, and LA), Table 3 presents a summary of all $\eta$ association/solvation parameters for pure/unlike interactions used in process simulation, along with their respective references. Other parameters used in the calculations with the Hayden-O'Connell equation are available in Table 4.

*Table 3. Hayden-O'Connell η association/solvation parameters for pure/unlike interactions used in process simulation. Data retrieved from Aspen Plus PURE32 databank,[46] unless otherwise stated.*

| | AA | ethanol | EL | FA | FF | HMF | LA | MTHF | water |
|---|---|---|---|---|---|---|---|---|---|
| AA | 4.5 | 2.5 | 2.0[b] | 4.5 | 0.8 | 0.8[d] | 4.5[b] | 1.2[c] | 2.5 |
| ethanol | 2.5 | 1.4 | 1.3[a] | 2.5 | 0.8 | 0.8[d] | 2,5[a] | 0.5[c] | 1.55 |
| EL | 2.0[b] | 1.3[a] | 0.53 | 2.0[b] | 0.75[b] | 0.75[d] | 2.0[a] | 0.4[c] | 1.3[a] |
| FA | 4.5 | 2.5 | 2.0[b] | 4.5 | 1.6 | 1.6[d] | 4.5[b] | 1.2[c] | 2.5 |
| FF | 1.6 | 0.8 | 0.75[b] | 1.6 | 0.58 | 0.58[d] | 1.6[b] | 0.4[c] | 0.8 |
| HMF | 1.6[d] | 0.8[d] | 0.75[d] | 1.6[d] | 0.58[d] | 0.58[d] | 1.6[d] | 0.4[d] | 0.8[d] |
| LA | 4.5[b] | 2.5[a] | 2.0[a] | 4.5[b] | 1.6[b] | 1.6[d] | 4.5[a] | 1.2[c] | 2.5[a] |
| MTHF | 1.2[c] | 0.5[c] | 0.4[c] | 1.2[c] | 0.4[c] | 0.4[d] | 1.2[c] | 0.4[c] | 0.5[c] |
| water | 2.5 | 1.55 | 1.3[a] | 2.5 | 0.8 | 0.8[d] | 2.5[a] | 0.5[c] | 1.7 |

a) Resk *et al.*, (2014)[61]

b) LA and EL interaction parameters were assumed to be the same as those of AA and ethyl acetate.

c) MTHF interaction parameters were assumed to be the same as those of tetrahydrofuran, and they were obtained from Aspen Plus PURE32 databank, except the interaction parameters with EL and itself, which were assumed to be 0.4 – very low for unlike interaction because of the functional groups of these molecules.

d) HMF interaction parameters were the same as FF.

*Table 4. Critical temperature ($T_c$), critical pressure ($P_c$), radius of gyration ($r_{gyr}$), and molecular dipole moment ($\mu$) of species in presence of carboxylic acids in the process simulation. All data retrieved from Aspen Plus PURE32 databank.*[46]

| | $T_c$ (°C) | $P_c$ (bar) | $r_{gyr}$ (Å) | $\mu$ (D) |
|---|---|---|---|---|
| AA | 318.80 | 57.86 | 2.610 | 1.73880 |
| EL | 392.95 | 29.24 | 4.827 | 1.26812 |
| EtOH | 240.85 | 61.37 | 2.259 | 1.69083 |
| FA | 314.85 | 58.10 | 1.847 | 1.41502 |
| FF | 397.00 | 56.60 | 3.350 | 3.59750 |
| HMF | 521.75 | 49.50 | 3.966 | 4.73674 |
| LA | 464.85 | 40.20 | 3.675 | 1.33708 |
| MTHF | 263.85 | 37.58 | 3.149 | 1.37998 |
| water | 373.95 | 220.64 | 0.615 | 1.84972 |

Other parameters used in the simulation of the sections using the Peng-Robinson equation of state with the Boston-Mathias modification of the alpha function were obtained from Aspen Plus databank PURE32.[46]

Table 5 summarizes the parameters used in the modeling of the liquid phase in the simulation using the NRTL activity coefficient model. In Table 5, entries 15 to 20 refer to parameters regressed from liquid-liquid equilibria (LLE) data obtained as part of this project. Details regarding methodology and equilibrium data are available in Appendix 1. Regarding the rest of binary interaction parameters, 10 entries were available in Aspen Plus databank PURE32, 5 entries were obtained from Resk *et al.* (2014),[61] 1 entry was obtained from Glass *et al.* (2017),[62] and the rest, corresponding to trace components and solute-solute interactions, was obtained via regression of LLE data estimated via group contribution method UNIFAC (universal quasichemical functional group activity coefficient model). All other thermodynamic parameters, such as coefficients for vapor pressure equation, coefficients of a heat capacity equation, transport properties, etc., were available in Aspen Plus databank PURE32.[46]

*Table 5. Summary of NRTL parameters used in process simulation.*

| $i$ | $j$ | $a_{ij}$ | $a_{ji}$ | $b_{ij}$ | $b_{ji}$ | $c_{ij}$ | $e_{ij}$ | $e_{ji}$ | $T_{min}$ (°C) | $T_{max}$ (°C) | Source |
|---|---|---|---|---|---|---|---|---|---|---|---|
| water | FF | 4.2362 | -4.7563 | -262.241 | 1911.42 | 0.3 | 0 | 0 | 58.2 | 161.7 | [46] |
| water | ethanol | 3.7555 | -0.9852 | -676.031 | 302.237 | 0.3 | 0 | 0 | 24.99 | 100 | [46] |
| water | FA | -2.5864 | 4.5156 | 725.017 | -1432.08 | 0.3 | 0 | 0 | 30 | 108 | [46] |
| water | AA | 3.3293 | -1.9763 | -723.888 | 609.889 | 0.3 | 0 | 0 | 20 | 229.75 | [46] |
| ethanol | AA | 0 | 0 | 225.476 | -252.482 | 0.3 | 0 | 0 | 35 | 115.8 | [46] |
| ethanol | FF | 0 | 0 | 73.3963 | 400.329 | 0.3 | 0 | 0 | 50 | 134 | [46] |
| FA | AA | 0 | 0 | 147.166 | -85.737 | 0.3 | 0 | 0 | 100.11 | 118.1 | [46] |
| FA | FF | 0 | 0 | 46.1655 | 289.216 | 0.3 | 0 | 0 | 100.7 | 161.7 | [46] |
| water | EL | 0 | 0 | 1014.969 | 64.60453 | 0.285 | 0 | 0 | 60[a] | 60[a] | [61] |
| LA | water | 0 | 0 | -342.585 | 880.5534 | 0.3 | 0 | 0 | 60[a] | 60[a] | [61] |
| ethanol | EL | 0 | 0 | 398.2682 | -74.662 | 0.3 | 0 | 0 | 60[a] | 60[a] | [61] |
| ethanol | LA | 0 | 0 | 585.396 | -376.308 | 0.3 | 0 | 0 | 60[a] | 60[a] | [61] |
| EL | LA | 0 | 0 | -285.428 | 336.234 | 0.3 | 0 | 0 | 60[a] | 60[a] | [61] |
| MTHF | water | -31.4449 | 142.132 | 1079.95 | -7712.72 | 0.405204 | 5.26904 | -19.8342 | 20 | 150 | [62] |
| FA | MTHF | 118.699 | 156.778 | -6321.66 | -8488.86 | 0.23123 | -17.0751 | -22.9672 | 6.85 | 66.85 | b |
| AA | MTHF | 643.401 | -618.802 | -34184.7 | 31978.9 | 0.01 | -93.0245 | 89.8341 | 6.85 | 66.85 | b |

*Table 3 (continued). Summary of NRTL parameters used in the process simulation.*

| $i$ | $j$ | $a_{ij}$ | $a_{ji}$ | $b_{ij}$ | $b_{ji}$ | $c_{ij}$ | $e_{ij}$ | $e_{ji}$ | $T_{min}$ (°C) | $T_{max}$ (°C) | Source |
|---|---|---|---|---|---|---|---|---|---|---|---|
| LA | MTHF | 917.977 | -1174.83 | -34035.4 | 47678.6 | 0.01 | -138.935 | 176.219 | 6.85 | 66.85 | b |
| FF | MTHF | -386.308 | -274.459 | 1147.47 | 29859.9 | 0.01 | 65.7725 | 32.1125 | 6.85 | 66.85 | b |
| water | $H_2SO_4$ | 12.4727 | -6.56916 | -1774.97 | 1222.7 | 0.3 | 0 | 0 | 6.85 | 66.85 | b |
| $H_2SO_4$ | MTHF | 14.0709 | 6.81485 | -3698.01 | 856.035 | 0.2 | 0 | 0 | 6.85 | 66.85 | b |
| FA | LA | 0 | 0 | -113.862 | 30.1136 | 0.3 | 0 | 0 | 0 | 200 | c |
| AA | FF | 0.476171 | 0.22581 | 1.15093 | 0.126298 | 0.5 | 0 | 0 | 95.97 | 149.18 | [46] |
| ethanol | MTHF | 0.222861 | 0.642818 | 0 | 0 | 0.484069 | 0 | 0 | 45 | 45 | [46] |
| AA | LA | 0 | 0 | -23.3344 | 38.3675 | 0.3 | 0 | 0 | 0 | 200 | c |
| LA | FF | 0 | 0 | 221.62 | -425.576 | 0.3 | 0 | 0 | 0 | 200 | c |

a) Equilibrium data (P-x) was determined in isothermal conditions (60 °C), and the model obtained through fitting of P-x data agrees with experimental T-x data over the range 11-39 °C.[61]

b) Based on the regression of experimental data obtained as part of this Masters' project. The manuscript of this work is available in Appendix 2 and will be submitted in due time.

c) Parameters were estimated using the UNIFAC group contribution method.

## 3.3. Technoeconomic analysis

### 3.3.1. Capital expenditures

The biorefinery was treated as a greenfield project. Capital expenditures (CAPEX) for sugarcane juice extraction, treatment, ethanol fermentation and recovery, and the cogeneration of heat and power facility using biomass as fuel were based on data from the Virtual Sugarcane Biorefinery of the Brazilian Bioethanol Science and Technology Laboratory (CTBE/CNPEM).[63] Data were available for 2014 and were updated to December 2017 using the IGP-M (General Index for Market Prices – specific for the Brazilian market).[64] It was assumed that the biomass furnace could handle the lignocellulosic residue of hydrolysis without any sort of special design that would increase its capital cost. CAPEX for the esterification of LA to EL was based on data from Novita *et al*. (2017).[65] CAPEX for the other sections was calculated using the software CAPCOST with the CEPCI (Chemical Engineering Plant Cost Index) of December 2017.[66,67] Distillations columns, reactors, and heat exchangers were dimensioned using Aspen Plus 8.6. Other equipment such as solids separators were dimensioned using appropriate literature guidelines.[68]

The sections of the biorefinery dedicated to biomass hydrolysis and its products handle acid streams in several classes of acid strength. As a result, different materials of construction were considered based on recommendations from the literature.[67,69] This factor has a heavy impact on capital expenditure, as most materials of construction were nickel-containing stainless steel alloys to withstand corrosion due to acid attack at high temperature or mechanical wear because of contact with solid particles. [70–72]

### 3.3.2. Operational expenditures and revenue

Prices of diesel, ethanol, FA, electricity, FF, and sulfuric acid were obtained for each month from 2013 to 2017. The values were updated using inflation to December 2017 and converted to United States dollars using an exchange rate of R$ 3.3074 = $1.00 (Table 6).[73] The series of values was used to calculate the average value and the standard deviation to be used in risk analysis. Sugarcane stalks and straw prices are updates of values estimated by other authors.[6,64]

*Table 6. Prices used in economic analysis.*

| Parameter | Average value | Standard deviation or limits of a triangular distribution |
|---|---|---|
| Sugarcane stalks ($/t)[6] | 22.27 | ±15%[a] |
| Sugarcane straw ($/t)[6] | 25.04 | ±15%[a] |
| Sulfuric acid ($/t)[74] | 28.56 | 14.57 |
| Inputs for ethanol production ($/$t_{cane}$)[75] | 0.7093 | ±15%[a] |
| MTHF ($/t)[29] | 853.5 | 149.9[b] |
| Ethanol ($/t)[76] | 661.7 | 69.35 |
| FF, current market price ($/t)[74] | 1824 | 320.4 |
| FF, as precursor of biofuels ($/t)[29] | 405.3 | 71.2[b] |
| FA, 50 wt% in water ($/t)[74] | 239.0[c] | 49.72[c] |
| Electricity ($/MWh)[77] | 57.03 | 16.53 |
| Diesel, ULSD ($/$m^3$)[78] | 607.4 | 16.75 |

a) a triangular distribution of probability with limits relative to the average price was used.

b) standard deviation is 18% of the average price, based on what is observed in the FF price series.

c) 60% off current pure FA price as a result of dilution.

The price of FF is a matter of discussion in the field of biofuels. The average price considering the last five years (2013-2017) is $1824/t (Table 6). This price is a consequence of the production by small facilities. Large-scale production of FF integrated to a sugarcane mill can produce FF at prices as low as R$600/t (2014),[79] which roughly equates to $215/t. This potential for low-price FF is an interesting observation because if large biorefineries start to focus on the production of LA to use it as fuel precursor, FF production will easily surpass market demand. For instance, one single FF plant integrated to a sugarcane mill processing 4 million tonnes of sugarcane per year can produce almost 50 kt/y of FF, and the market projection for FF in 2020 is 600 kt/y.[79] One of the options for furfural is the chemical upgrade to other chemicals. Still, other markets may become saturated with the additional production of typical FF derivatives such as furfuryl alcohol.

Therefore, another option would be to determine a selling price for FF to be used as a fuel precursor. As shown in Figure 3, FF can be used as an EL precursor to be blended with diesel. On the other hand, FF can be upgraded into MTHF to be blended with regular gasoline (Figure 5).[15]

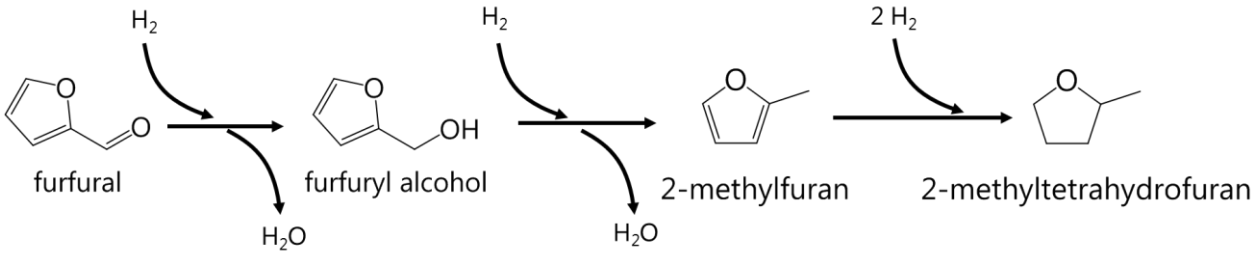


*Figure 5. Hydrogenation steps involved in the conversion of FF to MTHF.*

The maximum FF price to allow profitable conversion to MTHF or EL was determined in another step of this master's project, considering four possible markets (Brazil, China, European Union, and the United States) and three process options (two for MTHF and one for EL). In Brazil, which is the location of the biorefinery proposed in this work, FF maximum price should be $405/t in the best scenario, which considers the conversion of FF to MTHF in a two-step hydrogenation process using steam reforming of natural gas as a hydrogen source.[29] This value is higher than the minimum price required to make the conversion of biomass to FF profitable,[79] even though it represents only 22% of the current price. Consequently, this value was used to determine the revenues with FF in the biorefinery proposed in this work. The standard deviation used in risk analysis was the same as the current price relative to the average value.

Table 7 presents other parameters influencing operational expenditures (OPEX). Most values were based on others economic analyses of sugarcane mill projects.[75] The maintenance cost was set at 5%, higher than the 3% value that is commonly used for the sector because of the high risk of wear in equipment handling hydrolysis of biomass.

*Table 7. Parameters used in the cash flow analysis.*

| Parameter | Value |
|---|---|
| Working capital (% CAPEX) | 10% |
| Project lifespan (y) | 20 |
| Scrap value | 0 |
| Workers | 269[80] |
| Labor cost ($/mo) | 1301.27[81] |
| Maintenance (% CAPEX) | 5% |
| Income tax | 34%[82] |
| Depreciation, linear | 10% |
| Depreciation period (y) | 10 |

Results of each of the 25 simulated scenarios were used in the cash flow analysis to determine the MSP of EL: the price of EL was varied to achieve an internal rate of return (IRR) of 12% in any project. This value of IRR is commonly accepted as a minimum attractive rate of return for sugarcane mill projects in Brazil.[75]

## 3.4. Optimization and risk analysis

The list of values of MSP obtained via cashflow analysis for each case of the DOE was used to determine the optimized design of the biorefinery. The set of data including operating conditions and their resulting MSP were used to obtain a surrogate model, as described in Figure 6. In the situation in which the results of the surrogate model were inconclusive, the design space was changed according to technical limitations, such as availability of data or models used in the simulation of the process. With an adequate surrogate model, optimized conditions were obtained via gradient-based optimization, using the model's extreme values as lower and upper bounds. Last, the resulting optimized operating conditions were simulated to determine the MSP in optimized conditions, and the result was compared to the value predicted by the surrogate model.

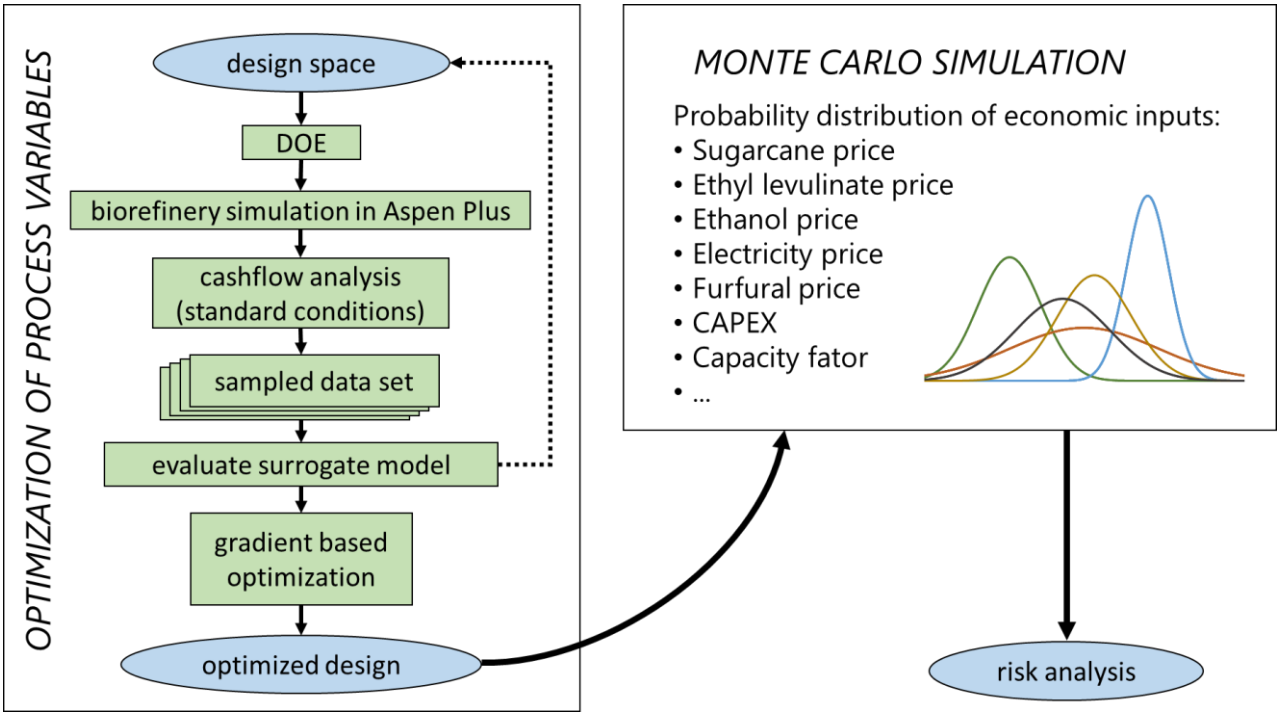


*Figure 6. Methodology of technoeconomic and risk analysis for the biorefinery.*

With the improved design of the biorefinery available, four scenarios were considered to discuss the implications of market conditions on the viability of EL production:

- EL-t: an optimized biorefinery for production of EL, whose conditions were developed in this work. The letter "t" stands for today, which means that the current FF price was used. As a consequence, the MTHF price was based on the current FF price. EL price was based on diesel price (Table 6).
- EL-f: the same biorefinery as in the previous scenario, but with FF price based on future (letter "f") perspectives of price reduction to use FF as a precursor to biofuels (MTHF).
- EL-p: same as the previous scenario, but a premium (letter "p") of 20% is paid over the price of FF and EL because either they come from renewable resources or because they present fuel additive properties.
- ET-t: an optimized autonomous ethanol distillery in which all sugarcane juice is fermented to ethanol and all bagasse is used for electricity production.[6]

Besides the simple comparison of economic indicators between scenarios, economic aspects were further analyzed using Monte Carlo simulation. Monte Carlo simulation helps to identify the most critical economic variables that may compromise the profitability and economic security of the biorefinery project.

In the cases in which a data series was available, a normal probability distribution of prices was assumed (Table 6). When a data series was unavailable, as in the case of sugarcane stalks and straw, a triangular probability distribution was used with limits defined as ±15% of average value. Capacity factor was included as one of the variables, with a triangular distribution of ±10%, to represent the effects of severe droughts on the yield of sugarcane per area harvested and the change of climatic conditions as well. CAPEX was considered to vary with a triangular distribution of probability. Considering sugarcane processing facilities, ethanol fermentation, and production of utilities (dubbed CAPEX base), limits of ±15% were attributed. For the areas working with hydrolysis of cellulose and their derivatives (dubbed CAPEX EL), a triangular probability distribution was assigned with ±40% limits. This difference in limit size for the triangular distributions is related to the maturity of each technology, which affects the accuracy of capital cost estimation.

Monte Carlo simulation was run using @RISK 7.5.2 (Palisade Corporation, USA, 2017) with 100000 iterations to obtain the probability distribution of IRR of the four different scenarios. In each of these iterations, values of each of the model inputs in the cash flow analysis (Figure 6) were randomly sampled according to their respective probability distribution. From these inputs, the model calculated the IRR for each iteration and stored these results to be used in statistical analysis. The obtained probability distribution of IRR was used to estimate the impact of each of the most important inputs in IRR via sensitivity analysis.

# 4. Process design and simulation

## 4.1. Defining the sections of the biorefinery

The biorefinery was structured as illustrated in Figure 7. The choice of integrating the LA process to the same biorefinery that can produce ethanol was based on two conclusions from previous literature: production of EL benefits from the availability of ethanol at a lower price and an integrated biorefinery has better economic performance than a standalone process.[12,15]

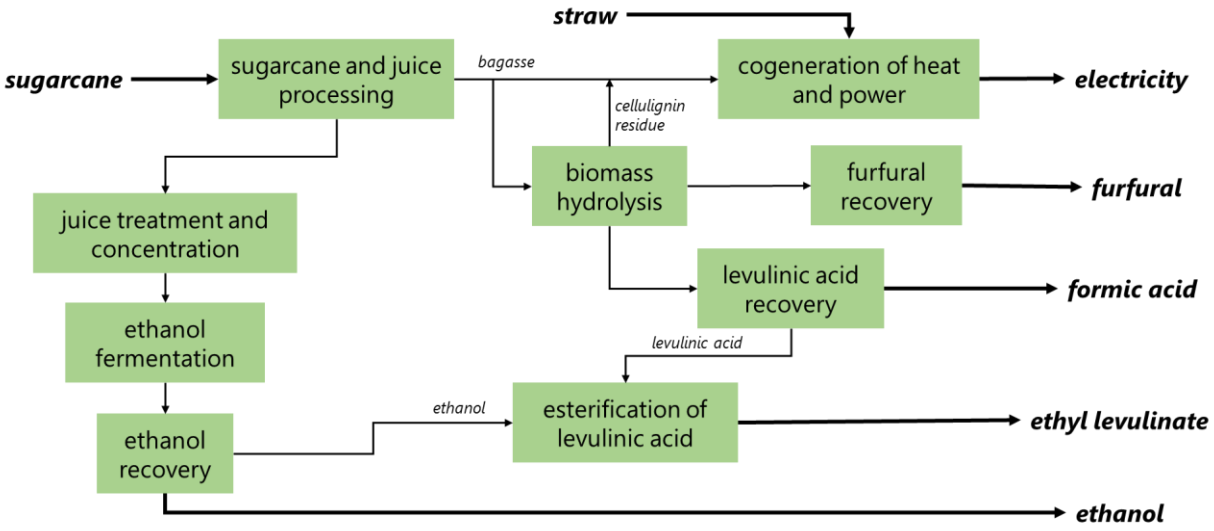


*Figure 7. Simplified block flow diagram of the biorefinery including the production of EL.*

Sugarcane processing and ethanol production from sugarcane juice were not simulated step-by-step. Instead, process simulation results of these sections based on data available in the literature were transferred into the simulation (mass and energy balances). Conditions used in the cogeneration of heat and power (CHP) section were the same used in the simulation of an optimized sugarcane mill with current technology. The furnace was fueled either by straw, bagasse, or residue from biomass hydrolysis. The amount of bagasse diverted to fuel application instead of LA production depends on the amount of LA produced (affected by optimization variable CC and selectivity). Backpressure turbines were employed since excess steam is produced. Parameters used in these sections are available in Table 8.

*Table 8. Process conditions included in the simulation for sugarcane processing, ethanol production, and CHP.*[59,63,83,84]

| Parameter | Value |
|---|---|
| Sugarcane processing capacity (Mt/y) | 4.0 |
| Operational year (d) | 200 |
| Bagasse (wet, 50 wt%) available for LA and CHP ($kg/t_{cane}$)[a] | 257 |
| Straw available as fuel ($kg/t_{cane}$) | 70 |
| Anhydrous ethanol yield from sugarcane ($L/t_{cane}$) | 85.4 |
| Steam consumption in the sugarcane mill and ethanol production | |
| *2.5 bar ($kg/kg_{EtOH}$)* | 4.61 |
| *6.0 bar ($kg/kg_{EtOH}$)* | 0.76 |
| Electricity consumption (mill and ethanol) ($kWh/t_{cane}$) | 30.0 |
| Boiler pressure (bar) | 90.0 |
| Boiler temperature (°C) | 520 |
| Boiler efficiency, LHV basis | 87.7% |
| Back pressure turbine efficiency | 85% |
| Electric generator efficiency | 98% |

a) Difference between total bagasse available after juice extraction and the amount of bagasse fines required in cake filter (6 $kg/t_{cane}$) and 5% of bagasse stored for boiler startup.

Sugarcane harvesting season is considered to last 200 days, thus limiting the biorefinery operational year. Some works in the literature consider an extended operational year of 330 days in second generation processes to reduce equipment size while keeping the same yearly production,[6] considering the storage of bagasse for operation during the off-season.[6] However, this approach seems unfeasible in real conditions because of the risk of bagasse fire and mold growth.[85,86] Moreover, the density of bagasse is low (dry: 102 kg/m$^3$).[85] Then, storing enough bagasse to keep the same production level running for 130 days during off-season requires vast storage space.

Ethanol was considered to be available for commercialization and use at a purity of 99.6 wt%.[12] Bagasse and straw were available for use with the composition detailed in Table 9.

*Table 9. Composition of sugarcane bagasse and straw.*[59]

| Component | Fraction of bagasse (wt%) | Fraction of straw (wt%) |
|---|---|---|
| Cellulose | 21.61% | 32.42% |
| Hemicelluloses | 11.81% | 22.53% |
| Acetyl group | 1.21% | 2.31% |
| Lignin | 11.72% | 20.59% |
| Ashes | 1.61% | 2.62% |
| Glucose | 0.08% | 0.19% |
| Sucrose | 1.96% | 4.34% |
| Water | 50.00% | 15.00% |

## 4.2. Hydrolysis of hemicelluloses

Operation of hydrolysis on the first pilot-scale project on LA production was regarded as one of the main problems because the first reactor often clogged.[15] Nevertheless, there are examples in the industry of reactors that handle biomass (sugarcane bagasse) hydrolysis without problems, such as the reactor used in the Rosenlew process for FF production.[20] The Rosenlew reactor operates with an innate catalyst derived from the own sugarcane bagasse, and most of the

reaction occurs in the middle section of the reactor, which is a vertical vessel with a length to diameter ratio (L/D) of 4.8.[20] The set of phenomena occurring in the reactor resembles a reactive distillation in a stripping column: as the solid biomass enters the reactor at room temperature, part of the vapors condenses; at the same time, steam is injected at the bottom to feed energy to the reactor and to rise hydrolysis products (FF and AA) to the top. In such fashion, AA derived from hydrolysis of acetyl groups in hemicelluloses accumulate in the middle section of the reactor and catalyzes the hydrolysis of polysaccharides. Due to the presence of vapor in large quantities, the vapor-liquid equilibrium between FF and water is at the side of the azeotrope in which FF is very volatile, and FF leaves the reactor at the top together with excess steam. This reactor successfully accomplishes the removal of a significant part of the hemicelluloses, which in turn will decrease the production of humins during synthesis of LA in more severe conditions.

Zeitsch (2000) gives operating conditions and yield of FF and other products only in the top stream of the reactor.[20] In the production of LA, the bottom product of the reactor is also of interest. Thus, conversion of biomass and sugars to heavy products was based on another reference. Batalha and co-workers (2015) studied the autohydrolysis of sugarcane bagasse. The more similar condition to that of the Rosenlew reactor corresponds to a residence time of 40 min – against 120 min in the Rosenlew reactor.[20,87] Even though this residence time represents one-third of the residence time of biomass in the Rosenlew reactor, it is important to remember that the hydrolysis reaction occurs in a small, central portion of the Rosenlew reactor. The rest of the reactor focuses on stripping off the produced FF. Therefore, these conversion data were used to complement the results from Zeitsch (2000).[20,87] Table 10 summarizes the conditions used to simulate this reactor.

*Table 10. Operating conditions of the Rosenlew reactor for hydrolysis of hemicelluloses.*[20,87]

| Parameter | Value |
|---|---|
| Conversion of hemicelluloses to xylose | 78.72% |
| Conversion of xylose to FF | 75.58% |
| Conversion of acetyl groups to AA | 87.88% |
| Conversion of cellulose to glucose | 11.81% |

*Table 10 (continued). Operating conditions for hydrolysis of hemicelluloses.[20,87]*

| | |
|---|---|
| Conversion of glucose to HMF | 42.21% |
| Conversion of HMF to LA and FA | 65.07% |
| Conversion of cellulose to low boilers[a] | 0.87% |
| Pressure (bar) | 10.01 |
| Temperature | 180.0 |
| Residence time (solids, min) | 120.0 |
| Steam[b] to FF ratio (kg/kg) | 30.00 |

a) Low boilers: methanol, ethanol, diacetyl, etc.

b) Steam is injected at the bottom at 10.01 bar and 265 °C.

The reactor, which is a single vessel, was simulated as a combination of three models of Aspen Plus: *RStoic*, *RadFrac*, and *Flash2*. Each of the two *RadFrac* blocks, with five equilibrium stages, represented the top and bottom parts of the reactor. These *RadFrac* blocks were simulated without condenser and reboiler. The reaction, which occurs in the middle section of the reactor, is represented by a combination of an *RStoic* and a *Flash2*, *i.e.*, another stage but with reaction. All blocks were set to operate adiabatically and at the operating pressure of the Rosenlew reactor: 10.01 bar.[20] The *Rstoic* block is required because Aspen Plus does not allow conversion of solids (biomass components) inside the *RadFrac* block.

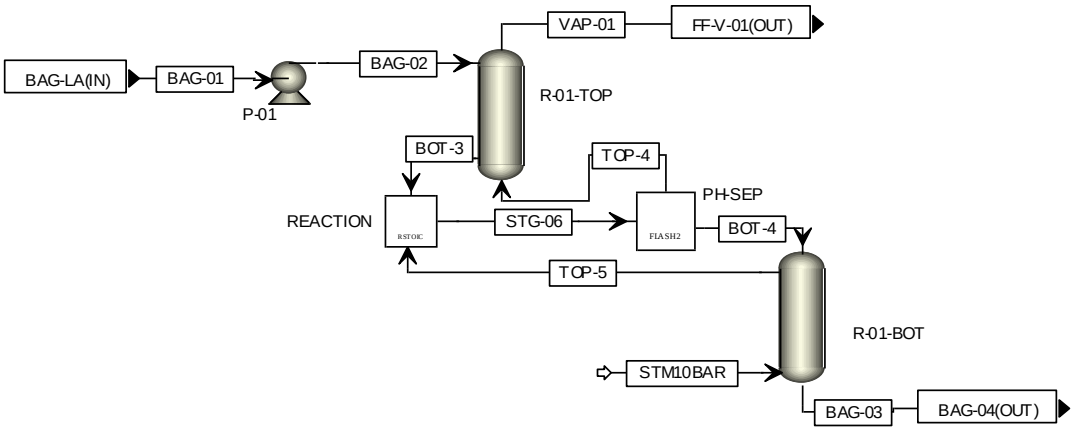


*Figure 8. Simulation of the reactor for hydrolysis of hemicelluloses based on the Rosenlew reactor.*

## 4.3. Hydrolysis of cellulose

Girisuta *et al.* (2013) studied the hydrolysis of cellulose in sugarcane bagasse in the presence of sulfuric acid in the range of 150-200 °C.[57] According to their model (Figure 9 and Eqs. 40-44), production of humins is a function of glucose concentration, catalyst concentration, and temperature. Humins correspond to a dark brown insoluble residue that forms during sugar degradation in an acid environment under severe conditions, compromising selectivity towards LA. Diverging from the aforementioned mechanism, other authors ascribe furanic compounds as the primary precursors of humins, since their formation mechanism is still unclear.[15] However, the differences between these two approaches do not affect the final result because the regressed reaction parameters is a good representation of the experimental data.

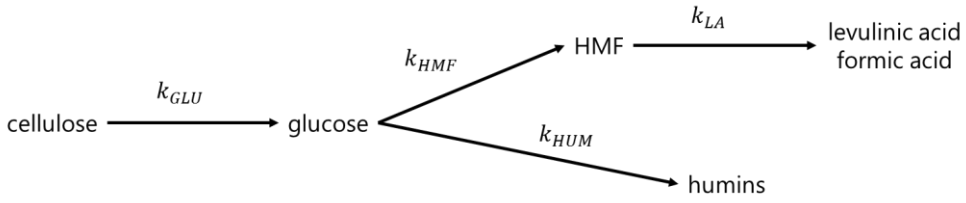


*Figure 9. Reaction scheme proposed by Girisuta* et al. *(2013) for hydrolysis of cellulose to LA.*[57]

Each reaction step depicted in Figure 9 is described by one of the following rate equations (Eqs. 40-43). The reaction rate is the product of a kinetic parameter and the concentration of the reactant (mol/L). In the case of cellulose, the monosaccharide units are used to calculate the concentration. The kinetic factor $k_i$ of each reaction rate equation is calculated using Eq. 44, whose constants are available in Table 11:

$$R_{GLU} = k_{GLU}[CELLULOSE] \quad (40)$$

$$R_{HUM} = k_{HUM}[GLUCOSE] \quad (41)$$

$$R_{HMF} = k_{HMF}[GLUCOSE] \quad (42)$$

$$R_{LA} = k_{LA}[HMF] \quad (43)$$

$$k_i = A_{0,i} \exp\left(-\frac{E_i}{RT}\right)[H_2SO_4]^{m_i} \quad (44)$$

in which $A_0$ is the pre-exponential factor, $E$ is the activation energy, $R$ is universal gas constant, $m$ is the exponent for sulfuric acid concentration and $i$ is the subscript which denotes each reaction step: $GLU$, $HUM$, $HMF$, or $LA$ for Eq. 40-43.

*Table 11. Kinetic parameters for the acid-catalyzed hydrolysis of cellulose in sugarcane bagasse.*[57]

| Reaction step | $A_0$($s^{-1}$) | $E$ (kJ/mol) | $m$(-) |
|---|---|---|---|
| $k_{GLU}$ | $1.59x10^{18}$ | 144.85 | 1.57 |
| $k_{HUM}$ | $6.94x10^{19}$ | 161.14 | 1.08 |
| $k_{HMF}$ | $6.58x10^{18}$ | 152.14 | 1.14 |
| $k_{LA}$ | $2.71x10^{14}$ | 101.63 | 1.32 |

These kinetic parameters were inserted in Aspen Plus using the LHHW (Langmuir-Hinshelwood-Hougen-Watson) rate equation format option of the general reaction formulary. Even though the kinetics of cellulose hydrolysis is not of the LHHW type, this formulary option has several possible entries. One of these entries, the adsorption term (Eq. 45 and 48), gives the possibility to indicate the rate dependency on sulfuric acid concentration:

$$r = \frac{(kinetic\ factor) \times (driving\ force\ expression)}{(adsorption\ term)} \quad (45)$$

$$(kinetic\ factor) = A_0(T)^n \exp\left(\left(-\frac{E}{RT}\right)\right) \quad (46)$$

$$(driving\ force\ expression) = k_1 \prod_{i=1}^{N} \boldsymbol{C}_i^{\alpha_i} - k_2 \prod_{j=1}^{N} \boldsymbol{C}_i^{\beta_j} \quad (47)$$

$$(adsorption\ term) = \left(\sum_{i=1}^{M} K_i \left(\prod_{j=1}^{N} \boldsymbol{C}_j^{\lambda_j}\right)\right)^{m'} \quad (48)$$

$$\ln(K_i) = A_i + \frac{B_i}{T} + C_i \ln(T) + D_i T \quad (49)$$

in which $n$ is the temperature exponent, $k_1$ and $k_2$ are the preexponential factor of the forward and

reverse (optional) reactions, $\alpha$ and $\beta$ are the exponents to indicate the reaction order in respect to concentration of the chemical species, $\boldsymbol{C}$ is the concentration of the chemical species (which can be given in several options of concentration basis), $N$ is the number of chemical species, $M$ is the number of terms in the adsorption expression, $K$ is a constant in the adsorption expression (given as a function of $T$ and coefficients $A$, $B$, $C$, and $D$), $\lambda$ is the concentration exponent for each chemical species used in the adsorption expression, and $m$' is the exponent of the adsorption term.

For the specific case of this simulation, the following was indicated: $n = 1$ in Eq. 46, $k_1 = 1$ and $k_2 = 0$ in Eq. 47, and the adsorption term in Eq. 48 is reduced to:

$$(adsorption\ term) = [H_2SO_4]^{m_i'} \tag{50}$$

in which $m_i' = -m_i$ (Table 11).

Although the work by Girisuta *et al.* (2013) describes a thorough study on conditions for hydrolysis of cellulose, almost all data for hemicelluloses conversion to FF are undisclosed.[57] The only data available show that hydrolysis of hemicelluloses to sugars was accomplished easily to totality in a few minutes, although most of the theoretical yield (about 80%, molar basis) was lost as degradation products other than FF.[57] Decomposition of FF as a consequence of the severity of the medium is an issue as demonstrated by other kinetic studies.[88] First, consider the reaction scheme depicted in Figure 10:


*Figure 10. Reaction scheme from xylose to FF and humins.*

Kinetic parameters for these two steps were determined based on disappearance rates of xylose and FF.[89] Although it is known that part of xylose and the intermediate in the reaction of xylose to FF are also consumed by condensation reactions,[20] these routes were discarded because: i) there are no kinetic parameters available since there is no practical method to determine the extension of such side reactions,[20] and ii) literature reports that concentration of xylose drops too fast and at a similar

time as the FF concentration peaks.[57,88] Therefore, considering only the consumption of xylose and consumption of FF (XYD and FFD, respectively), the kinetics of the reactions are described as follows:

$$R_{XYD} = 1.551 \times 10^{14} \left(\frac{L}{mol.min}\right)[XYLOSE][H^+] \exp\left(-\frac{140.457\left(\frac{kJ}{mol}\right)}{T\ (K)}\right) \quad (51)$$

$$R_{FFD} = 2.808 \times 10^{7} \left(\frac{L}{mol.min}\right)[FF][H^+] \exp\left(-\frac{92.352\left(\frac{kJ}{mol}\right)}{RT\ (K)}\right) \quad (52)$$

After the reactor, the hydrolysate stream was depressurized into an adiabatic vessel operating at 5 bar. The vapor obtained in this step had more than 3 wt% of FF and was mixed with the product of the Rosenlew reactor. Figure 11 depicts the operations related to the hydrolysis of cellulose.

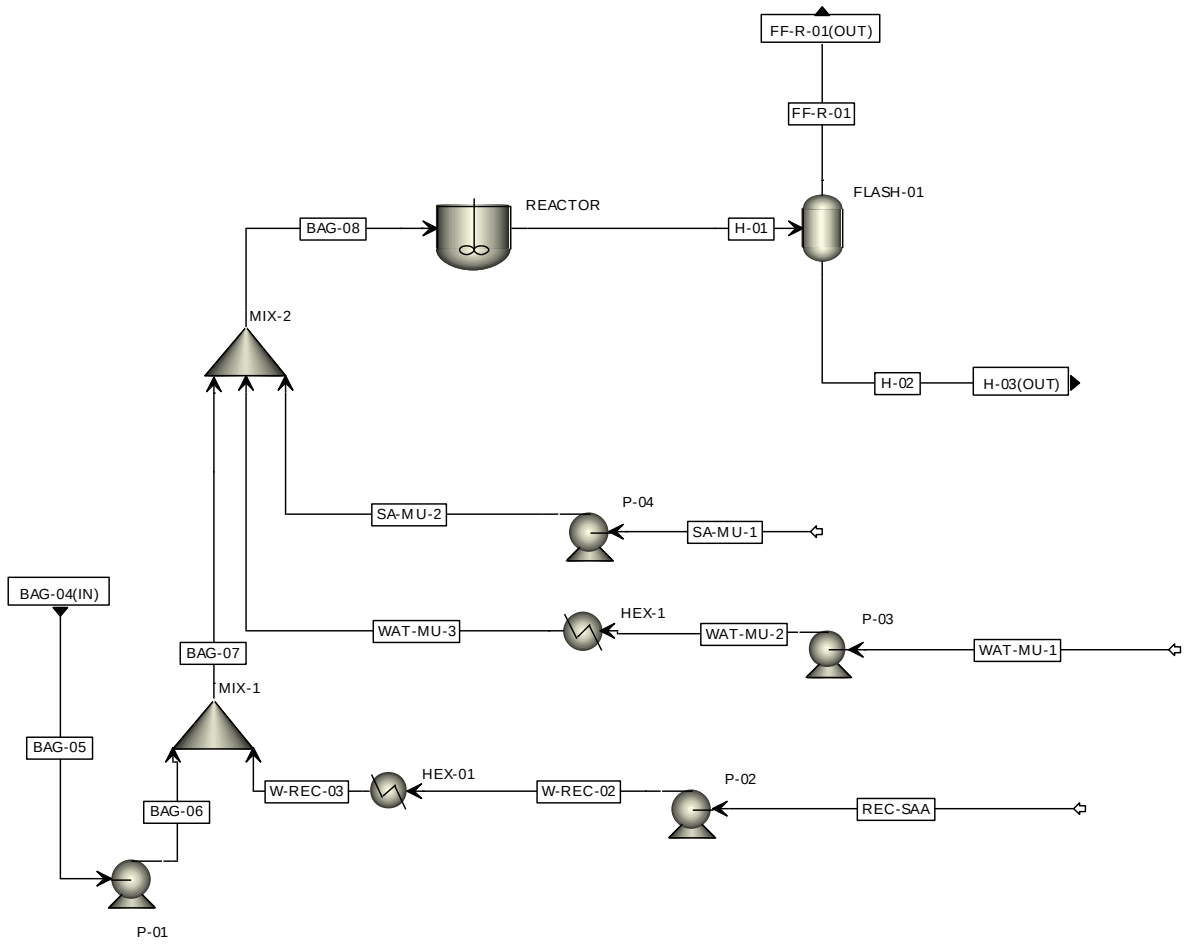


*Figure 11. Pre-heating of process water and hydrolysis reactor for cellulose conversion into LA.*

## 4.4. Recovery of solids and concentration of hydrolysate

The humins produced during hydrolysis form a coarse solid,[15,90] which in this design was suggested to be separated in the first step with a centrifuge because of the high liquid to solid proportion (around 10 in weight basis, depending on the case of the DOE). The centrifuge recovered 0.95 of the solids in a stream with a proportion of 2:1 of liquid to solids (~33% of solids). Energy spent by the centrifuge was not considered in process simulation because of the lack of process data and because the total energy required is too low compared to the rest of the process.[91] The liquid stream was then filtered, and this step considered complete recovery of the remaining solids in a cake with 50% of liquid. The feed pressure of the filter was 5 bar, and the pressure drop was 1 bar. The success of this step heavily depends on operability conditions regarding the handling of humins, which needs to be studied further as there is insufficient literature on the subject.[90]

Filter cake and centrifuge slurry were mixed and passed through a five-stage counter current solids washer with 95% mixing efficiency in each stage. Part of the water recovered from FF distillation (section 4.5) was used in this step, in a proportion of 1:1 to the liquid fraction of the slurry feeding the solids washer. This process recovered 98% of the LA which was present in the slurry. The washed solid was used as fuel in the furnace. Figure 12 depicts this process step.

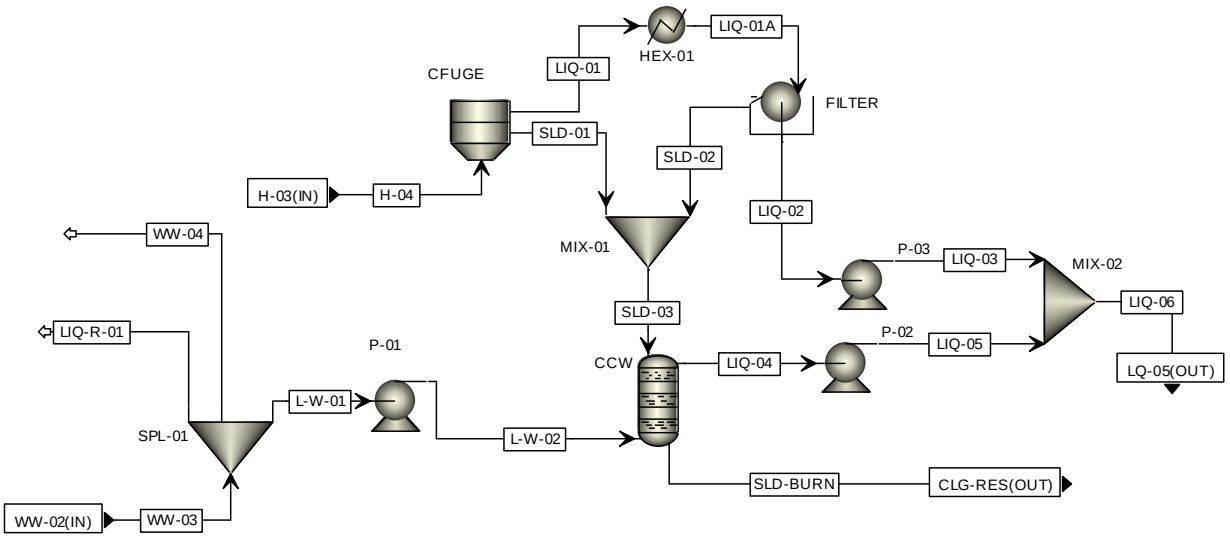


*Figure 12. Solids separation and washing. SPL-01 splits the water from FF distillation into a purge (5%), the required liquid to wash the solids in block CCW, and the balance was recycled to hydrolysis.*

The clear hydrolysate was sent to a concentration step. First, the hydrolysate was fed to a stripping column to recover most of the FF. This stripping column was simulated with 10 stages, no condenser, the feed entered at the top, condenser operated at 6.8 bar, and a pressure drop of 20 mbar per stage. The vapor leaving this column was used as a heating medium for the second evaporator of a series of six evaporator effects. This design was preferred for the first effect instead of a simple evaporator to recover a more concentrated stream of FF (the vapor stream became about thrice more concentrated in FF using this method). The following effects were simulated as simple evaporators, all with the same heat transfer area. Such condition was attained by adjusting the pressure drop between stages. The minimum temperature difference was set at the first effect (10 °C). This step is presented in Figure 13.

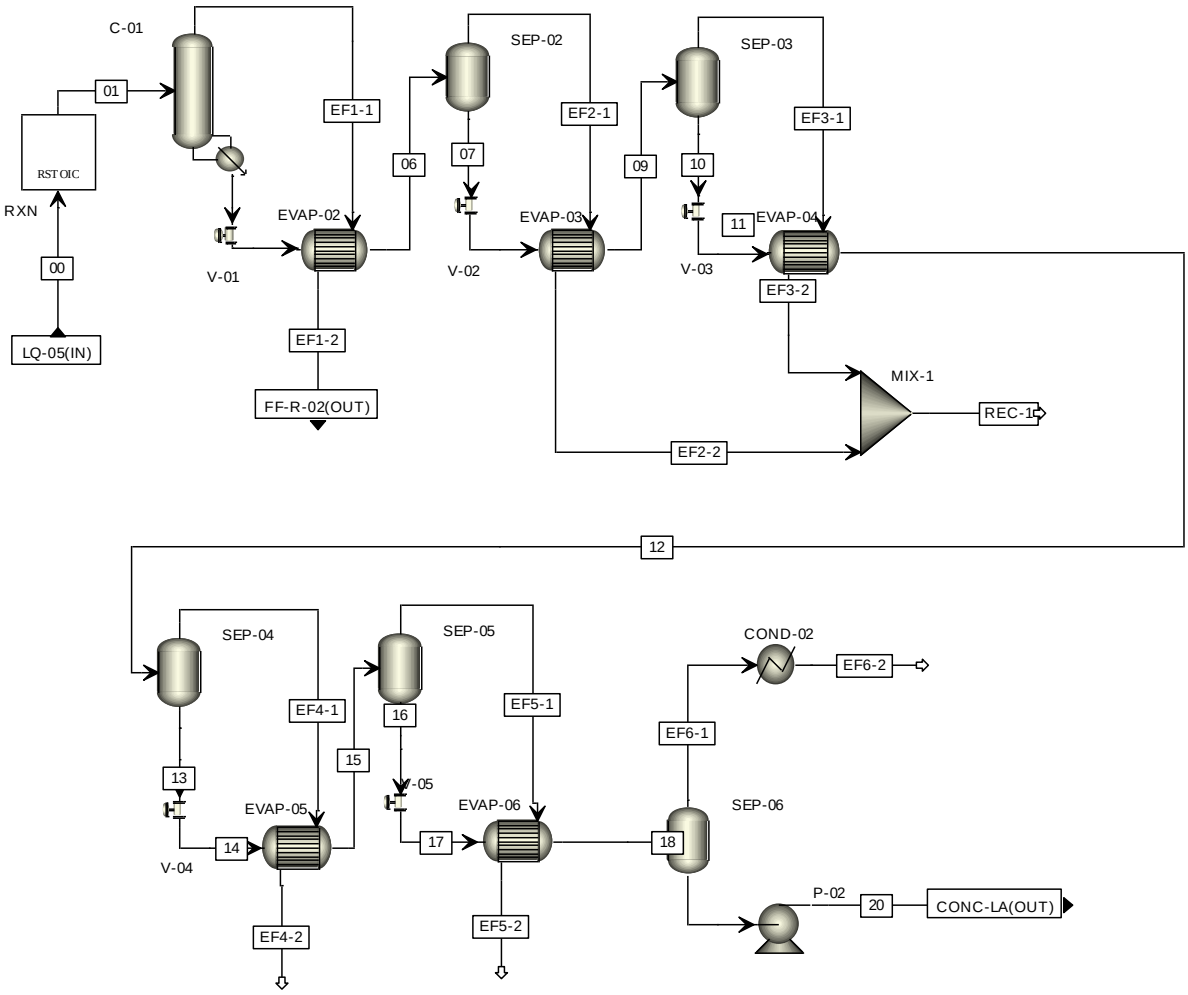


*Figure 13. Representation of the concentration step of hydrolysate with multiple-effect evaporators.*

During the concentration step, because of the increase of sulfuric acid concentration as part of the hydrolysate is evaporated, an *RStoic* model (adiabatic, no pressure drop) was used to convert all remaining hydrolyzed sugars into FF and LA. For each case of the DOE, the distillate to feed fraction in C-01 (Figure 13) was adjusted accordingly to obtain a hydrolysate with an LA content of 29.3 wt% without having a water content <40 wt%, based on results obtained in another part of this master's project.[92]

## 4.5. Recovery of furfural

FF is recovered in an azeotropic distillation scheme based on industrial process data.[20] First, the vapor streams containing FF were condensed. These streams were available with bubble points above 145 °C, and they were used to produce steam for other sections of the biorefinery that consumed low-pressure steam (2.5 bar, including sections in ethanol production – Figure 7). This approach provides a significant reduction of steam consumption.[17]

The condensed stream (~4 wt% of FF) was fed to a column that stripped FF out of the water, working on the side of the FF-water azeotrope in which FF is the most volatile component. This column had 38 stages (including reboiler and condenser), and the main feed entered in stage 11. The column had another feed in stage 8, consisting of an aqueous phase returned from a decanter, which was fed by a side stream drawn from stage 5 (liquid phase) that removed 17.85 wt% relative the main feed. This stream represented the main outlet of top products from the column, and the distillate recovered from the top of the column represented a small fraction: 0.486 wt% of the main feed. Thus, to provide enough contact between vapor and liquid phases at the top, the reflux ratio was high: 40. These conditions were based on industrial data, and they take advantage of the azeotrope and the occurrence of a LLE.[20] The pressure was set at 770 Torr in stage 1 and 1180 Torr in stage 38. The condenser had an off-gas outlet because of the operating temperature: 50 °C. This off-gas contained mainly very light gases produced during biomass hydrolysis. The liquid distillate (stage 1) contained low boilers (methanol, ethanol, diacetyl, etc.), water, and FF. The block convergence method was set to "azeotropic", with three valid phases.

The top product of the first column was sent to a small column to recover FF. This column had 10 stages, reflux ratio of 1, bottoms to feed ratio of 0.73 in mass basis, feed on stage 5, pressure

of 1.3 bar in the condenser, stage pressure drop of 15 mbar, and the condenser operated at 50 °C. The off-gas contained light gases, and the liquid distillate contained low boilers. The bottom product was sent to a decanter to separate FF and water. The block convergence method was “standard”.

The product stream from stage 5 of the azeotropic column containing more than 20 wt% of FF was cooled down to 61 °C and sent to a decanter for phase separation. The adiabatic decanter operated with a pressure drop of 100 mbar at the inlet. The aqueous phase was returned to the first column in stage 8, and the organic phase was sent to a third column which stripped off water from FF. This column had 5 stages, distillate to feed ratio of 0.05 (mass basis), feed on stage 1, and operated in vacuum conditions to avoid degradation of FF in high temperature: 400 mbar in stage 1 and 440 mbar in stage 5. The column had no reflux: the decanter feeding the organic phase to this column worked as its reflux drum. The top vapor product was cooled to 61 °C, and the off-gas was separated before mixing the liquid distillate with the other FF-rich streams that feed the decanter. Figure 14 illustrates the complete process for recovery of FF.

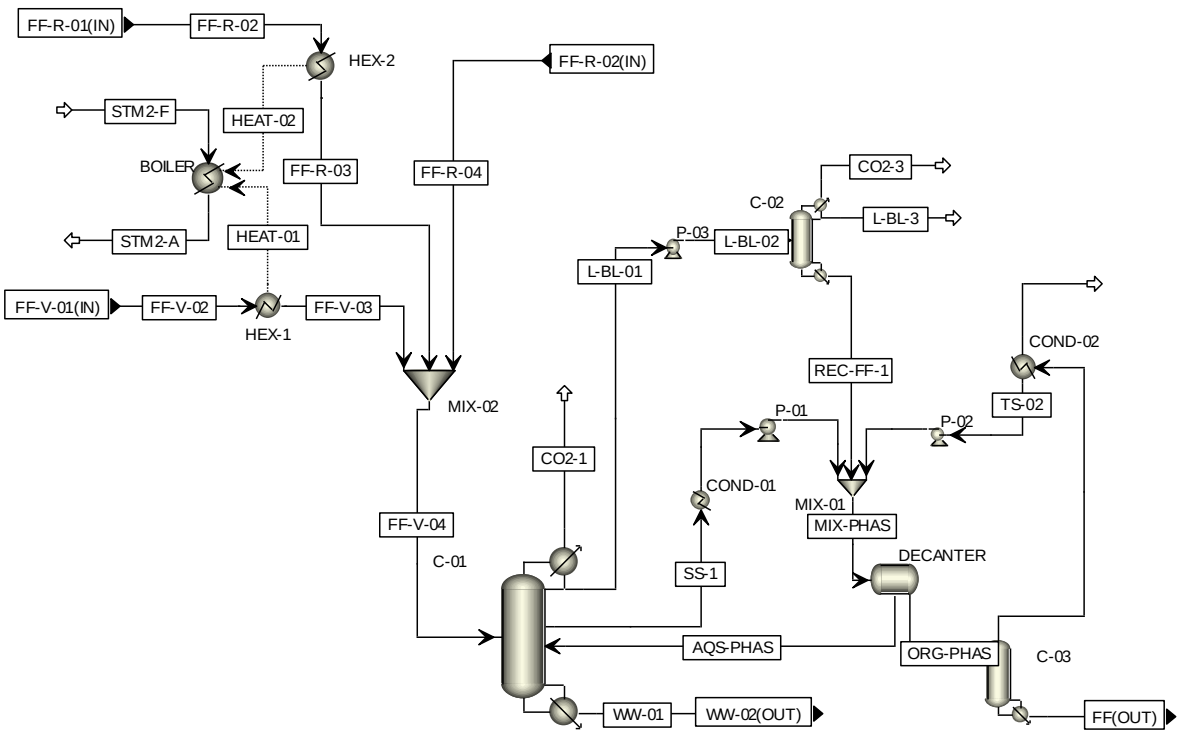


*Figure 14. Recovery of FF from FF-containing vapors via azeotropic distillation.*

## 4.6. Recovery of levulinic acid

LA was recovered via solvent extraction. The use of MTHF was suitable because it is very selective towards LA (oxygenated solute and oxygenated solvent). Operating conditions for this section were previously assessed using the UNIFAC group contribution method.[92] In the simulation of this biorefinery for production of EL, these same conditions were used since both NRTL and UNIFAC predict phase split and the differences in separation performance may not substantially affect the overall economic performance of the process as it represents a single step in a complete biorefinery. Moreover, a rigorous process simulation to yield definitive optimized operating conditions for this liquid-liquid extraction process also requires determination of process data for the dehydration of MTHF using molecular sieves. In the work which was used as the basis for the simulation of this step, the dehydration of MTHF had conditions based on those of dehydration of ethanol using molecular sieves to have an estimate of the recovery of MTHF per cycle.[92]

The concentrated hydrolysate was contacted in countercurrent with MTHF as shown in Figure 15. Both streams were fed to the extractor at 70 °C. MTHF and water present inverse solubility: the higher the temperature, the lower the mutual solubility. 70 °C was used as a limit because of the low boiling point of MTHF. Enough solvent (recycle and makeup) was supplied to recover 99% of LA.

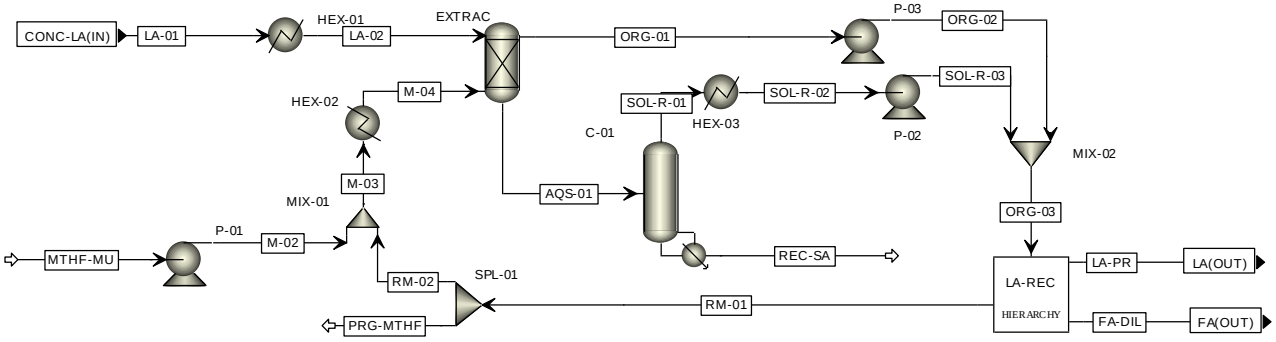


*Figure 15. Liquid extraction of LA from hydrolysate.*

The raffinate, which recovered more than 99% of sulfuric acid, was stripped off of traces of MTHF and recycled to be used in hydrolysis of cellulose. The stripping was carried out in a column

with 12 stages and no condenser, with the following conditions: top stage operating pressure of 1.05 bar, stage pressure drop of 15 mbar, distillate to feed ratio of 0.014 (mole basis), and convergence method as "azeotropic". The distillate product of this column was mixed with the extract stream and sent to a separation step (hierarchy block LA-REC in Figure 15) to recover MTHF and LA.

LA-REC in Figure 15 refers to the separation of LA and MTHF. As a result of the high difference in volatility between solvent and solute, a significant part of the MTHF was recovered in a three-effect evaporation to decrease steam consumption (Figure 16). Two out of the three evaporation steps were carried out using a column (*RadFrac* model) to minimize losses of FA and AA. In the first effect, a column with 10 stages operating at 9.15 bar in the first stage with a 20 mbar pressure drop per stage, about 20 wt% of the feed was recovered at the top. The amount of distillate recovered depended on previous steps (*i.e.,* LA yield, required MTHF amount to recover 99% of LA, etc., consequences of the DOE) and was changed to ensure a temperature approach of 10 °C in the reboiler of the third evaporator, which works as a condenser of the first evaporator. The bottom of the first evaporator was flashed into an adiabatic vessel (second evaporator effect), operating at 1.1 bar. Then, the bottom product was fed to the third evaporator, a 10-stage column without condenser, operating near atmospheric pressure conditions. Vapor from the first effect powered the reboiler of this column, simulated by a *HeatX* model (REB-01 in Figure 16). The liquid product and the condensed MTHF were used to preheat the feed of the first evaporator, considering a temperature approach of 10 °C, which is typically used in heat integration. The product from the third evaporator contained less than 20 wt% of MTHF, which was stripped off by injection of 10 bar, 265 °C steam at the bottom of a 10-stage column operating near atmospheric pressure. This approach removes MTHF and leaves most of FA behind. MTHF, FA, and water have azeotropes between any combinations of them. As MTHF must be recycled, the decision was to strip it off of the mixture of carboxylic acids using superheated steam and then recover the remaining FA as a mixture of FA and water, with no further separation because of the azeotrope and low relative volatility between them. The mixture of FA and water was separated from LA in a column with 21 stages, 0.041 of reflux ratio, 0.185 distillate to feed ratio, feed at stage 14, top pressure of 150 mbar and bottom pressure of 250 mbar. All streams containing a mixture of water and MTHF were sent to a dehydration step. Block DEHYD in Figure 16 represents the hierarchy in which dehydration of MTHF was simulated.

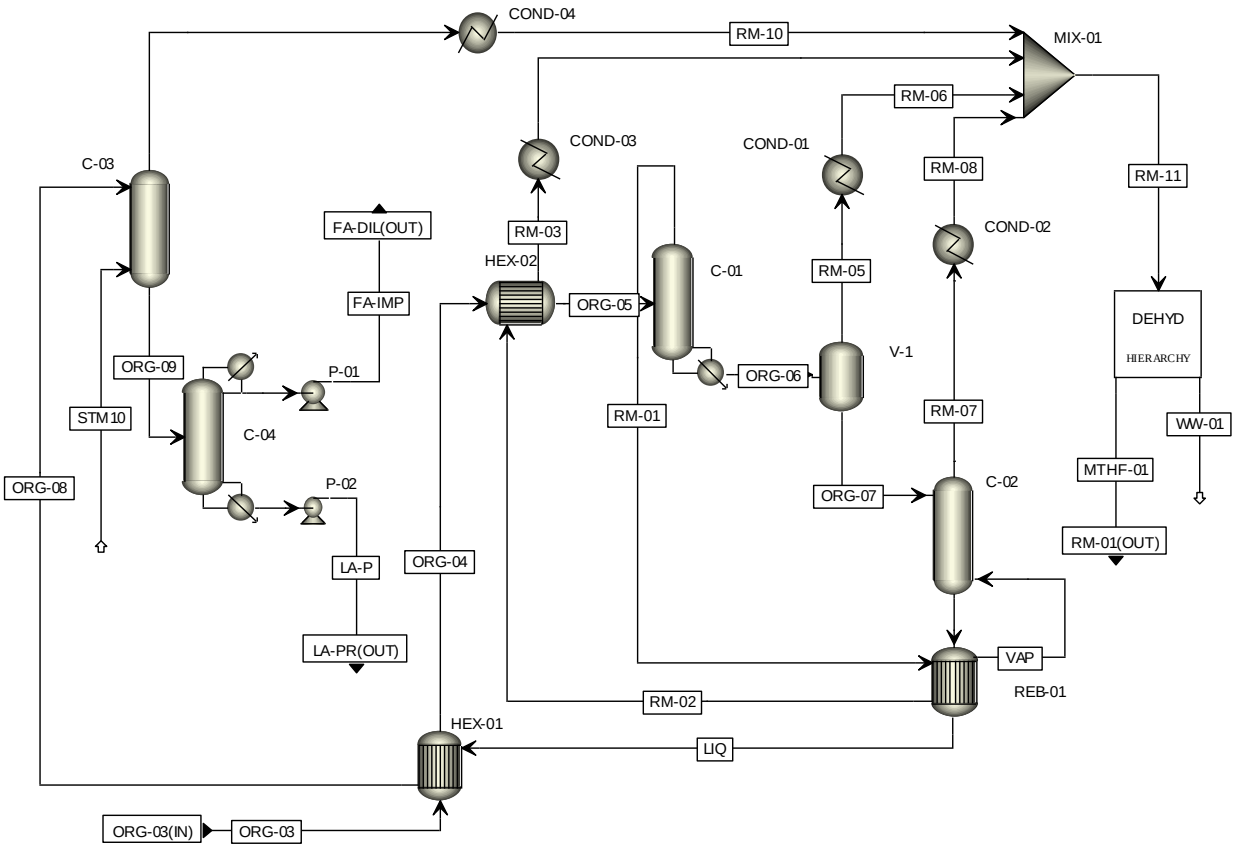


*Figure 16. Recovery of LA from the extract stream.*

Water and MTHF present an azeotrope at a concentration around 94 wt% of MTHF (1 atm). Consequently, because of the phase split proportion, only one side of the azeotrope is suitable for azeotropic distillation. The aqueous product of a decanter (Figure 17) was sent to a stripping column which removed MTHF and a small portion of water close to azeotropic proportion at the top. The column was simulated with 5 stages, distillate to feed ratio of 0.05 (mole basis), pressure of 1.01 bar at the condenser and a pressure drop of 10 mbar per stage. In this column, the aqueous phase from the decanter (stream AQS-01 in Figure 17) was fed at the top stage, acting both as column feed and reflux. The organic phase leaving the decanter (6 wt% of water) was pressurized (6.5 bar) and vaporized (150 °C). After passing the molecular sieve bed, 85% of organics were recovered with a water content of 0.4 wt%.[92,93] The purged stream was returned to the decanter and the dehydrated MTHF stream was reused as solvent for extraction after a purge of 2%.

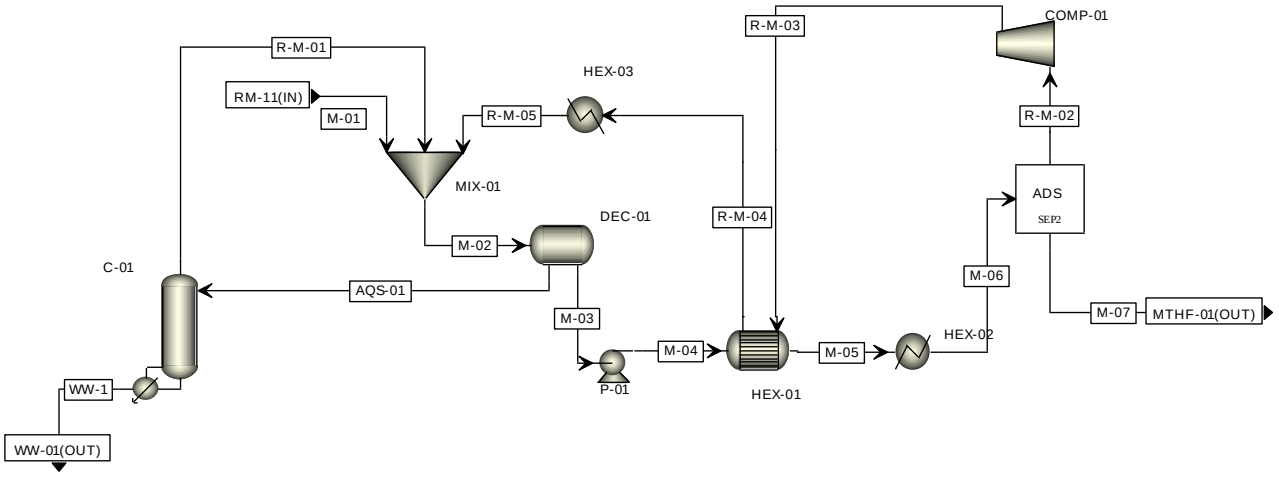


*Figure 17. Separation of MTHF and water (block DEHY in Figure 16).*

## 4.7. Esterification of levulinic acid

Esterification of LA to EL has been studied thoroughly for the development of this biorefinery. Based on a previous assessment, the uncatalyzed esterification in high temperature, presented by Bankole *et al.* (2014) seemed to be attractive.[15,94] However, a study considering the uncatalyzed esterification carried out in a reactive distillation column showed little improvements in economic performance when compared to a setup using a continuous reactor coupled to standard distillation columns, and the final upgrading cost of LA to EL was 55% higher than that of a process based on a catalyzed reactive distillation column of another recently published work.[65,95] Therefore, conditions for esterification were based on the work of Novita *et al.* (2017) and the results of mass and energy balances, including utility requirements, were used in the simulation of the biorefinery.[65]

## 4.8. Steam and electricity from biomass

Sugarcane straw, bagasse, and residue from hydrolysis were burned together to produce steam and electricity. Parameters used for the simulation of this part are available in Table 8. After burned, the boiler inefficiency was discounted from the flue gas, and the remaining energy recovered in decreasing the flue gas temperature to 150 °C was used to heat water and produce steam. Steam was expanded in turbines to yield steam at pressure conditions required by the process. Before use in the plant, a step to change the quality of the steam from superheated to near-saturation conditions was implemented with the addition of subcooled water. The required flow rate of steam at conditions

to be used in the ethanol plant was included in the extractions of steam at 2.5 bar and 6.0 bar. The total availability of steam at 2.5 bar included the additional steam produced via heat integration in the FF recovery section, as explained in section 4.5.

Total electricity required by the plant was calculated considering two parts: the power required by sugarcane extraction and ethanol plants (Table 8), and the power required by the part of the plant which was simulated in this work. For the plant simulated in this work, total electricity requirement was calculated using the process simulator, summed using the utility resource of Aspen Plus, and discounted from the total of electricity produced by the turbines. Surplus electricity was considered a product of the biorefinery.

Among the equipment requiring cooling media, none of them require temperatures below 50 °C, which dispenses the use of chilled water. Cooling water, the only cooling utility used in the biorefinery, was excluded from the simulations as it plays a minor role in the economics of the process. This same approach is used by other authors in the field of biorefinery simulation.[59,63]

# 5. Results and discussion

## 5.1. Simulation of DOE cases

Detailed process simulation results were included only for the optimized case, whereas key results were included for the 25 cases simulated as part of the DOE. Figure 18 shows the yields of products of the biorefinery. It is visible that in any of the 25 cases of the DOE, ethanol is still the main product, as its final yield varied slightly due to variations in the consumption of ethanol inside the biorefinery for esterification of LA. Production of chemicals derived from bagasse follows on average a very particular proportion: 1:3.1:5.4 of FA:FF:EL (mass basis). The proportion between FA and EL varies very little: they are produced in equimolar proportion from the same reaction, and the differences are a consequence of downstream processing. As for the proportion of FF to the others, it is greatly affected by the extension of the reactions that consume FF according to the operating conditions set in the second hydrolysis reactor, since the reactions of FF to humins do not have the same kinetics as the reactions that lead to humins using glucose or HMF as precursors.

Operational costs vary slightly because the only variables affected by the DOE are maintenance (indicated as a fraction of CAPEX, Table 7), consumption of sulfuric acid, and consumption of MTHF. Summed, the contribution of these factors to the yearly operational cost varies in the range of 19-22% for the 25 cases.

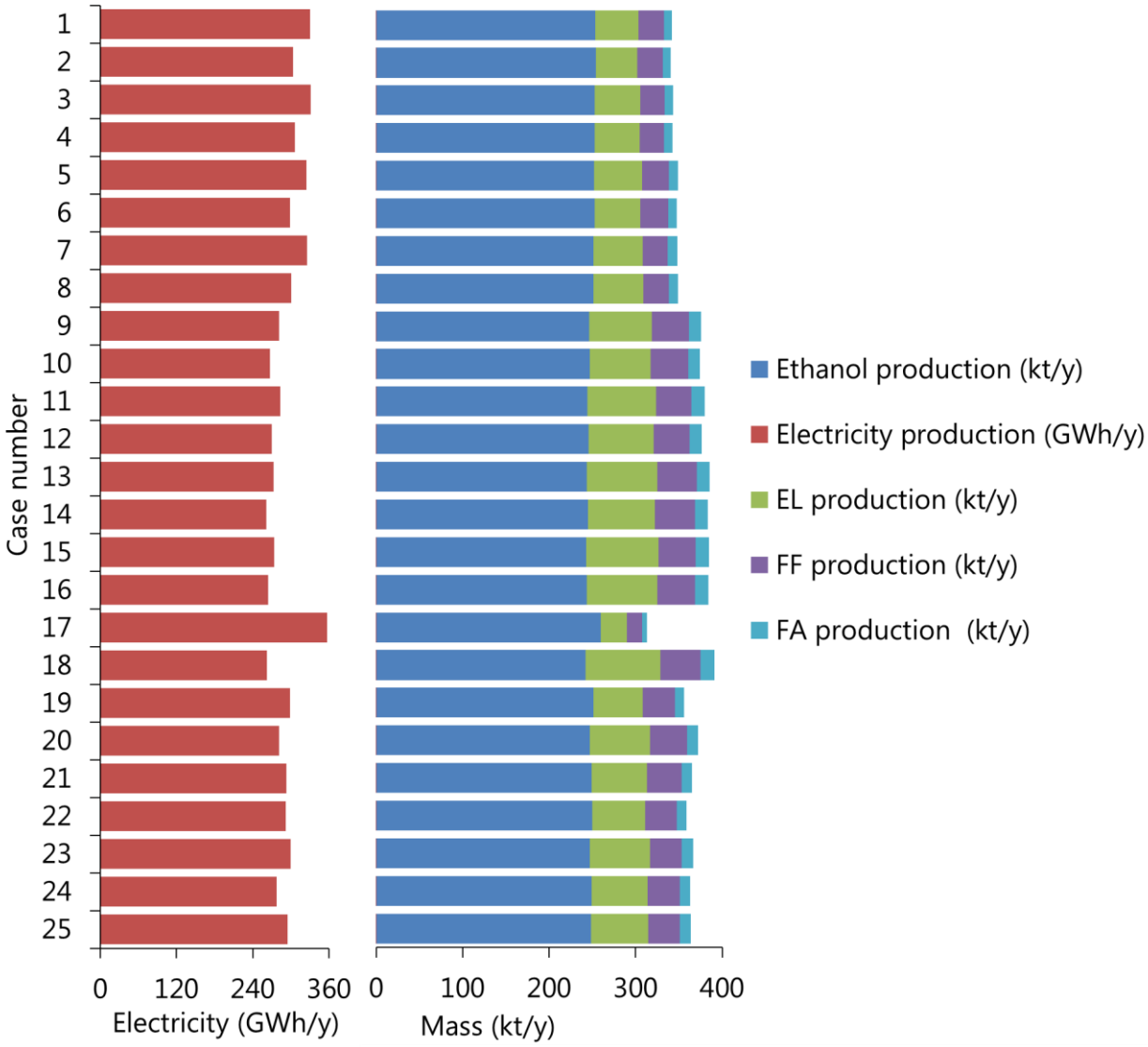


*Figure 18. Product yields of the biorefinery in each of the 25 cases of the DOE.*

Figure 19 presents the revenue and the revenue share for each case. It is observed that the contribution of EL to the revenue is in the same order of magnitude as the contribution of electricity. Albeit sounding counterintuitive, not always the scenarios with better revenue presented the best MSP of EL. Case 4 is an example: it has the 2$^{nd}$ best total revenue. However, the low SL of this case (8%) combined with the low CC (66%) results in a very dilute product, which demands more steam for product recovery. The CL is also high, which leads to increased equipment cost to withstand corrosion. Another factor is that the hydrolysis is carried out at 190 °C, which demands steam at high

pressure - hence, less electricity is obtained from steam expansion in turbines (red bar of case 4 in Figure 18 compared to others). Altogether, these factors lead to an increased MSP of EL.

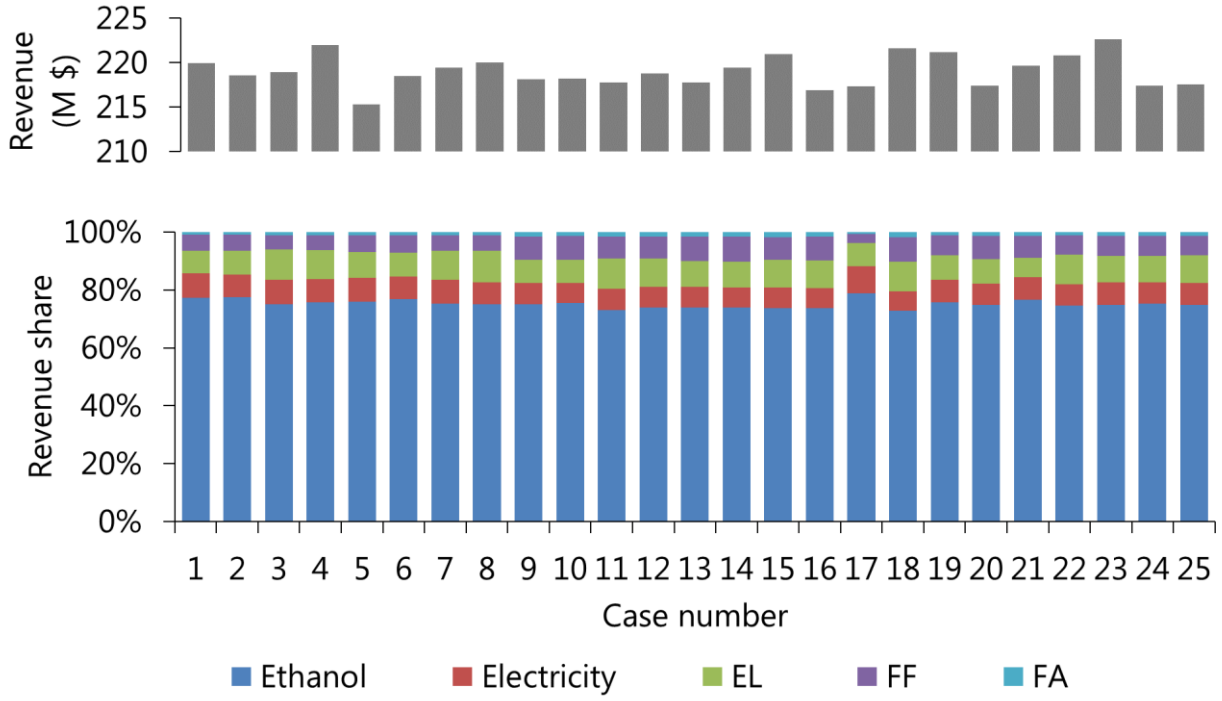


*Figure 19. Total revenue and revenue share for each product of the biorefinery in each of the 25 cases of the DOE.*

## 5.2. Surrogate model and statistical analysis

Table 12 presents the results of the MSP of EL for each of the 25 cases of the DOE. Many cases yielded an MSP above $0.40/kg, especially case 17, whose MSP was $0.806/kg. As a matter of comparison, the estimated price for EL to be sold in Brazil with the same price of diesel on an energy basis would be in the range of $0.42-0.47/kg.[15,29] As discussed before, the price of EL may be based on the energy price of diesel. However, due to its additive properties and its renewable origin, the final price may be even higher than the energy price of diesel. Policies benefiting the use of renewable fuels, such as the program RenovaBio, may contribute to an increase in revenues from biofuels as a consequence of higher blending mandates for diesel in the future.[96]

*Table 12. Results of MSP of EL for each case of the DOE.*

| Case | SL | CC | CL | RT | MSP ($/kg) |
|---|---|---|---|---|---|
| 1 | -1 | -1 | -1 | -1 | 0.479 |
| 2 | -1 | -1 | -1 | +1 | 0.515 |
| 3 | -1 | -1 | +1 | -1 | 0.566 |
| 4 | -1 | -1 | +1 | +1 | 0.563 |
| 5 | -1 | +1 | -1 | -1 | 0.477 |
| 6 | -1 | +1 | -1 | +1 | 0.467 |
| 7 | -1 | +1 | +1 | -1 | 0.510 |
| 8 | -1 | +1 | +1 | +1 | 0.535 |
| 9 | +1 | -1 | -1 | -1 | 0.338 |
| 10 | +1 | -1 | -1 | +1 | 0.344 |
| 11 | +1 | -1 | +1 | -1 | 0.379 |
| 12 | +1 | -1 | +1 | +1 | 0.376 |
| 13 | +1 | +1 | -1 | -1 | 0.319 |
| 14 | +1 | +1 | -1 | +1 | 0.344 |
| 15 | +1 | +1 | +1 | -1 | 0.329 |
| 16 | +1 | +1 | +1 | +1 | 0.341 |
| 17 | -2 | 0 | 0 | 0 | 0.806 |
| 18 | +2 | 0 | 0 | 0 | 0.339 |
| 19 | 0 | -2 | 0 | 0 | 0.451 |
| 20 | 0 | +2 | 0 | 0 | 0.365 |
| 21 | 0 | 0 | -2 | 0 | 0.337 |
| 22 | 0 | 0 | +2 | 0 | 0.484 |
| 23 | 0 | 0 | 0 | -2 | 0.392 |
| 24 | 0 | 0 | 0 | +2 | 0.416 |
| 25 | 0 | 0 | 0 | 0 | 0.423 |

Statistical analysis of the data in Table 12 was carried out in Statistica 13.3. The coefficient of determination of the data fitted to the quadratic surrogate model was 96.5%. Analysis of variance confirmed that the surrogate model represents a good fit of the regressed data.

*Table 13. Analysis of variance for the MSP of EL.*

| Source of variation | Sum of squares | Degrees of freedom | Mean sum of squares | F-test ratio |
|---|---|---|---|---|
| Treatment | 0.283 | 14 | 0.0202 | 19.499 |
| Error | 0.010 | 10 | 0.0010 | |
| Total | 0.293 | 24 | | |

Comparing the F-test statistic in Table 13 with the calculated $F_{14,10}$ with a p-value of 0.05:

$$19.499 \gg F_{14,10} \cong 0.3843$$

Therefore, the model is significant, and since the calculated F is more than ten times larger than the $F_{14,10}$ value calculated using the Probability Distribution Calculator tool of Statistica 13, one could infer that the model is useful for prediction and, consequently, can be used in process optimization via surrogate model.[97] It is important to indicate that, although the surrogate model is a good representation of the real model, this optimization is a fair approximation of the real optimized model, with a level of detail compatible with the process developed in this work.

The Pareto chart of standardized effects (Figure 20) considering a confidence interval of 95% shows that the main variables affecting the MSP of EL are the SL (both linear and quadratic coefficients), the CL (linear coefficient), and the CC (linear coefficient). All other variables or combinations of them have a similar effect on the MSP. The impact of SL is evident when comparing the MSP of cases 17 and 18, given the fact that they represent the extremes of SL in the DOE: MSP in case 17 is 2.4 times larger than in case 18. Case 17 produces a very dilute hydrolysis product, which requires more steam for recovery of LA. At the same that more steam is required, less bagasse is diverted to LA production: the CHP unit in case 17 produces 21% more steam than in case 18, whereas the production of EL/LA in case 17 is 65% less than in case 18. CC also has an important

impact owing to the final consequence of this variable: a higher feedstock conversion means higher product concentration and a decrease in steam requirement. Coefficients of the surrogate model are presented in Table 14, and the response surfaces obtained for the variable MSP using this surrogate model are presented in Figure 21.

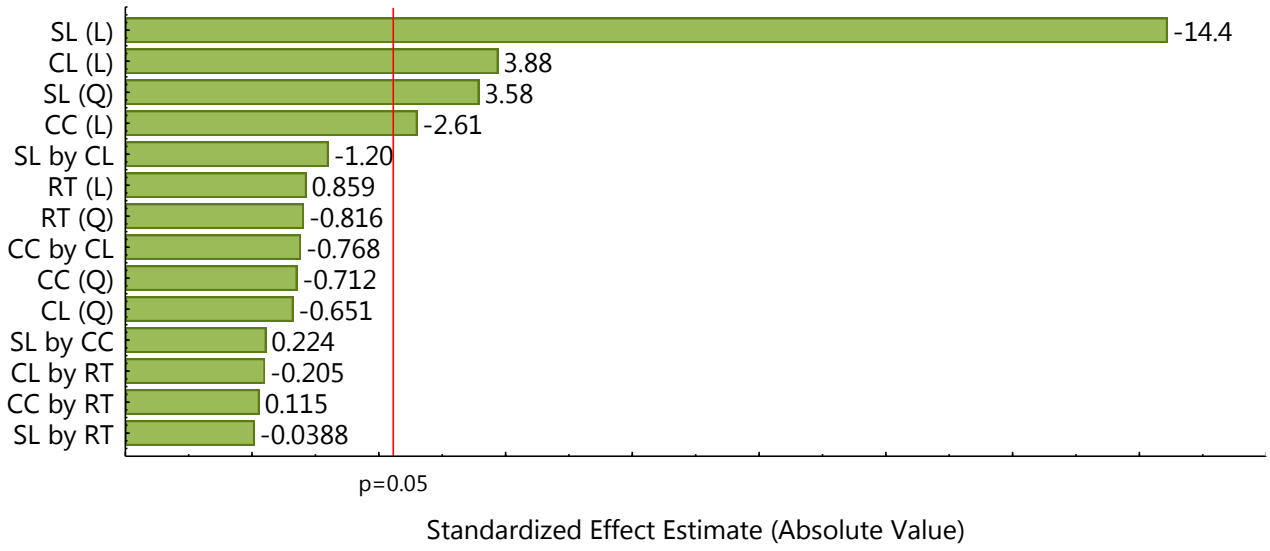


*Figure 20. Pareto chart of standardized effects for the MSP. (L) denotes a linear coefficient, (Q) denotes a quadratic coefficient, and the other terms correspond to the interactions between coefficients.*

*Table 14. Coefficients of the surrogate model obtained via DOE.*

| Term | Coefficient | Term | Coefficient |
|---|---|---|---|
| $Intercept$ | 0.422935 | $x_4^2$ | -0.007809 |
| $x_1$ | -0.094860 | $x_1x_2$ | 0.001801 |
| $x_1^2$ | 0.034295 | $x_1x_3$ | -0.009680 |
| $x_2$ | -0.017116 | $x_1x_4$ | -0.000312 |
| $x_2^2$ | -0.006819 | $x_2x_3$ | -0.006176 |
| $x_3$ | 0.025500 | $x_2x_4$ | 0.000927 |
| $x_3^2$ | -0.006232 | $x_3x_4$ | -0.001648 |
| $x_4$ | 0.005639 | | |

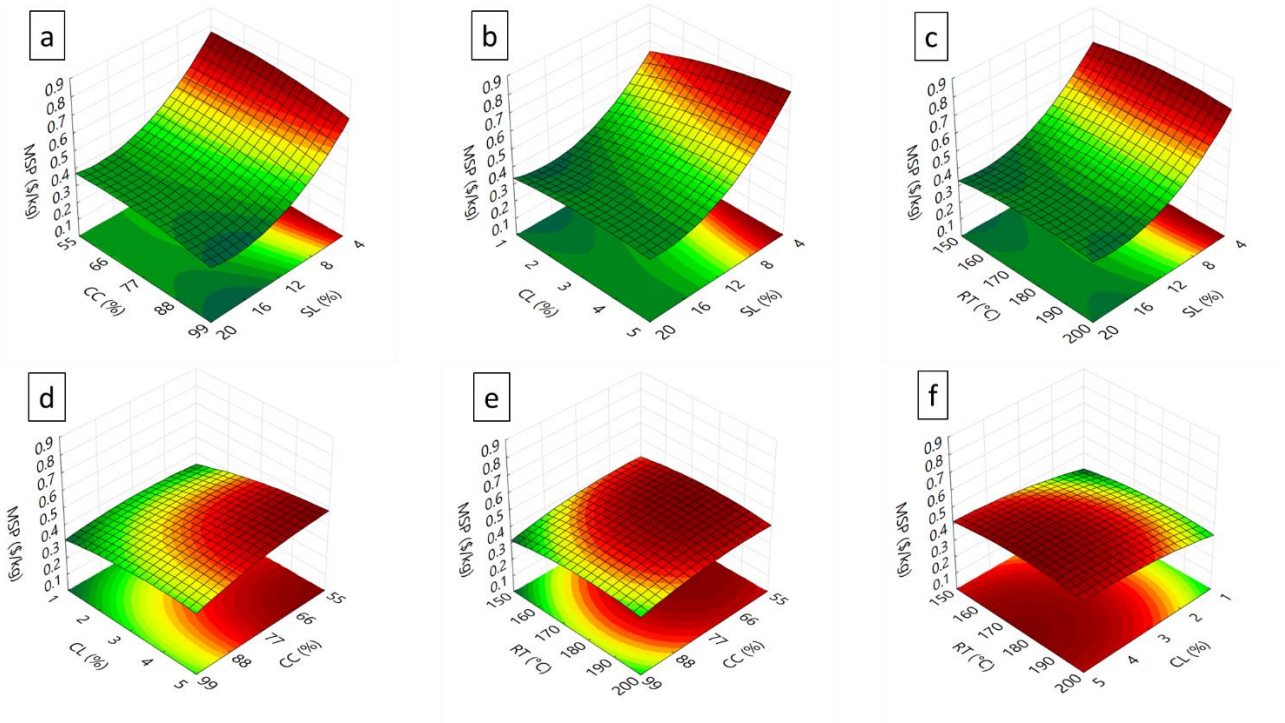


*Figure 21. Response surfaces obtained with the surrogate model for the MSP of EL: a) MSP (CC, SL), b) MSP (CL, SL), c) MSP (RT, SL), d) MSP (CL, CC), e) MSP (RT, CC), f) MSP (RT, CL). Variables not present in one graph were fixed at their respective central level. Directions of axes were adjusted to improve surface visualization.*

Comparison of graphs a, b, and c (in which SL is one of the variables) in Figure 21 to graphs d, e, and f makes the importance of SL in the response variable more evident: considering the same range of MSP, the effect of the other three variables is much less evident than the effect of SL. Indeed, the impact of SL in the production of biofuels has been investigated as one of the solutions to make their commercialization viable, including LA.[15]

As explained before, this is mainly a consequence of less steam demand for recovery of LA. High SL can impact other process variables as well. Svensson *et al.* (2016), when investigating a cellulosic ethanol process integrated to a pulp mill, determined that the highest impact of SL is in stillage (vinasse) production and the operations related to its treatment. High SL leads to high sugar concentration in hydrolyzed liquor. In cellulosic ethanol production, considering the scenario in which no concentration step is required, this would lead to a fermentation broth with more ethanol. However, ethanol is recovered as distillate. Hence, the amount of water has little impact in the steam

demand for distillation given that most of the energy spent by distillation columns is used to vaporize ethanol. Differences in steam consumption may rise as a consequence of the impact of broth composition in reflux demand to achieve a certain degree of purity in the distillate. Regarding environmental impact, Kadhum *et al.* (2017) demonstrated that a very high SL (30-45%) decreases global warming potential, which is not observed for an SL of 19%.[98]

On the other hand, this is not the situation for every biorefinery product: examples of products that cannot be distilled out of water include LA, succinic acid, and lactic acid. Even though FF and butanol have higher boiling points than water, these examples of green chemicals benefit from the effect of azeotropes and their low concentrations in water.[79,99] In the case of furfural, specifically, this makes its recovery a quite easy process, in which most of the energy is spent in the reaction.[20] Therefore, in the case of LA, an alternative to distillation processes are required.

Liquid extraction is an attractive alternative because of the opportunity to separate the product and leave the catalyst (a mineral acid) in the aqueous phase. This process makes the recovery of catalyst possible to a certain extent, granted that the losses of sulfuric acid in hydrolysis residue should be carefully evaluated in laboratory scale. This process step requires further study in laboratory scale followed by optimization to decrease CAPEX and OPEX. Extraction of LA does not necessarily require evaporation of water. However, since LA is a very oxygenated chemical, suitable solvents for extraction must be oxygenated to present a favorable partition coefficient for liquid extraction. Otherwise, the amount of solvent required would make the process unfeasible. This was demonstrated by Leal Silva *et al.* (2018) in the comparison of hexane and MTHF as extraction solvents for LA.[92] On the other hand, oxygenated solvents generally present greater mutual solubility with water. In this situation, a hydrolysate stream with higher LA content reduces the requirement of solvent and decreases the costs with solvent recycling and makeup. Thus, a higher SL is desirable to deliver a hydrolysate with a higher LA content, which may be increased even further after evaporation. The degree of conversion of the feedstock has a similar impact on the process, a factor which qualified CC as one of the main variables impacting the MSP, along with SL.

Analysis of Figure 21 clearly shows that temperature has little effect on MSP. In the study in which the kinetics for cellulose decomposition used in this process simulation was based, the

authors have shown that temperature and catalyst dosage have a significant impact in both yield and selectivity.[57] Regarding temperature, the conclusion was the same as what can be concluded from the results presented here, which consider the economics of a whole biorefinery: graphs c and e of Figure 21 shows that MSP decreases as temperature decreases. However, although it was shown by Girisuta *et al.* (2013) that higher CL is preferable to increase both yield and selectivity,[57] the same was not observed for MSP of EL. Figure 22 presents the simulated yield of products at several conditions. Graph d of Figure 22 clearly shows that higher yield and selectivity towards LA are obtained in low RT and higher CL.

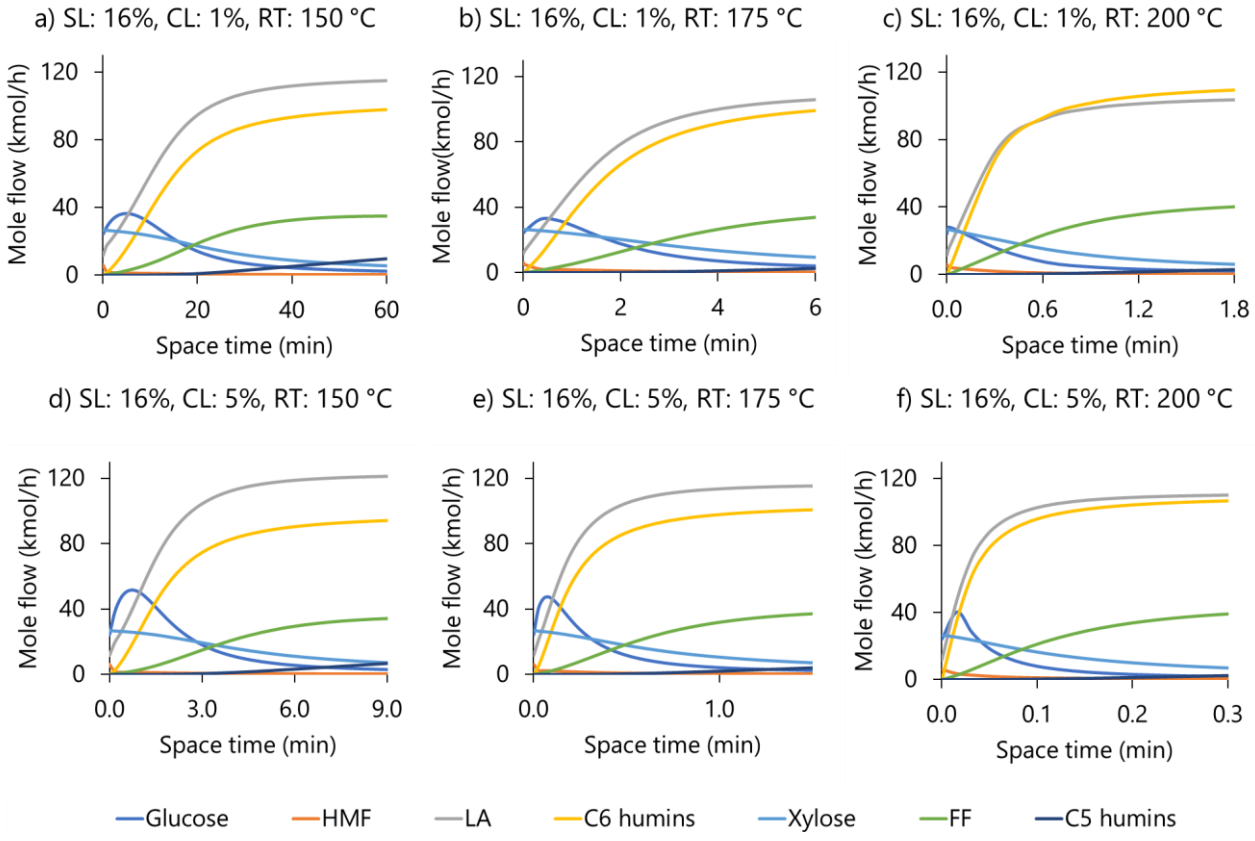


*Figure 22. Mole flow rate of selected hydrolysis products in different reaction conditions of RT (150 °C, 175 °C, 200 °C) and CL (1%, 5%) in the outlet of the second hydrolysis reactor. C6 humins represent the humins derived from cellulose, whereas C5 humins represent the humins derived from hemicelluloses. As the molecular structure of humins is not well established in the literature, the molar weights of the cellulose's and xylan's repeating units were used for C6 humins and C5 humins, respectively.*

For a fixed RT, the selectivity increases as the CL increases (graphs of Figure 22 compared in the vertical direction). On the other hand, for a fixed CL, the selectivity greatly decreases as RT increases (graphs of Figure 22 compared in the horizontal direction). The increase in CL from 1% to 5% increased selectivity in 8% (at CC: 99% CC, RT: 150 °C, SL: 16%). Nevertheless, the main factor that originated the divergence of the effect of CL between the results considering solely yield and selectivity of hydrolysis (Figure 22) and the analysis of MSP of EL (Figure 21) resides in process design and the consequences of dealing with a high concentration of sulfuric acid.

First, a high concentration of sulfuric acid, which optimizes selectivity, demands more expensive material of construction and maintenance. Therefore, as a result of the oxidizing strength of the contents being handled, a higher content of nickel is required in some equipment. For example, the material factor for a heat exchanger increases from 2.75 to 3.75 when switching from stainless steel to a high-nickel alloy such as Hastelloy.[67] In the economic analysis, the additional requirement of a more expensive material of construction was considered as a consequence of the increase in sulfuric acid use. The maintenance was fixed at 5% of the CAPEX, which in some way reflected the impact of the high use of sulfuric acid because of its direct effect on CAPEX.

Second, there is the limitation of the extraction solvent. In this process, both sulfuric acid and LA are solutes. The solvent, MTHF, has partial miscibility with water, and the addition of solutes in a proportion too high may yield in a concentration outside the two-phase region, thus preventing phase split. In view of the foregoing, the use of high CL increases the proportion of sulfuric acid to LA. Consequently, the maximum LA content in concentrated hydrolysate decreases and more solvent per mass of LA is required in the recovery process. The demand for more solvent impacts steam demand as a consequence of its recycling process.

Other factors that were not considered in this simulation also play a role regarding the use of high CL. First, chemicals degrade in the presence of sulfuric acid. Most of the FF is removed from hydrolysate in the flash vessel after the second hydrolysis reactor, and the remainder is removed in the first evaporator of the multiple-effect evaporator step. Even though both flash vessel and evaporator present low residence time, they may contribute to the oxidation of FF, which may be reduced using lower CL. Moreover, products of FF degradation can attach to vessel walls, thus

increasing maintenance frequency and decreasing heat transfer efficiency.[20] Also, the presence of sulfuric acid in a high proportion in the extractor may lead to increased losses of MTHF. Like most ethers, the C-O bond in MTHF is susceptible to cleavage in an acid environment. In stability trials, Aycock (2006) demonstrated a loss of 0.54% of MTHF after 4 h in a 4% solution of MTHF in a 5 mol/L solution of HCl.[100] Considering high CL, MTHF may be exposed to sulfuric acid concentrations higher than 20%, rendering the process impractical because of undesirable side reactions.

## 5.3. The optimized biorefinery

The surrogate model with coefficients presented in Table 14 was used in a gradient-based optimization to determine operating conditions that minimize the MSP of EL. Optimized conditions predicted by the model are presented in Table 15. Observe that three out of the four variables reached their upper or lower bounds. In the first trials with different design spaces, this behavior was observed, and the design space was changed to the final limits presented in section 3.1. Exploration beyond these limits was impossible for two reasons. First, in the case of CC, the limit of 99% is reasonable. Second, in the case of RT and CL, these were the limits to which the kinetics for cellulose degradation were obtained.[57]

*Table 15. Results for the optimized conditions to minimize MSP of EL.*

| Variable | Coded value | Model value |
|---|---|---|
| SL | +1.04 | 16.2% |
| CC | +2.00 | 99.0% |
| CL | -2.00 | 1.00% |
| RT | -2.00 | 150 °C |
| MSP | - | $0.22/kg |

Exploring the reaction below 150 °C of temperature and 1% of CL would be interesting to understand to which point the decrease of reaction rate and the exponential increase in reactor size is still economically attractive for this process. Observing graph f in Figure 21, it is possible to

notice a decrease in MSP for lower RT and CL, which might stop by the steep increase in capital cost as the reaction is carried out at lower rates. However, extrapolating the kinetics to this region could mislead conclusions. As the concentration of sulfuric in hydrolysis decreases, other less strong acids produced during hydrolysis (FA, AA, and LA) start having a more significant contribution in catalysis, and the model may render a negative deviation of the real conversion. On the other hand, mass and heat transfer resistances vary with temperature. Hence, the kinetics may yield divergent results compared to what would be observed experimentally because these phenomena were discarded in the modeling of the hydrolysis reactor or the kinetic model.

The obtained optimized conditions were used in the simulation of an optimized biorefinery. Key indicators obtained from the process simulation of this optimized case are presented in Table 16. Table 17 presents the estimated CAPEX for each section of the optimized biorefinery. As a matter of comparison of the impact of SL, case 17 of the DOE with the lowest SL has a CAPEX of $35.8 million for the sections including hydrolysis of cellulose, solids separations, and evaporators, which is 77% more than the CAPEX of the same sections in the optimized case.

*Table 16. Summary of results of the optimized biorefinery.*

| Parameter | Value |
|---|---|
| Yield of ethanol ($kg/t_{cane}$)[a] | 60.6 |
| Yield of EL ($kg/t_{cane}$) | 22.2 |
| Yield of FF ($kg/t_{cane}$) | 11.8 |
| Yield of FA[b] ($kg/t_{cane}$) | 2.10 |
| Yield of electricity ($kWh/t_{cane}$) | 71.1 |
| Steam consumption, biorefinery ($kg/t_{cane}$) | 640 |
| Steam consumption, EL ($kg/kg_{EL}$)[c] | 8.95 |
| Steam consumption, FF ($kg/kg_{FF}$)[c] | 9.07 |
| Steam consumption, FA ($kg/kg_{FA}$)[b,c] | 5.35 |
| Reactors for hydrolysis of hemicelluloses | 10x147 $m^3$ |
| Reactors for hydrolysis of celluloses | 5x210 $m^3$ |

*Table 16 (continued). Summary of results of the optimized biorefinery.*

| Parameter | Value |
|---|---|
| MTHF to LA mass ratio in liquid-liquid extraction | 2.62 |

a) does not include ethanol consumed in esterification of LA to EL.

b) considering real content of FA (49.2% FA, 2.6% AA, 0.7% LA, 0.3% MTHF, 47.2% water).

c) the required steam to produce the remaining ethanol which was not used for esterification was calculated using the steam consumption of an optimized autonomous distillery (Table 8); then, the balance was divided between FA, FF and EL using revenue as a weighting factor.

*Table 17. CAPEX of different sections of the optimized biorefinery.*

| Sector | CAPEX ($10^6$ $) |
|---|---|
| Sugarcane processing and ethanol production | 281.2 |
| Hydrolysis of hemicelluloses | 20.75 |
| Recovery of FF | 7.712 |
| Hydrolysis of cellulose and hydrolysate preparation | 20.16 |
| Recovery of LA and esterification to EL | 16.26 |
| CHP | 98.47 |

With these conditions, the determined MSP of EL for the optimized case was $0.240/kg, $0.0197/kg more than the value predicted by the surrogate model (8.21% of error). This result demonstrates the feasibility of the project to produce EL since the obtained MSP represents a fraction of what would be the equivalent price of EL based on the energy price of diesel ($0.412/kg).

Other routes for the use of LA have been proposed and economically assessed in the literature. Braden et al. (2011) suggested the conversion of LA to GVL via catalytic transfer hydrogenation using the coproduct FA as hydrogen source over a Ru/Re (3:4 metal proportion, 15% content) catalyst supported on carbon.[101] Then, the GVL is converted to butene and lastly to alkene oligomers which can be blended into gasoline (Figure 23). In this route, the authors obtained a price

of $4.31 per gasoline gallon equivalent considering an IRR of 10% (reference year: 2007).[101] Considering a LHV of 42.9 MJ/kg for gasoline,[102] this equates to a price of $41.6/GJ (value updated to 2017), [103] whereas the obtained energy price of EL in the optimized biorefinery developed in this study was $9.86/GJ (LHV of EL: 24.34 MJ/kg) for a MARR of 12%. Another suggested route is the conversion of LA to 5-nonanone (Figure 24).[104] In this route, the final price of the product is $8.49/kg, with prospects to be reduced to $1.29/kg, considering an LA price of $0.34/kg (reference year: 2007) and a MARR of 10%. Considering an LHV of 35.58 MJ/kg for 5-nonanone (calculated in Aspen Plus 8.6), the 5-nonanone price in the best scenario would be $42.9/kg (value updated to 2017). Therefore, the results indicate that EL produced in the optimized biorefinery scenario has a more significant market potential due to its low cost, which makes it competitive with petroleum-based products.

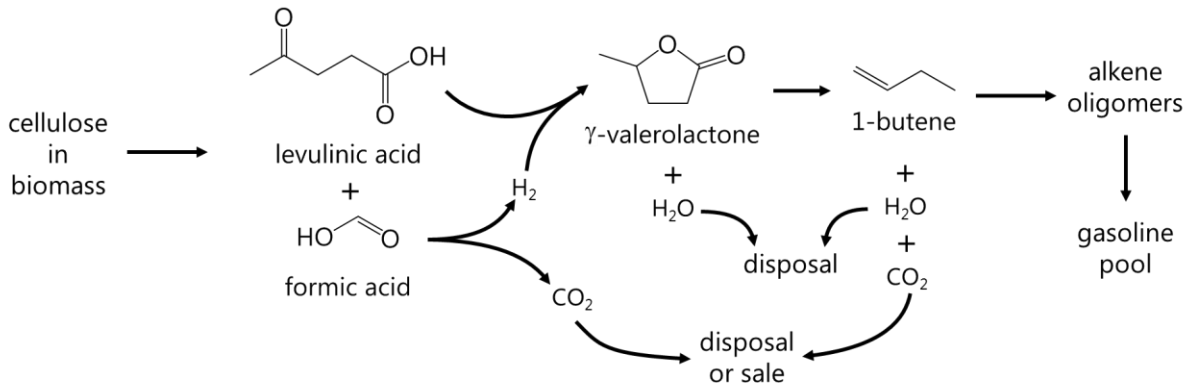


*Figure 23. An alternative use for LA: production of alkenes for gasoline blending. In the best price scenario, $CO_2$ is sold at $36/t.*[101]

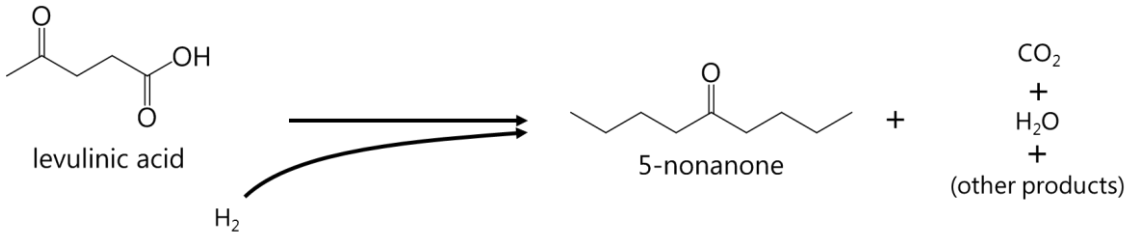


*Figure 24. An alternative use for LA: synthesis of 5-nonanone for solvent use.*[104]

## 5.4. Severity of hydrolysis and possible advances in reactor design

Advances in reactor design or better catalysts may improve process economics. Results of this study have shown that SL is by far the main variable impacting the MSP of EL. Preferred reaction conditions include the lowest CL and the lowest RT – which translates into low hydrolysis severity.[105] Therefore, the residence time in hydrolysis has low impact in process economics given that the SL is high enough. This is interesting because sulfuric acid has a very high acid strength, which motivated the use of costly material of construction and led to a capital-intensive investment (Table 17). The use of other acids (including organic acids such as FA) as catalysts may be enough to promote hydrolysis in less severe conditions and may require materials of construction with moderate cost. Moreover, other catalysts must be tested to verify the behavior of humins formation in their presence.

The study of humins formation is essential for several reasons owing to the impact of poor selectivity in economic performance. First, as observed from the results of the DOE, factors that affect the final concentration of LA in the hydrolysate product of the second reactor (SL and CC) play an important role in economics. Observing graph a in Figure 22, it is clear that, while it represents an optimized condition, the extension of the reaction to humins is almost the same as the extension of the reaction to LA. Literature reports several pathways to hinder humins formation in the synthesis of LA. In an investigation on the effect of reaction parameters on the formation of humins, it was observed that hydroxyl and carbonyl groups of furans and monosaccharides were protected against these side reactions by the presence of an alcohol.[106]

Protonation of the oxygen atom in carbonyl groups of FF or HMF is thought to be one of the mechanisms in humins formation.[107] The use of different solvents and catalysts may reduce the availability of free protons that lead to increased humins formation. On the other hand, these free protons are fundamental to catalyze the reaction of HMF to LA.[108] Therefore, conditions that foster LA formation and at the same time reduce humins formation sound mutually exclusive. The results showed here demonstrate that, although undesirable, a process with low selectivity for conversion of biomass to furans and their derivatives is still profitable. Moreover, the stepwise reactor design proposed in this study demonstrated the reduced formation of humins. Figure 25 shows the

difference in humins formation when a single step is used instead of a stepwise approach, as suggested for the optimized biorefinery. The curve for humins produced from the pentose fraction of biomass in graph a of Figure 25 appears to be linear instead of asymptotic because the resinification reaction assumed for decomposition of pentoses to humins was far from limiting conditions.

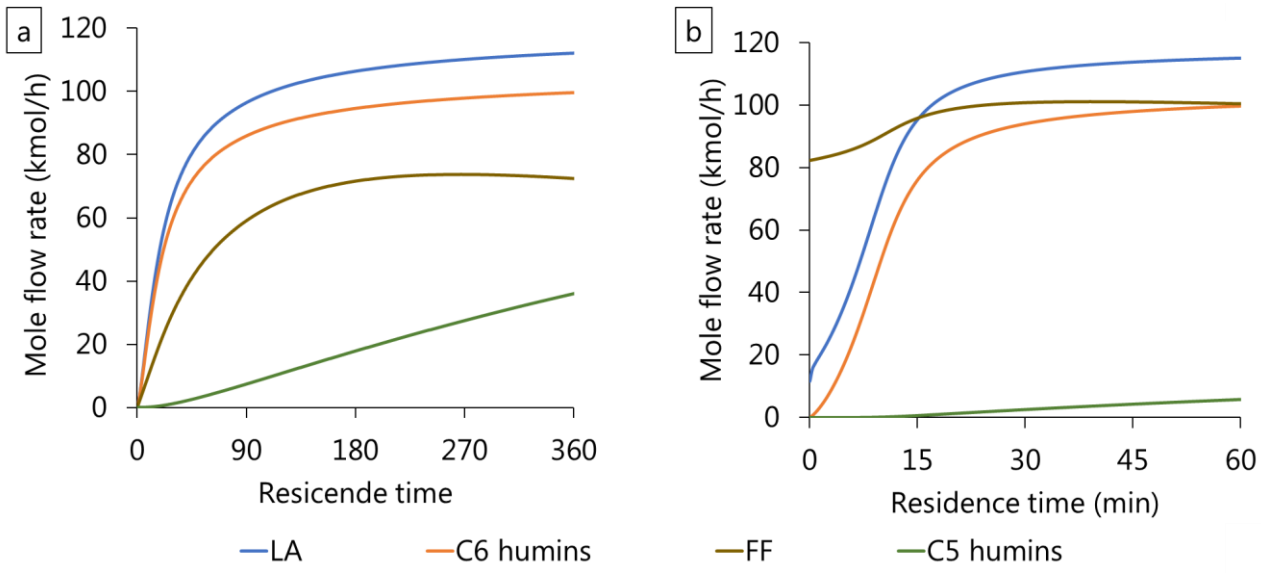


*Figure 25. The impact of stepwise biomass hydrolysis in the mole flow of products: a) single step hydrolysis on a continuous stirred tank reactor and b) Rosenlew reactor followed by a continuous stirred tank reactor. Conditions in the continuous stirred tank reactor: 16% SL, 1% CL, 150 °C RT.*

Removing furans from contact with sugars decrease humins formation.[15] This phenomenon was proven in trials with hydrolysis and simultaneous extraction of furans and other hydrolysis products with more affinity for any solvent.[109] This approach is very useful in the synthesis of HMF, and examples of solvents tested successfully include butanol, methyl isobutyl ketone, alkylphenols, and dimethyl sulfoxide, including combinations of solvents and addition of inorganic salts to modify partition coefficients.[110–114] Yet, solvent extraction parallel to hydrolysis should be considered carefully in the synthesis of LA given that the use of solvents in hydrolysis is demonstrated to increase the final cost of EL,[15] which is intended to be used as a low-cost biofuel.

Availability of protons in reaction media is shown to impact both products and side products formation. Thus, developing selective catalytic systems may improve process economics. Different studies have considered a combination of enzymatic hydrolysis followed by dehydration of sugars in different steps. Schmidt *et al.* (2017) observed losses of glucose of more than 30% using this approach.[115] Alipour and Omidvarborna (2017) attained a yield of LA of 70% of the theoretical after combining enzymes, solvent, and acidic ionic liquid in a simultaneous isomerization and reactive extraction followed by a back extraction process.[116] These studies focus on different catalytic systems to obtain sugars and do not show a great advantage over the simple and inexpensive approach of using sulfuric acid as a catalyst for all reactions, as the optimized process developed in this study presented a selectivity of 65% for LA. The study of Girisuta *et al.* (2013) obtained a yield of 63% at 150 °C. Another example of optimization attained a yield of 68% using HCl as a catalyst at long residence time and 149 °C.[117]

In LA synthesis, the problem of humins can be summarized as lack of selectivity in the conversion of monosaccharides and furans, not in lack of selectivity in the hydrolysis of polysaccharides. Hydrolysis of cellulose to glucose for cellulosic ethanol production represents a challenge because of the toxicity of the hydrolyzed liquor due to the presence of furans. However, the same glucose-rich liquor containing furans might be ideal for LA synthesis via other more selective catalysts. For example, 2,5-furandicarboxylic acid can be obtained from HMF via catalysis with metals,[118] or via highly-selective catalysis with enzymes.[119] For instance, the option of enzymatic catalysis is being developed by Corbion for the commercial production of 2,5-furandicarboxylic acid.[7]

One example of study in the direction of using a different catalyst in the dehydration of sugars was presented by Weingarten *et al.* (2013) and demonstrated the importance of developing a selective catalyst for LA synthesis: increasing the fraction of Brønsted acid sites from 12% to 38% reduced the selectivity to humins from 62% to 23% at a fixed conversion of 40% of glucose.

[7] Presentation given by Jan Wery (Corbion, The Netherlands) at the 3rd BBEST – Brazilian Bioenergy Science and Technology Conference, 17-19 October 2017, Campos do Jordão, Brazil.

Therefore, future studies may focus on the development of better catalysts for the dehydration of hydrolyzed hexoses to HMF followed by rehydration of HMF to LA.

## 5.5. Risk analysis and market uncertainties

As discussed in the methodology, four scenarios were drawn to examine the impact of market conditions on the production of EL. Scenarios EL-t, EL-f, and EL-p represent the optimized biorefinery proposed in this work for production of EL. Products of biomass hydrolysis are priced in three conditions:

- EL-t: prices compatible with current market conditions;
- EL-f: price of FF reduced to make viable its use as biofuel precursor;[29]
- EL-p: both FF and EL receive a premium of 20% over their future price.

These scenarios were compared to a fourth benchmark scenario producing only ethanol and electricity using current technology in optimized conditions, ET-t. Economic results of these four scenarios are available in Table 18. Scenario EL-t presents the best results at the coondition of FF being sold at the current price. This condition is incompatible with the main goal of the production of EL, which is to focus on the sizeable fuel market. Yet, this solution may become interesting for a pioneering company willing to invest in EL production because the high FF price may be used to pay for the investment faster and FF price will not drop from the current price to the possible future price instantly.

*Table 18. Results of the different scenarios considered in the economic analysis.*

| Scenario | EL-t | EL-f | EL-p | ET-t |
|---|---|---|---|---|
| CAPEX ($10^6$ $) | 445 | 445 | 445 | 396 |
| Sulfuric acid requirement (kt/y) | 0.87 | 0.87 | 0.87 | 0.0 |
| MTHF requirement (kt/y) | 1.99 | 1.99 | 1.99 | 0.0 |
| Ethanol production (kt/y) | 241 | 241 | 241 | 269 |
| FF production (kt/y) | 47.0 | 47.0 | 47.0 | 0.0 |

*Table 18 (continued). Results of the different scenarios considered in the economic analysis.*

| Scenario | EL-t | EL-f | EL-p | ET-t |
|---|---|---|---|---|
| FA production (kt/y) | 17.1 | 17.1 | 17.1 | 0.0 |
| Electricity production (kt/y) | 285 | 285 | 285 | 742 |
| EL production (kt/y) | 89.5 | 89.5 | 89.5 | 0.0 |
| Yearly total costs ($10^6$ $) | 133 | 127 | 127 | 123 |
| Yearly revenues ($10^6$ $) | 302 | 236 | 247 | 221 |
| IRR | 20.5% | 13.9% | 15.0% | 14.0% |
| Net present value | 299 | 60.6 | 98.8 | 57.5 |
| Profitability index | 67% | 14% | 22% | 22% |
| Payback period | 3.9 | 5.6 | 5.3 | 5.6 |

Comparing scenario EL-f in which FF is sold at a price that makes the production of FF-derived biofuels viable, it is noticed that using bagasse to produce more electricity instead of using it to produce chemicals is more attractive by a narrow margin. However, considering a premium over the energy price of FF and EL has a great result: even though the CAPEX in scenario EL-p is 12% higher than in scenario ET-t, the increase in revenue makes scenario EL-p more attractive than scenario ET-t. Assuming a 20% premium over the current energy price of a lignocellulosic biofuel is adequate as long as biofuel mandates are being increased all over the world: the higher requirement of biofuels may increase demand and price of these chemicals.[120–122] Even though higher figures have been observed in the literature, this value considers a safe margin because biofuel standards are not currently enforced for several reasons, and these changes may take time to be established.[123]

Figure 26 presents the probability distribution of IRR for the four scenarios. As explained before, EL-t, though very attractive, includes mutually exclusive conditions that make it completely unrealistic in the long run. Yet, it demonstrates that in the short term, an IRR higher than 12% is an event that happens almost surely. It is interesting that, even though the IRR of ET-t is higher than the IRR of EL-f, the probability of presenting an IRR higher than 12% is higher for scenario EL-f. This happens as a result of the revenues of EL-f being complemented by revenue sources other than ethanol and electricity, hence decreasing the dependence on the revenue of these only two sources,

which is an important aspect for biorefineries. Although a great part of the market for chemicals is dependent on crude oil price, the price of each of these chemicals is not affected by fluctuations to the same extent. Therefore, diversifying product portfolio decreases the risk of an investment.[16,79]

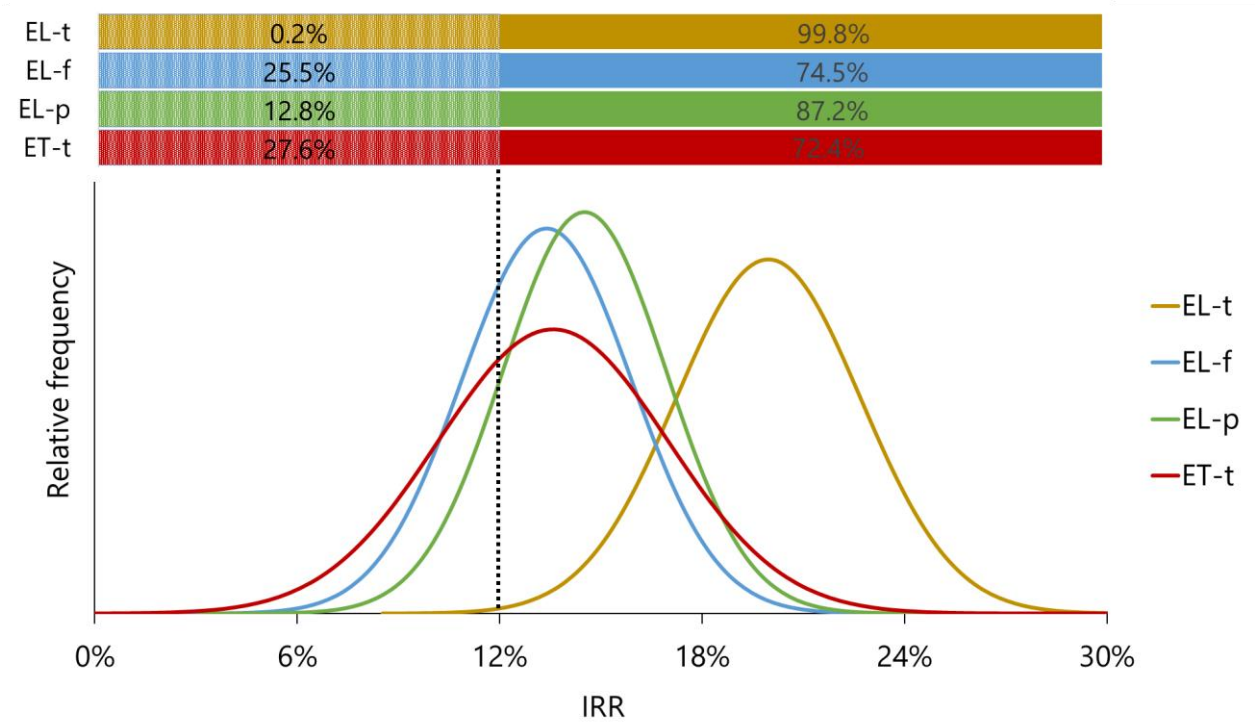


*Figure 26. Probability distribution of IRR for the four scenarios considered in the economic analysis and the probability of resulting in an IRR lower or higher than 12%.*

Figure 27 to Figure 30 present the sensitivity analysis of IRR at different percentiles of inputs. Since all variables of economic analysis were supplied as probability distributions (or functions of them), cumulative distributions were calculated to link the probability of an input assuming certain value to the respective resulting IRR. For instance, the probability of ethanol assuming a value less than \$548/t (5$^{th}$ percentile) is less than 5%. On the other side, assuming a value higher than \$776/t (95$^{th}$ percentile) is less than 5%. This analysis is more useful than the usual sensitivity analysis based on parameter variation inside a range because it links the probability of a variable to assume a certain value with its corresponding impact in the dependent variable (in this situation, the IRR).

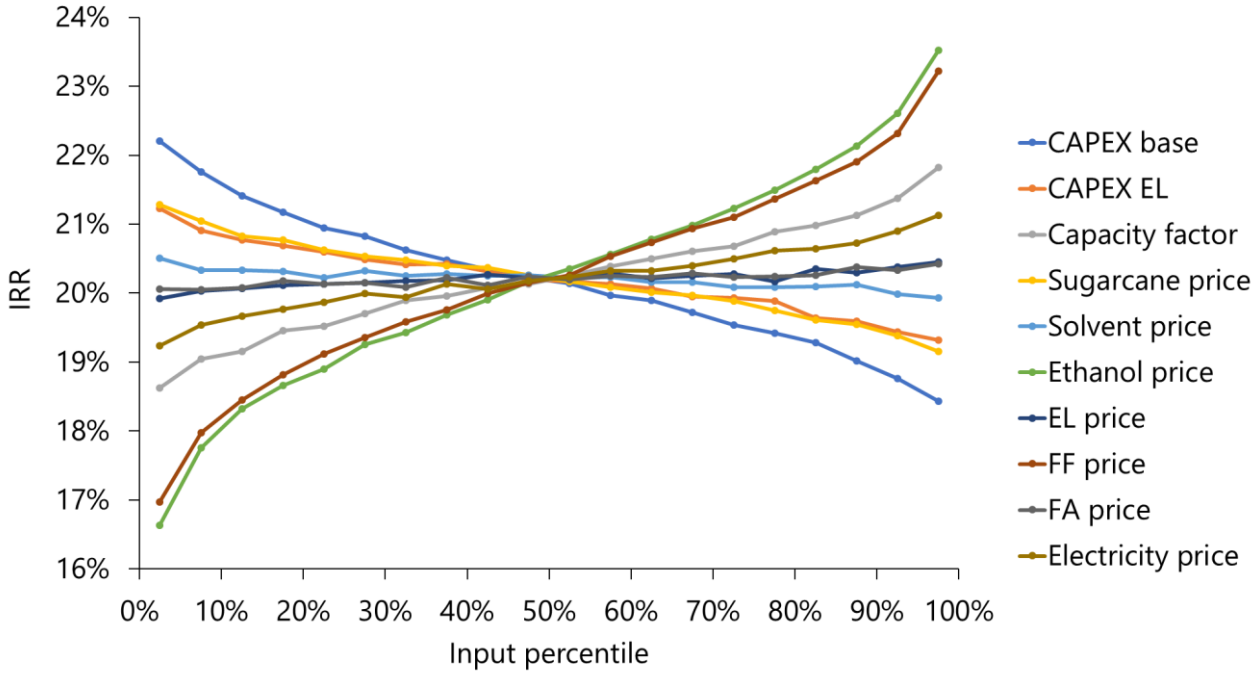


*Figure 27. Sensitivity analysis of input variables for scenario EL-t.*

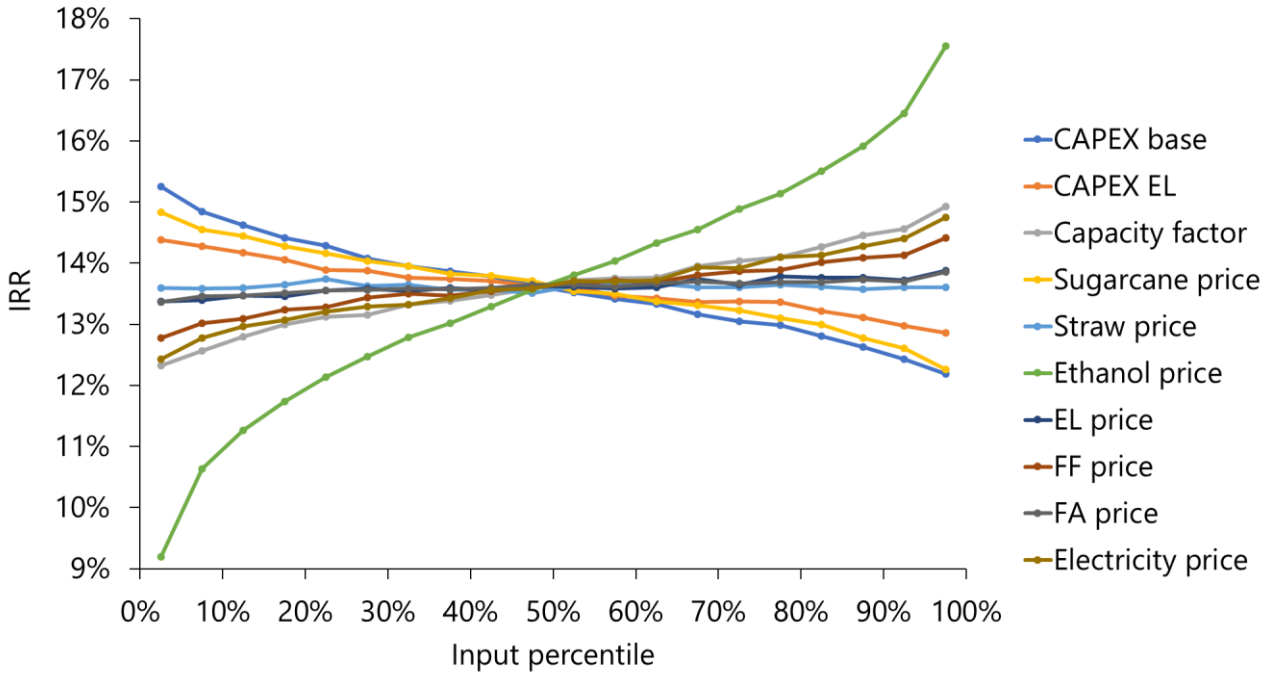


*Figure 28. Sensitivity analysis of input variables for scenario EL-f.*

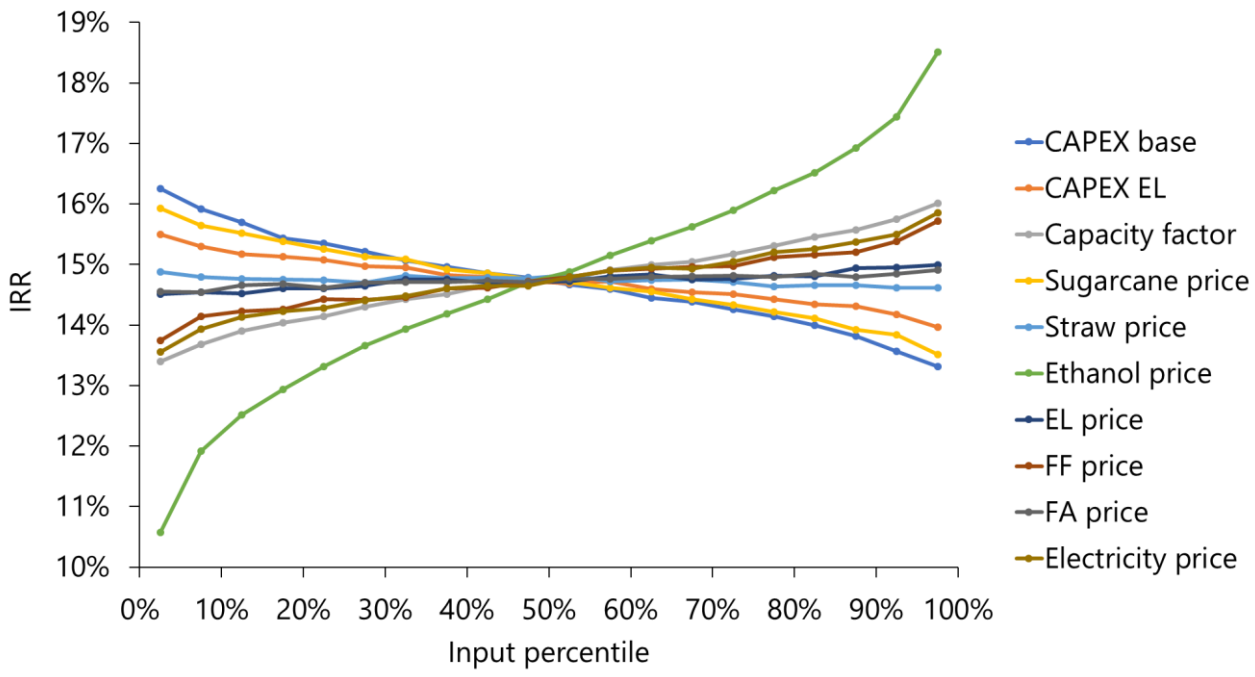


*Figure 29. Sensitivity analysis of input variables for scenario EL-p*

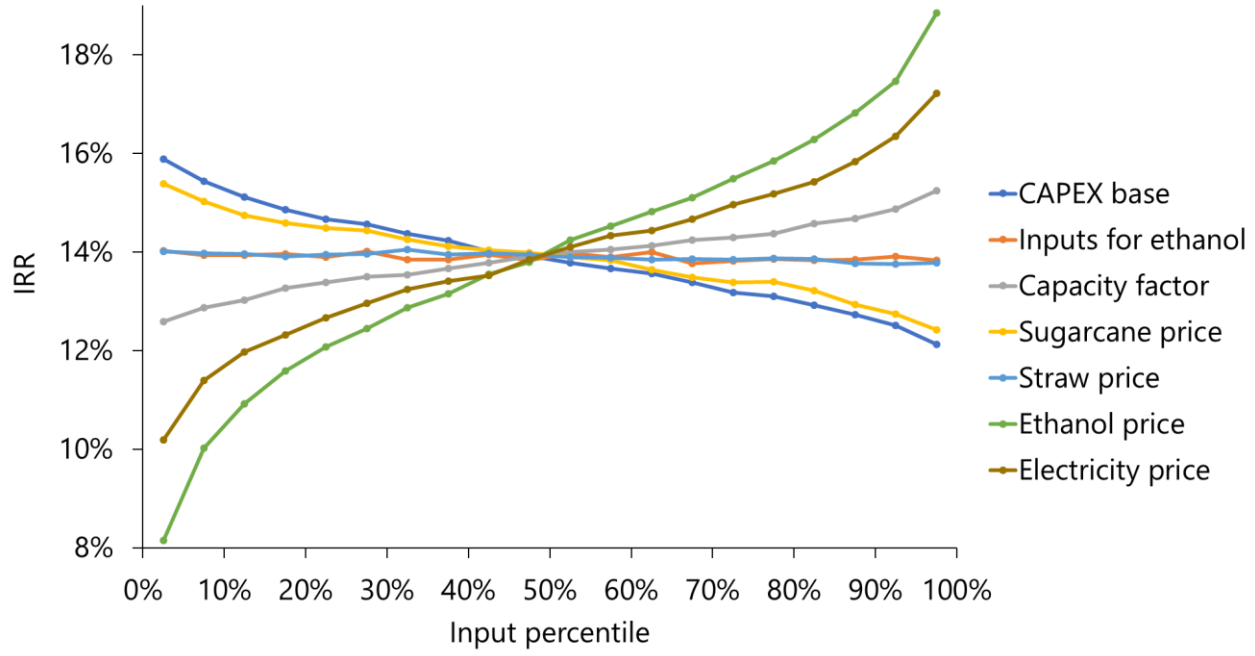


*Figure 30. Sensitivity analysis of input variables for scenario ET-t*

In all scenarios, ethanol is the main factor impacting the IRR. Especially in scenario EL-t, in which FF is sold at the current market price, FF and ethanol prices have almost the same impact in IRR. In this scenario, FF contributes to 28% of the total revenue whereas ethanol contributes to 53%. Although FF contribution to revenue is about half of the ethanol, the probability distribution of its price is more dispersed: the standard deviation of FF represents 18% of its average value, whereas, in the case of ethanol, its standard deviation represents 10% of its average value, as consequence of the difference in price fluctuation for these two commodities.

Sulfuric acid is inexpensive and has a low requirement. Consequently, it was not ranked among the 10 most important variables affecting cost in scenarios producing EL. This is a direct consequence of process design, which made recycling of sulfuric acid possible with the solvent extraction of LA. If not recycled, sulfuric acid would need to be neutralized, and a proper destination for the residue would need to be included in technoeconomic analysis. Processes for the production of carboxylic acids from fermentation, such as lactic acid or succinic acid, include neutralization steps and produce large quantities of gypsum whose destination is uncertain and represents a burden in process development.[6,124,125]

EL has a low impact over the IRR of scenarios EL-t, EL-f, and EL-p despite its high contribution to revenues (in the range of 12% to 18%) as a result of its low standard deviation based on diesel price (Table 6). This low standard deviation reflects the fact that the price of diesel has been regulated by the Brazilian Government for a long time. Parity with the international fluctuation of oil price has only been established recently.[126]

The impact of the capacity factor demonstrates the effect of droughts, aging of sugarcane fields, lack of investments, or poor yield. The 2017/2018 harvesting season in Brazil registered a decrease in total sugarcane harvested of 3.6%, with another reduction of 1.2% expected for 2018/2019, even though ethanol is facing a higher demand because of the spike in gasoline price.[127] Variations in capacity factor also cover variations in the operational year due to differences in dry and wet season observed year after year. Sensitivity analysis demonstrated that the capacity factor is very important for the economic success of the biorefinery, and its variation has a similar effect over any scenario considered in this study.

Nevertheless, the effect of variations in electricity price was especially different between scenario ET-t and the other scenarios diverting part of the bagasse to the production of chemicals. Again, this is a consequence of portfolio diversification observed in robust biorefinery designs. The electricity market in Brazil observed a crisis recently as a consequence of a severe drought that affected the region in which most of the Brazilian hydroelectric dams are located, and electricity prices soared.[128,129] Yet, lately, wind power has been expanding in Brazil and played a decisive role in decreasing the electricity price in renewable energy auctions for electricity supply contracts.[77] Therefore, this may open more opportunities for lignocellulosic biofuels in the future than for electricity as an alternative destination for bagasse in biorefineries, which qualifies the use of bagasse for production of biofuel a safer investment in the long run.

# 6. Conclusions and outlook

Production of levulinates represents a challenge in the biofuels sector. Reactor operability, operating conditions that lead to attractive economic results, poor selectivity, and market uncertainties are among the factors that hinder the large-scale production of LA and EL.

## 6.1. Recovery of products

In this study, use of MTHF as an extraction solvent for recovery LA from hydrolysate was proposed with positive results. The choice of solvent demonstrated great results as a consequence of the affinity between solvent and solute – both oxygenated chemicals. The lack of affinity between LA and another extraction solvent such as hexane yields a costly process.

The recovery of LA from dilute hydrolysate had a large impact in process economics. The requirement of high concentration of LA comes as a consequence of the mutual solubility of MTHF and water and the requirement to distillate MTHF before recycling. Yet, other oxygenated solvents need to be tested and economically assessed to determine promising options for LA recovery other than MTHF. Solvents with a high boiling point should be explored to avoid an azeotrope with water, FA, and AA, which may render overly complicated recycling schemes.

An alternative use for FF was included in the economic analysis, whereas analternative use for FA was not proposed because it has a large market and several applications. Still, the

applications of FA can be found inside the production of LA. Large amounts of FA can be produced as a coproduct of LA biorefineries. Thus, FA can be applied in the catalysis of the same process in appropriate conditions. FA has lower acid strength compared to sulfuric acid. Yet, the high availability of FA inside an EL biorefinery and the proven positive effect of lower severity on the economics of an EL biorefinery aid to the need of studying the hydrolysis of bagasse catalyzed by FA.

## 6.2. Stepwise approach and selectivity

Losses of products in the form of humins represent a burden because they are a inferior hydrolysis product which compromise reactor operability. Humins formation is ascribed to condensation reactions between furans and sugars. This study demonstrated that removal of FF in a first, less severe reaction stage is fundamental to decrease the production of these products significantly and increase overall process yield.

The stepwise approach might be explored even further to break down the function of the second hydrolysis reactor according to the three desirable reactions which take place on it, namely: hydrolysis of cellulose, dehydration of glucose, and rehydration of HMF to LA. Moreover, the appropriate study of humins, including applications, handling, and impacts on operability need to be studied further to understand if the assumption that they can be considered as a residue that can be burned in the biomass furnace of the biorefinery is adequate. The contamination of this residue with sulfur from sulfuric acid and its implications in the emission of pollutants should be evaluated as well.

## 6.3. Catalysis focused on different reaction steps

Continuing the question of focusing on different steps of the reactions towards LA, it is important to notice that not all steps require the same catalyst. As observed in this study, the autocatalyzed hydrolysis of hemicelluloses increases process yield. This evidence demonstrates the power of using less strong acids as catalysts for hydrolysis. Moreover, other investigators have tried to apply different catalysts to hydrolysis and dehydration/rehydration reactions. Possibly this approach can yield improved results in the future with the development of more selective combinations of catalysts tailored to each reaction step. Reaction solvent should be considered as

well as another variable to be studied considering the different reaction steps, though carefully because of the costs associated with solvent losses and recycling. Overall, fractioning the biomass as it is done with crude oil in refineries has demonstrated great potential, and breaking down the process into more steps may increase selectivity and improve economic results.

## 6.4. Solids loading, catalyst loading, temperature, and conversion

The analysis of MSP of EL considering several reaction variables has demonstrated that SL has a notorious impact on economics. A high concentration of LA in the hydrolysate is highly desirable, and SL and CC are the key variables that affect this parameter and decrease the steam requirement. Decreasing steam requirement is fundamental because both steam and LA production compete for bagasse availability.

The desirable reactor temperature was observed to be aligned with previous findings in the literature. However, it was found that lower catalyst dosage and higher residence time are preferable to make the process more economically attractive, even though it has a negative effect on selectivity. The use of high concentration of sulfuric acid makes the recovery of LA costlier. Moreover, the increased use of a catalyst may come with other negative implications which were not included in the conception of this biorefinery model, such as losses of products in downstream processing due to the strongly oxidizing environment. These results demonstrate the possibility to achieve desirable economic performance through the sacrifice of process selectivity.

The results of reactor optimization also proved that EL can be produced at a very low price. Indeed, the MSP to achieve an IRR of 12% represented about half of the expected price of EL considering the energy price of diesel in Brazil. Besides its application as an energy carrier, EL has fuel additive properties fundamental to biodiesel and diesel, which may justify the same price of diesel on energy basis as a lower bound for EL price.

## 6.5. Diversification of product portfolio

Comparison of the optimized EL biorefinery to an equivalent autonomous ethanol distillery with the production of electricity showed that producing EL, FF, FA, and electricity from bagasse instead of only producing electricity represent a better investment. Of course, these results

depend on the successful operation of hydrolysis of biomass to LA, which is still recognized as a challenge regarding operability. Yet, the results indicated that albeit selectivity is low (a factor which can be worked upon with development of better catalytic systems), the economics of the process is still promising.

Therefore, using bagasse as feedstock for production of furans and derivatives such as LA and EL is proven to be an attractive route, even though there is a long pathway in the development and maturation of biomass conversion processes. Although this study is based on assumptions for successful reactor operability, it provides insights of the impact of reaction parameters on economics and demonstrates directions for researchers and industry to develop better processes and make the production of EL truly viable in the future.

□

# References

[1] G. A. Florides, P. Christodoulides, *Environ. Int.* **2009**, *35*, 390–401.

[2] R. Stein, *The Automobile Book*, Paul Hamlyn, **1967**.

[3] T. Wilberforce, Z. El-Hassan, F. N. Khatib, A. Al Makky, A. Baroutaji, J. G. Carton, A. G. Olabi, *Int. J. Hydrogen Energy* **2017**, *42*, 25695–25734.

[4] Ö. Simsekoglu, *Transp. Policy* **2018**, DOI 10.1016/j.tranpol.2018.03.009 (in press).

[5] S. M. Jowitt, T. T. Werner, Z. Weng, G. M. Mudd, *Curr. Opin. Green Sustain. Chem.* **2018**, *13*, 1–7.

[6] B. C. Klein, J. F. L. Silva, T. L. Junqueira, S. C. Rabelo, P. V. Arruda, J. L. Ienczak, P. E. Mantelatto, J. G. C. Pradella, S. V. Junior, A. Bonomi, *Biofuels, Bioprod. Biorefining* **2017**, *11*, 1051–1064.

[7] G. Z. Papageorgiou, D. G. Papageorgiou, Z. Terzopoulou, D. N. Bikiaris, *Eur. Polym. J.* **2016**, *83*, 202–229.

[8] J. McEniry, P. O'Kiely, P. Crosson, E. Groom, J. D. Murphy, *Biofuels, Bioprod. Biorefining* **2011**, *5*, 670–682.

[9] B. Dale, *Biofuels, Bioprod. Biorefining* **2018**, *12*, 5–7.

[10] T. Stevanovic, in *Lignocellul. Fibers Wood Handb.*, John Wiley & Sons, Inc., Hoboken, NJ, USA, **2016**, pp. 49–106.

[11] H. Guo, B. Zhang, Z. Qi, C. Li, J. Ji, T. Dai, A. Wang, T. Zhang, *ChemSusChem* **2017**, *10*, 523–532.

[12] M. O. S. Dias, T. L. Junqueira, O. Cavalett, M. P. Cunha, C. D. F. Jesus, C. E. V. Rossell, R. Maciel Filho, A. Bonomi, *Bioresour. Technol.* **2012**, *103*, 152–161.

[13] S. Fernando, S. Adhikari, C. Chandrapal, N. Murali, *Energy and Fuels* **2006**, *20*, 1727–1737.

[14] S. Kim, B. E. Dale, *Biofuels, Bioprod. Biorefining* **2015**, *9*, 422–434.

[15] J. F. Leal Silva, R. Grekin, A. P. Mariano, R. Maciel Filho, *Energy Technol.* **2018**, *6*, 613–639.

[16] G. C. Q. Pereira, D. S. Braz, M. Hamaguchi, T. C. Ezeji, R. Maciel Filho, A. P. Mariano, *Bioresour. Technol.* **2018**, *250*, 345–354.

[17] J. F. L. Silva, T. L. Junqueira, B. C. Klein, S. V. Jr, A. M. Bonomi, R. M. Filho, in *39th Symp. Biotechnol. Fuels Chem.*, **2017**.

[18] A. Morone, M. Apte, R. A. Pandey, *Renew. Sustain. Energy Rev.* **2015**, *51*, 548–565.

[19] S. Kang, J. Yu, *Biomass and Bioenergy* **2016**, *95*, 214–220.

[20] K. J. Zeitsch, *The Chemistry and Technology of Furfural and Its Many By-Products*, Elsevier, **2000**.

[21] J. J. Bozell, L. Moens, D. . Elliott, Y. Wang, G. . Neuenscwander, S. . Fitzpatrick, R. . Bilski, J. . Jarnefeld, *Resour. Conserv. Recycl.* **2000**, *28*, 227–239.

[22] T. Werpy, G. Petersen, *Top Value Added Chemicals from Biomass Volume I—Results of Screening for Potential Candidates from Sugars and Synthesis Gas Energy Efficiency and Renewable Energy*, Oak Ridge, **2004**.

[23] F. D. Pileidis, M.-M. Titirici, *ChemSusChem* **2016**, *9*, 562–582.

[24] T. Werpy, J. Frye, J. Holladay, in *Biorefineries - Ind. Process. Prod.* (Eds.: B. Kamm, P.R. Gruber, M. Kamm), Wiley-VCH Verlag GmbH, Weinheim, Germany, **2005**, pp. 367–379.

[25] K. Kon, W. Onodera, K. Shimizu, *Catal. Sci. Technol.* **2014**, *4*, 3227–3234.

[26] J. C. Serrano-Ruiz, D. Wang, J. A. Dumesic, *Green Chem.* **2010**, *12*, 574.

[27] S. Sitthisa, D. E. Resasco, *Catal. Letters* **2011**, *141*, 784–791.

[28] S. S. R. Gupta, *Catal. Today* **2018**, *309*, 189–194.

[29] J. F. Leal Silva, A. P. Mariano, R. Maciel Filho, *Biomass and Bioenergy* **2018**, *119*, 492–502.

[30] E. Christensen, A. Williams, S. Paul, S. Burton, R. L. McCormick, *Energy & Fuels* **2011**, *25*, 5422–5428.

[31] H. Joshi, B. R. Moser, J. Toler, W. F. Smith, T. Walker, *Biomass and Bioenergy* **2011**, *35*, 3262–3266.

[32] A. English, J. Brown E&C, J. Rovner, S. Davies, U. by Staff, in *Kirk-Othmer Encycl. Chem. Technol.*, John Wiley & Sons, Inc., Hoboken, NJ, USA, **2015**, pp. 1–19.

[33] E. Christensen, J. Yanowitz, M. Ratcliff, R. L. McCormick, *Energy & Fuels* **2011**, *25*, 4723–4733.

[34] F. Zhu, in *Hydroprocessing for Clean Energy* (Eds.: F. Zhu, R. Hoehn, V. Thakkar, E. Yuh), John Wiley & Sons, Inc., Hoboken, New Jersey, **2016**, pp. 23–49.

[35] G. Dwivedi, M. P. Sharma, *Renew. Sustain. Energy Rev.* **2014**, *31*, 650–656.

[36] T. Lei, Z. Wang, Y. Li, Z. Li, X. He, J. Zhu, *BioResources* **2013**, *8*, 2696–2707.

[37] T. Lei, Z. Wang, X. Chang, L. Lin, X. Yan, Y. Sun, X. Shi, X. He, J. Zhu, *Energy* **2016**, *95*, 29–40.

[38] D. Singh, K. A. Subramanian, M. Juneja, K. Singh, S. Singh, R. Badola, N. Singh, *Environ. Prog. Sustain. Energy* **2017**, *36*, 214–221.

[39] K. H. Nothnαgel, D. S. Abrams, J. M. Prausnitz, *Ind. Eng. Chem. Process Des. Dev.* **1973**, *12*, 25–35.

[40] J. G. Hayden, J. P. O'Connell, *Ind. Eng. Chem. Process Des. Dev.* **1975**, *14*, 209–216.

[41] AspenTech Inc., *Aspen Physical Property System: Physical Property Methods*, Burlington, **2013**.

[42] D. E. Stogryn, J. O. Hirschfelder, *J. Chem. Phys.* **1959**, *31*, 1531–1545.

[43] AspenTech Inc., *Aspen Plus 8.6 Manual*, AspenTech, Inc., Bedford, MA, USA, **2014**.

[44] J. F. Boston, P. M. Mathias, in *Proc. 2nd Int. Conf. Phase Equilibria Fluid Prop. Chem. Process Ind. (17-21 March 1980)*, West Berlin, **1980**, pp. 823–849.

[45] D.-Y. Peng, D. B. Robinson, *Ind. Eng. Chem. Fundam.* **1976**, *15*, 59–64.

[46] Aspentech Inc., *Aspen Plus PURE32 Databank*, AspenTech, Inc., Bedford, MA, USA, **2014**.

[47] S. M. Walas, *Phase Equilibria in Chemical Engineering*, Butterworth, **1985**.

[48] H. Renon, J. M. Prausnitz, *AIChE J.* **1968**, *14*, 135–144.

[49] D. Gorissen, I. Couckuyt, P. Demeester, T. Dhaene, K. Crombecq, *J. Mach. Learn. Res.* **2010**, *11*, 2051–2055.

[50] Z.-H. Han, K.-S. Zhang, in *Real-World Appl. Genet. Algorithms* (Ed.: Olympia Roeva), Intech, Rijeka, **2012**, pp. 343–362.

[51] C. Daniel, *Applications of Statistics to Industrial Experimentation*, John Wiley & Sons, Inc., Hoboken, NJ, USA, **1976**.

[52] S. W. Fitzpatrick, (Biofine Incorporated), US4897497 A, **1990**.

[53] S. W. Fitzpatrick, (Biofine Incorporated), **n.d.**

[54] M. Jin, C. Sarks, B. D. Bals, N. Posawatz, C. Gunawan, B. E. Dale, V. Balan, *Biotechnol. Bioeng.* **2017**, *114*, 980–989.

[55] J. Zhang, D. Chu, J. Huang, Z. Yu, G. Dai, J. Bao, *Biotechnol. Bioeng.* **2009**, n/a-n/a.

[56] J. . Cha, M. . Hanna, *Ind. Crops Prod.* **2002**, *16*, 109–118.

[57] B. Girisuta, K. Dussan, D. Haverty, J. J. Leahy, M. H. B. Hayes, *Chem. Eng. J.* **2013**, *217*, 61–70.

[58] K. Kroenlein, V. Diky, *ThermoData Engine*, **2017**, https://www.nist.gov/mml/acmd/trc/thermodata-engine, accessed December 20, 2017.

[59] E. R. Morais, T. L. Junqueira, I. L. M. Sampaio, M. O. S. Dias, M. C. A. F. Rezende, C. D. F. de Jesus, B. C. Klein, E. O. Gómez, P. E. Mantelatto, R. Maciel Filho, et al., Springer, Cham, **2016**, pp. 53–

132.

[60] R. J. Wooley, V. Putsche, *Development of an ASPEN PLUS Physical Property Database for Biofuels Components*, Golden, CO, USA, **1996**.

[61] A. J. Resk, L. Peereboom, A. K. Kolah, D. J. Miller, C. T. Lira, *J. Chem. Eng. Data* **2014**, *59*, 1062–1068.

[62] M. Glass, M. Aigner, J. Viell, A. Jupke, A. Mitsos, *Fluid Phase Equilib.* **2017**, *433*, 212–225.

[63] M. O. S. Dias, T. L. Junqueira, I. L. M. Sampaio, M. F. Chagas, M. D. B. Watanabe, E. R. Morais, V. L. R. Gouveia, B. C. Klein, M. C. A. F. Rezende, T. F. Cardoso, et al., Springer, Cham, **2016**, pp. 189–256.

[64] Instituto Brasileiro de Economia - Fundação Geúlio Vargas, *IBRE - IGP*, **2018**, http://portalibre.fgv.br/main.jsp?lumChannelId=402880811D8E34B9011D92B6B6420E96, accessed May 8, 2018.

[65] F. J. Novita, H.-Y. Lee, M. Lee, *Ind. Eng. Chem. Res.* **2017**, *56*, 7037–7048.

[66] S. Jenkins, *Chem. Eng. Mag.* **2018**.

[67] R. Turton, R. C. Bailie, W. B. Whiting, J. A. Shaeiwitz, D. Bhattacharyya, *Analysis, Synthesis, and Design of Chemical Processes*, Prentice Hall, **2012**.

[68] R. H. Perry, D. W. Green, *Perry's Chemical Engineers' Handbook*, McGraw-Hill, **2008**.

[69] L. M. L. Delong, **2013**, pp. 245–254.

[70] The International Nickel Company Inc., *The Corrosion Resistance of Nickel-Containing Alloys in Sulfuric Acid and Related Compounds*, Suffern, NY, **1983**.

[71] The International Nickel Company Inc., *Corrosion Resistance of Nickel-Containing Alloys in Organic Acids and Related Compounds*, Suffern, **1979**.

[72] The Nickel Institute, *Stainless Steels and Specialty Alloys for Pulp, and Biomass Conversion: A Practical Guide for Mill Engineers*, Toronto, **2017**.

[73] Central Bank of Brazil, *Exchange Rates*, **2018**, http://www4.bcb.gov.br/pec/taxas/ingl/ptaxnpesq.asp?id=quotations, accessed May 8, 2018.

[74] MDIC - Brazilian Ministry of Industry and Foreign Trade, *AliceWeb2* **2018**.

[75] A. Y. Milanez, D. Nyko, M. S. Valente, L. C. Sousa, A. M. F. L. J. Bonomi, C. D. F. de Jesus, M. D. B. Watanabe, M. F. Chagas, M. C. A. F. Rezende, O. Cavalett, et al., *De Promessa a Realidade: Como o Etanol Celulósico Pode Revolucionar a Indústria Da Cana-de-Açúcar-Uma Avaliação Do Potencial Competitivo e Sugestões de Política Pública*, Rio de Janeiro, **2015**.

[76] CEPEA, *Ethanol - Center for Advanced Studies on Applied Economics*, **2018**, https://www.cepea.esalq.usp.br/en/indicator/ethanol.aspx, accessed February 25, 2018.

[77] Empresa de Pesquisa Energética, *Leilões de Energia*, **2018**, http://www.epe.gov.br/pt/leiloes-de-energia/leiloes, accessed February 15, 2018.

[78] Agência Nacional do Petróleo, *Série histórica do levantamento de preços e de margens de comercialização de combustíveis*, **2018**, http://www.anp.gov.br/wwwanp/precos-e-defesa/234-precos/levantamento-de-precos/868-serie-historica-do-levantamento-de-precos-e-de-margens-de-comercializacao-de-combustiveis, accessed February 13, 2018.

[79] J. F. L. Silva, M. A. Selicani, T. L. Junqueira, B. C. Klein, S. Vaz Júnior, A. Bonomi, *Brazilian J. Chem. Eng.* **2017**, *34*, 623–634.

[80] M. A. F. D. de Moraes, *Econ. Apl.* **2007**, *11*, 605–619.

[81] U.S. Bureau of Labor Statistics, *International Labor Comparisons (ILC)*, **2018**, https://www.bls.gov/fls/, accessed February 19, 2018.

[82] KPMG, *Corporate tax rates table*, **2018**, https://home.kpmg.com/xx/en/home/services/tax/tax-tools-and-resources/tax-rates-online/corporate-tax-rates-table.html, accessed February 23, 2018.

[83] M. O. S. Dias, T. L. Junqueira, C. E. V. Rossell, R. Maciel Filho, A. Bonomi, *Fuel Process. Technol.* **2013**, *109*, 84–89.

[84] M. O. S. Dias, T. L. Junqueira, C. D. F. Jesus, C. E. V. Rossell, R. Maciel Filho, A. Bonomi, *Energy*

**2012**, *43*, 246–252.

[85] A. T. Conag, J. E. R. Villahermosa, L. K. Cabatingan, A. W. Go, *J. Environ. Chem. Eng.* **2017**, *5*, 5411–5419.

[86] N. M. Garzón-Barrero, M. A. Shirakawa, S. Brazolin, R. G. de F. N. de Barros Pereira, I. A. R. de Lara, H. Savastano, *Int. Biodeterior. Biodegradation* **2016**, *115*, 266–276.

[87] L. A. R. Batalha, Q. Han, H. Jameel, H. Chang, J. L. Colodette, F. J. Borges Gomes, *Bioresour. Technol.* **2015**, *180*, 97–105.

[88] H. Liu, H. Hu, M. M. Baktash, M. S. Jahan, L. Ahsan, Y. Ni, *Biomass and Bioenergy* **2014**, *66*, 320–327.

[89] D. F. Root, J. F. Saeman, J. F. Harris, W. K. Neill, *For. Prod. J.* **1959**, *9*, 158–165.

[90] I. van Zandvoort, Y. Wang, C. B. Rasrendra, E. R. H. van Eck, P. C. A. Bruijnincx, H. J. Heeres, B. M. Weckhuysen, *ChemSusChem* **2013**, *6*, 1745–1758.

[91] W. W.-F. Leung, *Centrifugal Separations in Biotechnology*, Elsevier, **2007**.

[92] J. F. Leal Silva, R. Maciel Filho, M. R. Wolf Maciel, *Chem. Eng. Trans.* **2018**, *69*, 373–378.

[93] M. Simo, C. J. Brown, V. Hlavacek, *Comput. Chem. Eng.* **2008**, *32*, 1635–1649.

[94] K. S. Bankole, G. A. Aurand, *Res. J. Appl. Sci. Eng. Technol.* **2014**, *7*, 4671–4684.

[95] J. F. Leal Silva, M. R. Wolf Maciel, R. Maciel Filho, *Chem. Eng. Trans.* **2018**, *69*, 379–384.

[96] *LEI Nº 13.576, de 26 de Dezembro de 2017 - Política Nacional de Biocombustíveis*, Brasília, **2017**.

[97] B. de Barros Neto, I. S. Scarminio, R. E. Bruns, *Como Fazer Experimentos: Pesquisa e Desenvolvimento Na Ciência e Na Indústria*, Bookman, Porto Alegre, **2000**.

[98] H. J. Kadhum, K. Rajendran, G. S. Murthy, *Bioresour. Technol.* **2017**, *244*, 108–116.

[99] A. P. Mariano, N. Qureshi, R. Maciel Filho, T. C. Ezeji, *J. Chem. Technol. Biotechnol.* **2012**, *87*, 334–340.

[100] D. F. Aycock, *Org. Process Res. Dev.* **2007**, *11*, 156–159.

[101] D. J. Braden, C. A. Henao, J. Heltzel, C. C. Maravelias, J. A. Dumesic, *Green Chem.* **2011**, *13*, 1755.

[102] M. Pan, G. Shu, J. Pan, H. Wei, D. Feng, Y. Guo, Y. Liang, *Fuel* **2014**, *132*, 36–43.

[103] U.S. Bureau of Labor Statistics, *Consumer Price Index (CPI)*, **2018**.

[104] A. D. Patel, J. C. Serrano-Ruiz, J. A. Dumesic, R. P. Anex, *Chem. Eng. J.* **2010**, *160*, 311–321.

[105] N. Abatzoglou, E. Chornet, K. Belkacemi, R. P. Overend, *Chem. Eng. Sci.* **1992**, *47*, 1109–1122.

[106] X. Hu, C. Lievens, A. Larcher, C.-Z. Li, *Bioresour. Technol.* **2011**, *102*, 10104–10113.

[107] S. J. Dee, A. T. Bell, *ChemSusChem* **2011**, *4*, 1166–1173.

[108] A. Mukherjee, M.-J. Dumont, V. Raghavan, *Biomass and Bioenergy* **2015**, *72*, 143–183.

[109] L. Shuai, J. Luterbacher, *ChemSusChem* **2016**, *9*, 133–155.

[110] Y. Román-Leshkov, J. N. Chheda, J. A. Dumesic, *Science* **2006**, *312*, 1933–7.

[111] J. C. Serrano-Ruiz, J. A. Dumesic, *Energy Environ. Sci.* **2011**, *4*, 83–99.

[112] B. F. M. Kuster, H. J. C. Der Van Steen, *Starch - Stärke* **1977**, *29*, 99–103.

[113] Y. Román-Leshkov, J. A. Dumesic, *Top. Catal.* **2009**, *52*, 297–303.

[114] E. I. Gürbüz, S. G. Wettstein, J. A. Dumesic, *ChemSusChem* **2012**, *5*, 383–387.

[115] L. M. Schmidt, L. D. Mthembu, P. Reddy, N. Deenadayalu, M. Kaltschmitt, I. Smirnova, *Ind. Crops Prod.* **2017**, *99*, 172–178.

[116] S. Alipour, H. Omidvarborna, *J. Clean. Prod.* **2017**, *143*, 490–496.

[117] R. Weingarten, J. Cho, R. Xing, W. C. Conner, G. W. Huber, *ChemSusChem* **2012**, *5*, 1280–1290.

[118] A. B. Gawade, A. V. Nakhate, G. D. Yadav, *Catal. Today* **2018**, *309*, 119–125.

[119] H. Yuan, J. Li, H. Shin, G. Du, J. Chen, Z. Shi, L. Liu, *Bioresour. Technol.* **2018**, *247*, 1184–1188.

[120] W. Thompson, R. Johansson, S. Meyer, J. Whistance, *Energy Policy* **2018**, *113*, 368–375.

[121] G. Kim, L. Anderson, *Biofuels Demand Expands, Supply Uncertain*, Washigton, **2017**.

[122] Jim Lane, *Don't spill that ethanol! Those cellulosic fuels are worth $4.33 a gallon.: Biofuels Digest*, **2018**, http://www.biofuelsdigest.com/bdigest/2017/06/13/dont-spill-that-ethanol-those-cellulosic-fuels-are-worth-4-33-a-gallon/, accessed May 13, 2018.

[123] R. van Rijn, I. U. Nieves, K. T. Shanmugam, L. O. Ingram, W. Vermerris, *BioEnergy Res.* **2018**, *11*, 414–425.

[124] P. Pal, J. Sikder, S. Roy, L. Giorno, *Chem. Eng. Process. Process Intensif.* **2009**, *48*, 1549–1559.

[125] J. Qin, X. Wang, Z. Zheng, C. Ma, H. Tang, P. Xu, *Bioresour. Technol.* **2010**, *101*, 7570–7576.

[126] Petrobras, *Petrobras - Fatos e Dados - Adotamos nova política de preços de diesel e gasolina*, **2016**, http://www.petrobras.com.br/fatos-e-dados/adotamos-nova-politica-de-precos-de-diesel-e-gasolina.htm, accessed May 14, 2018.

[127] CONAB, *Companhia Brasileira de Abastecimento - Safra Brasileira de Cana-de-açúcar*, **2018**, https://www.conab.gov.br/info-agro/safras/cana, accessed May 14, 2018.

[128] R. Corrêa da Silva, I. de Marchi Neto, S. Silva Seifert, *Renew. Sustain. Energy Rev.* **2016**, *59*, 328–341.

[129] J. D. Hunt., D. Stilpen, M. A. V. de Freitas, *Renew. Sustain. Energy Rev.* **2018**, *88*, 208–222.

[130] K. L. Carleton, D. M. Sonnenfroh, W. T. Rawlins, B. E. Wyslouzil, S. Arnold, *J. Geophys. Res.* **1997**, *102*, 6025–6033.

[131] S. M. Walas, S. M. Walas, in *Phase Equilibria Chem. Eng.*, **1985**, pp. 343–394.

# 7. Appendix 1

This section provides the methodology and the results of the experimental part of the master's project to which this dissertation is related. Binary interaction parameters for the NRTL activity coefficient model used to simulate the extraction of levulinic acid from aqueous solution were obtained with the data presented here.

## 7.1. Methodology

### 7.1.1. Quality and purification of analytes

The purity of chemicals is available in Table 19. The purity of chemicals as supplied by the manufacturer was consulted in their respective certificates of analysis. Among the chemicals used, only FA, LA, and FF were purified. The mass purity of purified chemicals was attested using HPLC (method details available in section 7.1.3). FA and LA were purified using fractional crystallization because of their melting points (FA: 8.4 °C, LA: 33-35 °C). Even though FF has a very high purity according to the certificate of analysis, it was further purified to remove oxidation products, since it is very unstable. Thus, FF was purified via fractional distillation under vacuum conditions (~25 mbar) to avoid oxidation, and the fraction distilling around 60-65 °C was collected. The vacuum decreases the system temperature, yielding an almost colorless heart product. Head and tail products were

discarded. Although sulfuric acid has a purity of 97.0%, it was not further purified because of three reasons: i) sulfuric acid forms an azeotrope with water, ii) sulfuric acid in this proportion crystalizes as sulfuric acid monohydrate,[130] iii) 2.92% of the 3.00% impurity is water, as verified by Karl Fisher titration (method details available in section 7.1.3). Type I reagent water was used in all trials (Megapurity, Brazil, resistivity < 18.2 MΩ.cm).

*Table 19. Manufacturer information and mass purity of chemicals.*

| Chemical | CAS number | Supplier | Purity, manufacturer | Purity, after purification |
|---|---|---|---|---|
| AA | 64-19-7 | Vetec | 99.9% | - |
| FA | 64-18-6 | Êxodo científica | 99.4% | 99.898% |
| FF | 98-01-1 | Sigma-Aldrich | 99.5% | 99.901% |
| MTHF | 96-47-9 | Sigma-Aldrich | 99.9% | - |
| LA | 123-76-2 | Sigma-Aldrich | 98.6% | 99.899% |
| Sulfuric acid | 7664-93-9 | Vetec | 97.0% | - |

### 7.1.2. Equilibrium cells

Data were obtained using a Marconi MA 505/5FEAQ (Marconi, Brazil), which consists of a series of five jacketed vessels equipped with individual temperature sensors and two sample ports, one for each phase (Figure 31). The temperature was controlled using a thermostatic bath Marconi MA 108/9 (Marconi, Brazil). Temperature uncertainty is 0.1 K for this model. Samples were withdrawn from equilibrium cells using 1 mL syringes (BD ultrafine, Brazil).

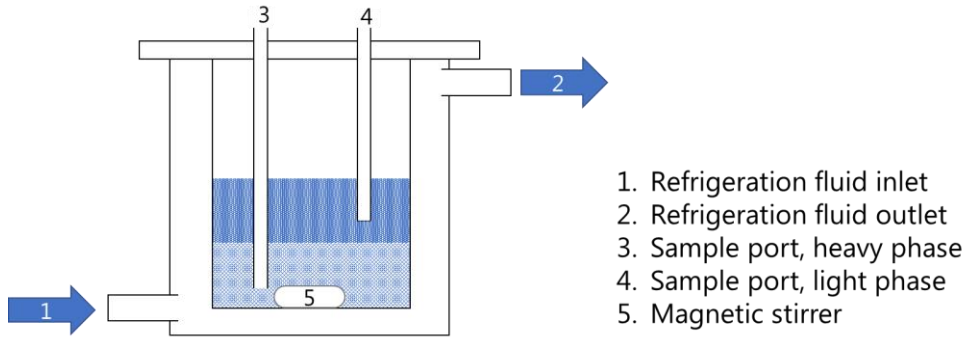


*Figure 31. Illustration of the apparatus used to obtain equilibrium compositions.*

For each sample point, the chemicals were mixed in proportions based on a previous determination of a binodal curve and tie-lines estimated using the UNIFAC activity coefficient model with the databank for LLE in Aspen Plus 8.6 (AspenTech, Inc., USA).

### 7.1.3. Quantification of analytes

The concentration of FA, AA, LA, FF, and MTHF was determined using a diode array detector coupled to an HPLC system (Agilent 1260 Infinity II). The method consisted of eluting the analytes through a Poroshell 120 EC-18 4.6 x 50 mm 2.7 µm (Agilent, USA), using a 5 mmol/L sulfuric acid aqueous mixture of 15% acetonitrile (Sigma-Aldrich, HPLC grade) by volume (type I water added to complete volume) as the mobile phase. With a flow rate of 1 mL/min, all analytes elute in 2.3 min. The detector was set at a wavelength of 194 nm for detection of MTHF, which is above the cutoff for both water and acetonitrile. Higher wavelengths do not detect MTHF. FA, AA, and LA were detected at 210 nm, and FF at 264 nm. Samples were diluted in the mobile phase, and the dilution factor was used on a weight basis. Samples were weighed with XP205DR (Mettler Toledo, Switzerland, uncertainty of 0.01 mg). For each sample point, a dilution triplicate was completed to estimate the uncertainty of the analysis method by including the step more susceptible to human error.

The concentration of water was determined via Karl Fischer titration in an 841 Titrando (Metrohm AG, Switzerland). Two problems are related to this method. First, carboxylic acids might react with the methanol present in the Karl Fischer reagent, producing water and interfering with measurements. Second, low pH affects negatively the kinetics of the reaction occurring in Karl Fischer titration. Thus, titration was carried out with small samples (according to the lower limit recommended by the manufacturer), and the titration media was changed frequently based on experience and titration time. Titrating agent was Composite 5 (Honeywell Fluka) and titrating medium was Hydranal™ Methanol Rapid (Honeywell Fluka). Samples were weighed with XP205DR. Triplicates were completed to estimate uncertainty for water concentration in samples. The concentration of sulfuric acid was determined via titration using a standardized 0.01 mol/L NaOH solution. All acid-base titrations were conducted in an 809 Titrando (Metrohm AG, Switzerland). NaOH solution was standardized with potassium biphthalate (Sigma-Aldrich). Samples were weighed with XP205DR. Triplicates were completed to estimate the uncertainty of sulfuric acid concentration.

### 7.1.4. Data curation

After all mass concentrations were determined, they were normalized under the condition that if the sum of mass fractions determined individually was out of the range of 3% of the unity, the tie-line was to be repeated. Data regression was carried out using the regression module of Aspen Plus Properties 8.6. The NRTL liquid activity model was used because it presents better agreement for the classes of components used.[62,131] The regression method implemented in Aspen Plus Properties considers Gibbs energy minimization to yield stable results. Aspen Plus uses the uncertainty as weighing factor in data regression. However, it only accepts a general uncertainty for each parameter (temperature and concentration of each chemical in each phase). Therefore, the uncertainty used was the average of the standard deviations of all points for the same variable.

## 7.2. Results

Tables 20-24 present the composition of the two phases in equilibrium. The parameters regressed from these data are available in the main text of the dissertation, in Table 5.

*Table 20. Equilibrium compositions (mol fraction) for the system MTHF+FA+water.*

| T (K) | organic phase | | | aqueous phase | | |
|---|---|---|---|---|---|---|
| | MTHF | FA | water | MTHF | FA | water |
| 0.1* | 0.0013 | 0.0013 | 0.0052 | 0.0007 | 0.0006 | 0.0025 |
| 280 | 0.8113 | 0.0000 | 0.1887 | 0.0420 | 0.0000 | 0.9580 |
| 280 | 0.4901 | 0.1022 | 0.4077 | 0.0430 | 0.0230 | 0.9340 |
| 280 | 0.3528 | 0.1353 | 0.5119 | 0.0444 | 0.0436 | 0.9120 |
| 280 | 0.2362 | 0.1432 | 0.6206 | 0.0583 | 0.0770 | 0.8648 |
| 280 | 0.2744 | 0.1470 | 0.5786 | 0.0503 | 0.0648 | 0.8849 |
| 310 | 0.8182 | 0.0000 | 0.1818 | 0.0215 | 0.0000 | 0.9785 |
| 310 | 0.5536 | 0.1024 | 0.3440 | 0.0202 | 0.0267 | 0.9532 |
| 310 | 0.4163 | 0.1421 | 0.4416 | 0.0242 | 0.0503 | 0.9255 |

*Table 20 (continued). Equilibrium compositions (mol fraction) for the system MTHF+FA+water.*

| T (K) | organic phase | | | aqueous phase | | |
|---|---|---|---|---|---|---|
| | MTHF | FA | water | MTHF | FA | water |
| 310 | 0.3109 | 0.1672 | 0.5219 | 0.0314 | 0.0787 | 0.8899 |
| 310 | 0.3346 | 0.1600 | 0.5055 | 0.0279 | 0.0722 | 0.9000 |
| 340 | 0.8230 | 0.0000 | 0.1770 | 0.0147 | 0.0000 | 0.9853 |
| 340 | 0.5615 | 0.1112 | 0.3272 | 0.0141 | 0.0317 | 0.9542 |
| 340 | 0.4340 | 0.1455 | 0.4205 | 0.0214 | 0.0590 | 0.9196 |
| 340 | 0.2802 | 0.1766 | 0.5431 | 0.0358 | 0.1012 | 0.8630 |
| 340 | 0.3886 | 0.1696 | 0.4419 | 0.0252 | 0.0811 | 0.8937 |

*Table 21. Equilibrium compositions (mol fraction) for the system MTHF+AA+water.*

| T (K) | organic phase | | | aqueous phase | | |
|---|---|---|---|---|---|---|
| | MTHF | AA | water | MTHF | AA | water |
| 0.1* | 0.0013 | 0.0011 | 0.0052 | 0.0004 | 0.0001 | 0.0017 |
| 280 | 0.8113 | 0.0000 | 0.1887 | 0.0420 | 0.0000 | 0.9580 |
| 280 | 0.5931 | 0.0648 | 0.3421 | 0.0494 | 0.0105 | 0.9401 |
| 280 | 0.4196 | 0.0937 | 0.4866 | 0.0542 | 0.0221 | 0.9236 |
| 280 | 0.2810 | 0.1124 | 0.6066 | 0.0753 | 0.0454 | 0.8793 |
| 280 | 0.2463 | 0.1088 | 0.6448 | 0.0800 | 0.0514 | 0.8686 |
| 310 | 0.8182 | 0.0000 | 0.1818 | 0.0215 | 0.0000 | 0.9785 |
| 310 | 0.6328 | 0.0617 | 0.3055 | 0.0235 | 0.0113 | 0.9652 |
| 310 | 0.5131 | 0.1033 | 0.3836 | 0.0266 | 0.0227 | 0.9507 |
| 310 | 0.3946 | 0.1377 | 0.4677 | 0.0334 | 0.0400 | 0.9266 |
| 310 | 0.2990 | 0.1478 | 0.5531 | 0.0453 | 0.0596 | 0.8951 |
| 340 | 0.8230 | 0.0000 | 0.1770 | 0.0147 | 0.0000 | 0.9853 |
| 340 | 0.6680 | 0.0501 | 0.2819 | 0.0146 | 0.0110 | 0.9744 |
| 340 | 0.5490 | 0.0970 | 0.3540 | 0.0173 | 0.0233 | 0.9595 |

*Table 21 (continued). Equilibrium compositions (mol fraction) for the system MTHF+AA+water.*

| T (K) | organic phase | | | aqueous phase | | |
|---|---|---|---|---|---|---|
| | MTHF | AA | water | MTHF | AA | water |
| 340 | 0.4269 | 0.1313 | 0.4418 | 0.0224 | 0.0391 | 0.9385 |
| 340 | 0.3365 | 0.1524 | 0.5111 | 0.0314 | 0.0569 | 0.9117 |

*Table 22. Equilibrium compositions (mol fraction) for the system MTHF+LA+water.*

| T (K) | organic phase | | | aqueous phase | | |
|---|---|---|---|---|---|---|
| | MTHF | LA | water | MTHF | LA | water |
| 0.1* | 0.0020 | 0.0013 | 0.0051 | 0.0007 | 0.0003 | 0.0047 |
| 280 | 0.8113 | 0.0000 | 0.1887 | 0.0420 | 0.0000 | 0.9580 |
| 280 | 0.7566 | 0.0268 | 0.2166 | 0.0429 | 0.0040 | 0.9531 |
| 280 | 0.6780 | 0.0385 | 0.2835 | 0.0456 | 0.0054 | 0.9490 |
| 280 | 0.6291 | 0.0502 | 0.3208 | 0.0485 | 0.0075 | 0.9440 |
| 280 | 0.5566 | 0.0554 | 0.3879 | 0.0507 | 0.0096 | 0.9397 |
| 310 | 0.8182 | 0.0000 | 0.1818 | 0.0215 | 0.0000 | 0.9785 |
| 310 | 0.7511 | 0.0362 | 0.2126 | 0.0220 | 0.0051 | 0.9729 |
| 310 | 0.6798 | 0.0504 | 0.2698 | 0.0234 | 0.0067 | 0.9699 |
| 310 | 0.6226 | 0.0648 | 0.3126 | 0.0235 | 0.0084 | 0.9682 |
| 310 | 0.6073 | 0.0776 | 0.3150 | 0.0269 | 0.0132 | 0.9599 |
| 340 | 0.8230 | 0.0000 | 0.1770 | 0.0147 | 0.0000 | 0.9853 |
| 340 | 0.7697 | 0.0263 | 0.2040 | 0.0155 | 0.0038 | 0.9807 |
| 340 | 0.7222 | 0.0420 | 0.2358 | 0.0158 | 0.0060 | 0.9782 |
| 340 | 0.6453 | 0.0524 | 0.3023 | 0.0171 | 0.0080 | 0.9749 |
| 340 | 0.6042 | 0.0608 | 0.3350 | 0.0199 | 0.0102 | 0.9698 |

*Table 23. Equilibrium compositions (mol fraction) for the system MTHF+FF+water.*

| T (K) | organic phase | | | aqueous phase | | |
|---|---|---|---|---|---|---|
| | MTHF | FF | water | MTHF | FF | water |
| 0.1* | 0.0013 | 0.0011 | 0.0042 | 0.0003 | 0.0001 | 0.0017 |
| 280 | 0.8113 | 0.0000 | 0.1887 | 0.0420 | 0.0000 | 0.9580 |
| 280 | 0.6669 | 0.0841 | 0.2490 | 0.0366 | 0.0030 | 0.9604 |
| 280 | 0.5096 | 0.1930 | 0.2974 | 0.0300 | 0.0065 | 0.9635 |
| 280 | 0.3472 | 0.3299 | 0.3228 | 0.0257 | 0.0106 | 0.9637 |
| 280 | 0.1853 | 0.5408 | 0.2740 | 0.0150 | 0.0146 | 0.9704 |
| 310 | 0.8182 | 0.0000 | 0.1818 | 0.0215 | 0.0000 | 0.9785 |
| 310 | 0.6683 | 0.0854 | 0.2463 | 0.0201 | 0.0029 | 0.9770 |
| 310 | 0.5141 | 0.1957 | 0.2902 | 0.0178 | 0.0063 | 0.9759 |
| 310 | 0.3553 | 0.3271 | 0.3176 | 0.0154 | 0.0109 | 0.9737 |
| 310 | 0.1765 | 0.5036 | 0.3200 | 0.0078 | 0.0155 | 0.9767 |
| 340 | 0.8230 | 0.0000 | 0.1770 | 0.0147 | 0.0000 | 0.9853 |
| 340 | 0.6320 | 0.1021 | 0.2660 | 0.0140 | 0.0035 | 0.9824 |
| 340 | 0.4894 | 0.2264 | 0.2842 | 0.0134 | 0.0079 | 0.9787 |
| 340 | 0.3023 | 0.3835 | 0.3142 | 0.0113 | 0.0140 | 0.9748 |
| 340 | 0.1403 | 0.4928 | 0.3669 | 0.0063 | 0.0183 | 0.9755 |

*Table 24. Equilibrium compositions for the system MTHF+sulfuric acid+water.*

| T (K) | organic phase | | | aqueous phase | | |
|---|---|---|---|---|---|---|
| | MTHF | sulfuric acid | water | MTHF | sulfuric acid | water |
| 0.1* | 0.0018 | 0.0001 | 0.0084 | 0.0009 | 0.0007 | 0.0046 |
| 280 | 0.8113 | 0.0000 | 0.1887 | 0.0420 | 0.0000 | 0.9580 |
| 280 | 0.8107 | 0.0006 | 0.1888 | 0.0439 | 0.0124 | 0.9437 |
| 280 | 0.8102 | 0.0012 | 0.1885 | 0.0462 | 0.0240 | 0.9298 |
| 280 | 0.7980 | 0.0021 | 0.1999 | 0.0566 | 0.0359 | 0.9075 |

*Table 24 (continued). Equilibrium compositions for the system MTHF+sulfuric acid+water.*

| T (K) | organic phase | | | aqueous phase | | |
|---|---|---|---|---|---|---|
| | MTHF | sulfuric acid | water | MTHF | sulfuric acid | water |
| 280 | 0.7930 | 0.0048 | 0.2023 | 0.1020 | 0.0400 | 0.8580 |
| 310 | 0.8182 | 0.0000 | 0.1818 | 0.0215 | 0.0000 | 0.9785 |
| 310 | 0.8183 | 0.0002 | 0.1814 | 0.0202 | 0.0127 | 0.9671 |
| 310 | 0.8187 | 0.0002 | 0.1811 | 0.0205 | 0.0252 | 0.9543 |
| 310 | 0.8408 | 0.0007 | 0.1585 | 0.0220 | 0.0381 | 0.9399 |
| 310 | 0.8324 | 0.0015 | 0.1660 | 0.0309 | 0.0556 | 0.9135 |
| 340 | 0.8230 | 0.0000 | 0.1770 | 0.0147 | 0.0000 | 0.9853 |
| 340 | 0.8237 | 0.0000 | 0.1762 | 0.0149 | 0.0131 | 0.9721 |
| 340 | 0.8256 | 0.0001 | 0.1743 | 0.0153 | 0.0263 | 0.9584 |
| 340 | 0.8261 | 0.0003 | 0.1736 | 0.0163 | 0.0389 | 0.9448 |
| 340 | 0.8325 | 0.0006 | 0.1669 | 0.0179 | 0.0496 | 0.9325 |